
Evaluating the decay of sound

Die Vermessung des [Aus]Klangs

PhD Thesis conducted at the
Signal Processing and Speech Communications Laboratory
Graz University of Technology, Austria

by
Jamilla Balint

Supervisors:
Gerhard Graber
Gernot Kubin

Assessors/Examiners:
Michael Vorländer
Gerhard Graber
Gernot Kubin

Graz, December 3, 2020

Abstract

The absorption coefficient is a central parameter in the room acoustic design process. It can be measured in an impedance tube for normal sound incidence or in the reverberation chamber for random incidence. To guarantee a standardized test environment for reverberation chambers, the international standard ISO 354 suggests a measurement procedure to increase the diffusivity of a sound field inside a laboratory environment by installing diffusers. The quality of the sound field diffusivity is evaluated by measuring the reverberation time and calculating the absorption coefficient of a sample. Unfortunately with this procedure it is not possible to achieve comparable results between different laboratories. As a consequence, the measured absorption coefficient shows unacceptable deviations in laboratories around the world. Therefore one of the most important input parameters for the room acoustic design process is not reliable.

In this thesis, the decay of sound in rooms of different shapes and sizes is investigated experimentally. A different framework to linear regression is proposed to calculate decay parameters, when the fundamental assumptions for the application of the reverberation formula in acoustics is not applicable (uniform distribution of absorption). The decay parameters form the basis for calculating the absorption coefficient measured in the reverberation chamber. Results indicate that the beginning of the sound decay contains valuable information, which is mostly discarded for the evaluation of the reverberation time. The idea of absorption coefficient measurements leads to the topic of this work, namely the fundamental principle of measuring and calculating the reverberation time in various rooms.

In addition to the scientific contributions on the topic of sound decays and absorption coefficient measurements, the interconnection between acoustics and architecture is addressed. The benefit of joint work is demonstrated with examples from collaborative projects.

Kurzfassung

Der Absorptionsgrad ist ein zentraler Parameter des raumakustischen Planungsprozesses. Er kann in einem Impedanzrohr ermittelt werden für senkrechten Schalleinfall oder in einem Hallraum für diffusen Schalleinfall. Um eine standardisierte Messumgebung für Hallräume zu schaffen, empfiehlt die ISO 354 eine Messprozedur, um die Diffusität des Schallfeldes zu erhöhen. Eine ausreichende Diffusität wird mittels einer Nachhallzeitmessung sowie der Bestimmung des Absorptionsgrades eines hochabsorbierenden Materials ermittelt. Bedauerlicherweise kann durch diese Methode nicht sichergestellt werden, dass in unterschiedlichen Hallräumen gleiche Messergebnisse bei Absorptionsgraden erzielt werden. Bei Ringversuchen konnte gezeigt werden, dass es bei Absorptionsgradmessungen von gleichen Proben in unterschiedlichen Hallräumen zu großen Abweichungen kommt. Somit ist einer der wichtigsten Eingangsparameter für den raumakustischen Planungsprozess nicht verlässlich.

In der vorliegenden Arbeit werden Ausklingvorgänge in unterschiedlichen Räumen und Besetzungszuständen experimentell untersucht. Eine alternative Berechnungsmethode für Ausklingzeiten wird vorgeschlagen, wenn die grundlegenden Annahmen für die Anwendung der Nachhallformel nicht gegeben sind (u.a. die gleichmäßige Verteilung der Absorption). Die Ausklingzeiten dienen als Grundlage für die Berechnung des Absorptionsgrades aus Hallraummessungen. Die Ergebnisse führen zu der Annahme, dass der Teil zu Beginn des Ausklingvorganges wichtige Informationen enthält, jedoch meistens vom Auswertevorgang ausgeschlossen wird. Die Idee von Absorptionsgradmessungen führt zum Thema der vorliegenden Arbeit: das grundlegende Prinzip der Messung und der Berechnung der Nachhallzeit in unterschiedlichen Räumen.

Zusätzlich zu den wissenschaftlichen Beiträgen zu Ausklingvorgängen und Absorptionsgradmessungen wird die Verbindung zwischen Akustik und Architektur erörtert. Mit Beispielen aus gemeinsam durchgeführten Projekten werden die Vorteile der interdisziplinären Arbeit hervorgehoben.

Contents

| | | |
|----------|---|-----------|
| 1 | Introduction | 13 |
| 1.1 | Motivation | 16 |
| 1.2 | Contributions and outline | 17 |
| 2 | Multi-exponential decay model & Bayesian decay time estimation | 21 |
| 2.1 | Coupled Spaces | 23 |
| 2.2 | Single Spaces | 25 |
| 2.3 | Double slope indicators | 27 |
| 2.4 | Multi-exponential decay model | 27 |
| 2.5 | Bayesian decay time estimation | 29 |
| 2.5.1 | Framework | 29 |
| 2.5.2 | Numerical example | 32 |
| 3 | Calculating the absorption coefficient | 37 |
| 3.1 | Measurements | 40 |
| 3.2 | Theoretical absorption coefficient | 41 |
| 3.3 | Linear regression | 42 |
| 3.4 | Use of shortest decay time | 44 |
| 3.5 | Discussion | 48 |
| 4 | Experimental investigation of absorber placement | 51 |
| 4.1 | Absorber placement | 52 |
| 4.2 | Measurements | 52 |
| 4.2.1 | Difficulties with comparing absorber setups | 54 |
| 4.2.2 | Evaluation of decay parameter | 61 |
| 4.3 | Discussion | 62 |
| 5 | Experimental investigation of artificial reverberation | 67 |
| 5.1 | Measurements | 70 |
| 5.2 | Discussion | 73 |
| 6 | Conclusion | 77 |
| 6.1 | Rethinking reverberation time | 80 |
| 6.2 | The process of standardization | 81 |
| 6.3 | Further thoughts on (architectural) acoustics | 81 |
| 6.3.1 | W. C. Sabine, a lecture hall, and TU Graz | 84 |
| 6.3.2 | Why concert halls should please the ear AND the eye | 85 |
| 6.3.3 | Sonic environment | 88 |
| 6.3.4 | Y. Toyota and why he prays a lot | 89 |

| | |
|---|------------|
| Appendix A - Contributions | 91 |
| Bayesian decay time estimation in a reverberation chamber for absorption measurements | 92 |
| Architectural Acoustics extended, between two languages new space is discovered . | 103 |
| Humming Room | 109 |
| Appendix B - Data Sheets | 113 |
| Data sheet: Lecture Hall i9 | 114 |
| Data sheet: Seminar Room Kronesgasse | 118 |
| Appendix C - Student Projects | 122 |
| Prevention of flutter echoes in architecturally demanding spaces | 123 |
| Sound propagation in a reverberation chamber | 125 |
| Entwurf und Bau einer variablen Akustik | 129 |
| Raumakustische Optimierung eines Aufnahme-raumes im Tonstudio der KUG | 131 |
| Adaptive Acoustics | 133 |
| Statistical energy analysis for room acoustics | 135 |
| Entwurf und Bau eines Modellhallraums im Massstab 1:10 | 137 |
| Raumakustik: Grundlagen, Konzepte und Anwendungsbeispiele | 139 |
| Grenadier Acoustics | 141 |
| Appendix D - Derivation of decay times | 145 |
| Bibliography | 150 |

Statutory Declaration

I declare that I have authored this thesis independently, that I have not used other than the declared sources/resources, and that I have explicitly marked all material which has been quoted either literally or by content from the used sources.

date

signature

Preface

When entering a concert hall, I perceive the environment as a musician, as an engineer and as an acoustician. Listening to recitals at various concert halls is therefore one of my greatest passions. I continuously ask myself, what makes a certain hall special. Sometimes I enter a room and immediately feel comfortable, warm and have a sense of well-being. When thinking about it from a more scientific point of view, there are so many factors which add up to generating such an atmosphere: the amount of early reflections, the side reflections, the reverberation time, the diffusivity of the sound field, the aesthetics of the space, the light - and these are just a couple to be mentioned. It is fascinating how physics and aesthetics work in this context - they all add up like a piece of art. Nevertheless, I often wondered how such halls can be designed. An architect might have a vision, makes a sketch and an acoustician has to translate the pictures into an acoustic design. Suggestions have to be made about the materials which work in a certain way to absorb, reflect or scatter the sound.

After finishing my master thesis and working as an acoustic consultant, I had the impression that the input parameters for the acoustic design process are not very reliable. Then I started to investigate the mystery of acoustics and its connections to architecture...

To my family and friends.

1

Introduction



Two listening examples (impulse responses) are prepared to illustrate the fundamental topic of this work (either scan the QR code or use this [LINK](#)).

- What kind of space do you hear?
- What kind of space do you visualize?
- What is the difference between the two examples?
- Try to guess the reverberation time.
- Is the acoustics good or bad?

A picture of the rooms will be shown within the thesis, as well as a short description and some room acoustic parameters.

1 Introduction

*Because of the reverberation, there's always more to the sound than just the sound.
Listen to everything all the time and remind yourself when you are not listening.*

Pauline Oliveros [Oliveros, 2010]

The architectural design of a space has to fulfill several purposes, among others, it has to satisfy the expectations of the creators, users, and visitors on many levels. Pleasing the senses is highly complex since the taste of human beings is very heterogeneous and the range of applications is wide. From an acoustic point of view, a concert hall for classical music should envelop the listener with its sound, a lecture hall should provide the best solution to ensure a high speech intelligibility. The requirements and expectations can be expressed very clearly but what *good acoustics* is in the end, is a matter of perspective. Nevertheless, architectural acoustics as an academic discipline has been established ever since the end of the 19th century, when Wallace Clement Sabine was asked to improve the intelligibility of a lecture hall. The problem was stated as follows [Sabine, 1936]:

*Why is the lecture room of the Fogg Art Museum acoustically poor,
and what can be done about it?*

which was translated by W. C. Sabine to:

*What is the behaviour of vibrational energy in a three-dimensional medium bounded by
imperfectly reflecting walls and what light does the answer to this question throw
on the age old problem of the acoustic properties of rooms?*

He conducted a series of listening test with an organ pipe during the night and found out that by adding seat cushions from a theatre to the lecture room, the reverberation decreases and the speech intelligibility increases. This sounds very obvious nowadays but it has to be pointed out that at the end of the 19th century putting wires into a room was considered as an effective acoustic measure. [Sabine, 1922] After several experiments in different rooms, the relationship between the reverberation time, the room volume and the room surfaces was established, known as Sabine's reverberation formula:

$$T = \frac{4 \cdot 6 \cdot \ln(10) \cdot V}{c \cdot A}, \quad (1.1)$$

where T is the time where the sound pressure level drops 60 dB below the initial level, V the room volume, c is the speed of sound and A is the equivalent absorption area. Equation 1.1 forms the basis for measuring the absorption coefficient of a material in the reverberation chamber [ISO 354, 2003]:

$$\alpha = \frac{55.3 \cdot V}{c \cdot S} \left(\frac{1}{T_o} - \frac{1}{T_e} \right), \quad (1.2)$$

where V is the volume of the chamber, c the speed of sound, S the area of the specimen, T_o is the reverberation time measured with the sample and T_e is the reverberation time in the empty chamber. It was also W.C. Sabine who was responsible for the construction of the first reverberation chamber; sadly he passed away soon after the building has been completed at the Riverbank Laboratories in 1915. His work was continued by his cousin P. E. Sabine, who published several articles on the topic of absorption measurements and its difficulties [Sabine, 1931, Sabine, 1935]. At that time the measurements were called *the organ pipe and ear method*, as illustrated in fig. 1.1. The picture shows a person sitting in a wooden box next to

1 Introduction

organ pipes in a reverberation chamber covered with non absorbing material listening to the decay of sound. Extensive analysis included listening to the sound decay in one setup 1400 times.

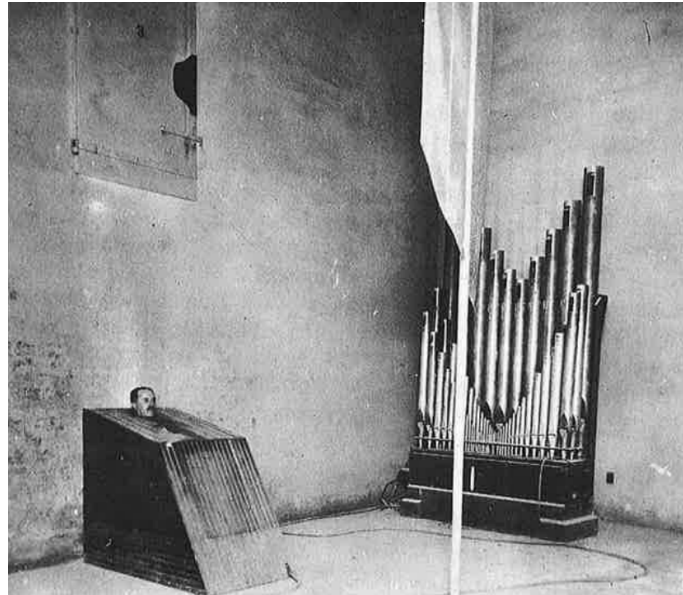


Figure 1.1: Conducting an absorption coefficient test at Riverbank Laboratories in 1919 [Sabine, 1922]

After conducting several measurements in different laboratories, a major concern was the poor interlaboratory reproducibility of absorption measurements. But the problem were not the organ pipes nor the ear. The first round robin test was conducted in 1933, where seven different laboratories took part and measured the absorption coefficient of the same sample [Sabine, 1935]. The results showed a large deviation within different laboratories, leading to the question if there is any such single value that can describe the acoustic properties of a material. Unfortunately the results did not improve over the next 100 years, and absorption coefficient measurements are still a topic of concern [C.W.Kosten, 1960, Davern and Dubout, 1980, R.E.Halliwell, 1983, ASTM, 2006, Thysell, 2011, Nolan et al., 2014].

1.1 Motivation

The introductory statement by Pauline Oliveros about reverberation is fundamental to this thesis. Reverberation is a central parameter in physics and in art. A sound is played back in a room and the sound is modified due to the reverberation in the room. The surrounding space acts like a filter and gives the sound a certain character. Acoustics surrounds us in our everyday lives and influences how we communicate with each other. To achieve a certain sound in a room within the architectural design process is crucial for the room to function according to the requirements.

Two of the most important parameters for the acoustic design of a space are the reverberation time and absorption coefficient. But inconsistencies in absorption coefficient measurements have been a topic of various previous research. Several round robin tests have shown that the absorption coefficient of a given area of the same material can take virtually any value. Therefore the most important input parameter for room acoustic design is not very reliable. In this thesis the approach described in ISO 354 to measure the sound absorption coefficient is investigated and certain aspects of the evaluation procedure are assessed. The basic approach of reverberation chamber measurements is to ensure a diffuse sound field by adding scattering elements to the space. But it is not possible to measure sound field diffusion yet, to be able to tell if a chamber is more diffuse than the other. Therefore it is very challenging to quantify the quality of a chamber. Many ISO certified chambers vary in shape and equipment (rectangular, non rectangular, boundary or panel diffusers, etc.) but they can all be used for absorption measurements according to ISO 354.

The calculation of the absorption coefficient is carried out via Sabine's equation for the reverberation time. But already Sabine stated that his equation is only valid in a diffuse sound field with uniform distribution of absorption. Until now it is not possible to quantify sound field diffusion and in the reverberation chamber a non-uniform distribution of absorption is present when following the measurement standard ISO 354. Therefore it is worth taking a closer look at the method for calculating the reverberation time. Linear regression is applied to a certain range of the energy decay curve (EDC). Previous research shows that it is not valid to use linear regression since the underlying data exhibits multiple slopes under different circumstances.

What if the input parameter RT for calculating the absorption coefficient is not determined with the highest accuracy possible? What if the reverberation time that we calculate is not the physically correct value which represents the decay of sound (the sum of all decaying modes within an enclosure)?

When multiple sloped decays are present, we state the hypothesis that the reverberation time obtained by fitting a linear regression to the data will lead to questionable results. As a consequence, the absorption coefficient will be questionable, too.

In this thesis sound decays in rooms of different shapes and sizes are investigated experimentally. A different framework to linear regression is proposed to calculate decay parameters. The idea of absorption coefficient measurements leads to the topic of this work, namely the fundamental principle of measuring and calculating the reverberation time in various rooms.

1.2 Contributions and outline

The main contributions of this work (Ch. 2 - Ch. 6) are all motivated by the desire to investigate absorption coefficient measurements in reverberation chambers and the large deviations which have been a topic of interest for almost 100 years. This part of the thesis is

based on materials that have been published in journals and conference proceedings over the last years [Balint et al., 2016, Balint et al., 2018, Balint and Graber, 2018, Balint and Kaiser, 2018, Balint et al., 2019, Balint and Muralter, 2019]. An effort has been made to tackle the very fundamental topics regarding absorption coefficient measurements, namely estimating the reverberation time with a different framework to linear regression. This led to the topic of decay analysis in a broad context.

Chapter 2: Multi-exponential decay model & Bayesian decay time estimation

In this chapter a brief overview on sound decay analysis is given, followed by a short introduction to the concept of multi-exponential decays. A Bayesian framework is introduced to estimate decay parameters. The need for such a framework to estimate decay parameters from multiple sloped decays as an alternative to linear regression is argued with the fact that energy decays are not linear (on a logarithmic scale) in most real world scenarios, especially in reverberation chambers at low frequencies and with non-uniform distribution of absorption. Examples will be given for the sake of demonstration.

Chapter 3: Calculating the absorption coefficient

In this chapter we discuss the method of calculating the absorption coefficient with the smallest decay time (obtained with the Bayesian framework) from measurements carried out in a reverberation chamber. Initial decay times as well as multiple decay parameters are estimated with a Bayesian framework from energy decay functions.

Chapter 4: Experimental investigation of absorber placement

In this chapter five different absorber placements and the influence of three different diffuse field conditions on the decay rates in the reverberation chamber are analysed experimentally. Measurements are carried out in a rectangular reverberation chamber and impulse responses are measured when the absorber is placed in a typical testing situation as well as split apart and spread in the edges of the room. The amount of diffusion is varied by changing the number of panel diffusers in the chamber. Conventional decay parameters like EDT , T_{20} , and T_{30} are analysed.

Chapter 5: Experimental investigation of artificial reverberation

In this chapter an artificial reverberation system is analysed with respect to the modification of the early and late energy decay and the consequences for conventional reverberation times. With active acoustic systems it is possible to create a curved energy decay if desired. As well as the early part of the decay and the late part can be modified by adding reflections or reverberation to the signal. Acoustics of coupled volumes can be simulated regarding the shape of the energy decay curve.

Finally, **Chapter 6** points to open questions and future research topics. A review is given which highlights the assumptions on why we need to rethink how the reverberation time is obtained in laboratory procedures followed by a comment on the process of including the findings into the concerning standard. Although this thesis deals with (1) the topic of sound

decay analysis, (2) the fundamentals of acoustics, and (3) absorption coefficient measurements in many ways, it is by no means complete. Many open questions remain to be answered and yield the possibility for future research.

In the last part of the thesis, further thoughts on acoustics in a more general way are presented as short comments. As a supplement to the scientific contributions, the subject of acoustics and its connections to architecture in research and teaching is brought up. Inspired by the collaboration with Milena Stavric at the Institute of Architecture and Media, several projects were realised with both students from architecture and audio engineering [Stavric and Balint, 2019b, Stavric and Balint, 2019a, Stavric and Balint, 2020]. The author of this thesis firmly believes that working together inspires the sphere of activity and can lead to novel approaches in both fields. Although this part was not intended to be included in the thesis, the work as a teaching and research associate and the results are always inspired by the interactions and discussions with students and therefore need to be a part of the thesis. Selected examples presented here and in the Appendices open up a field where future research and teaching activities will emerge.

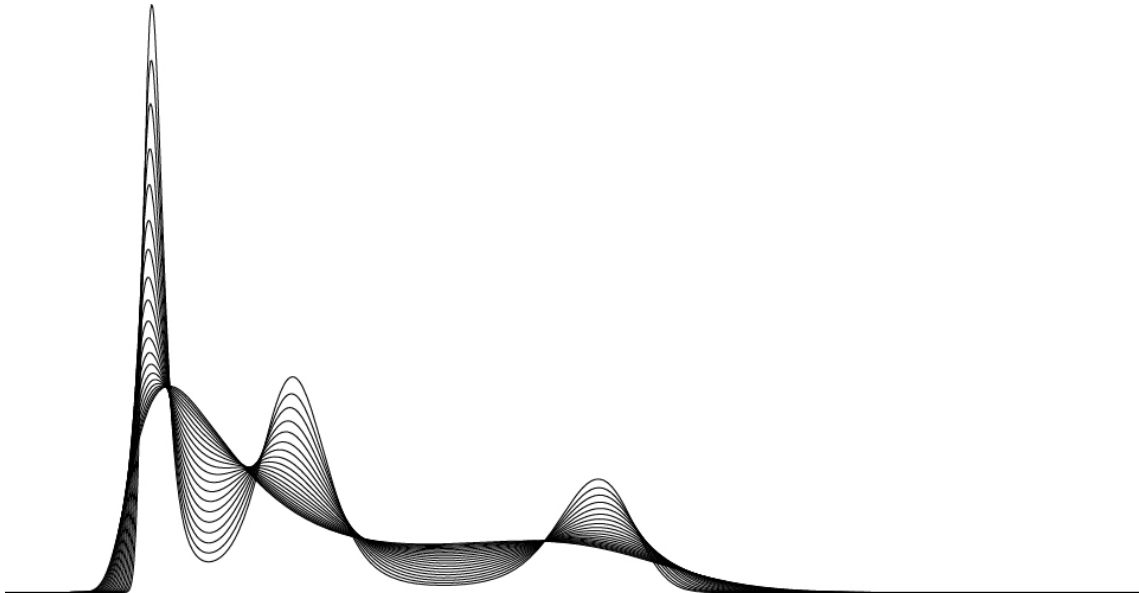
In **Appendix A** one journal publication is included [Balint et al., 2019] (which in the author's humble opinion is the main scientific contribution within this thesis), selected pages from a book publication where the author served as an editor together with colleague Milena Stavric (this joint work is a showcase project for the successful collaboration between acoustics and architecture) and some impressions from an interdisciplinary art project with Elisabeth Harnik and Milena Stavric (which combines acoustics, architecture, and art in the most inspiring way).

In **Appendix B** two data sheets from a lecture hall and a seminar room are shown. They were created within the Bachelor Projects, where the acoustic conditions were assessed in 26 halls of Graz University of Technology [Frischmann et al., 2019, Mülleder et al., 2019]. The reason for adding the data sheets lies in a rather historical context: W. C. Sabine, a pioneer in acoustics, made his first experiments in the lecture hall of the Fogg Art Museum (around 1897). He was asked to suggest improvements because it was too reverberant. Years of hard work led him finally to the derivation of the reverberation formula that we use today. Over 100 years later, together with students we assessed the acoustics in the lecture halls of TU Graz to forge the bridge and take a look how the situation evolved over the last decades.

Appendix C is a collection of student projects which were supervised during the author's time as a research and teaching associate at the Signal Processing and Speech Communication Laboratory. Additionally, impressions from a collaborative teaching project are included, where despite the extraordinary circumstances great projects were realised by students of architecture in the field of acoustics.

2

Multi-exponential decay model & Bayesian decay time estimation



In this chapter a brief summary is given on energy decay analysis. The benefit of using a multi-exponential rather than a single-exponential decay model is discussed. At first the well known theory of coupled systems is summarized, followed by a theoretical introduction to multi-exponential decays in single spaces. Parts of this Chapter have been previously published in [Balint et al., 2016, Balint et al., 2018, Balint and Graber, 2018, Balint et al., 2019].

2.1 Coupled Spaces

Multi-exponential decays are a well known phenomenon in coupled spaces [Bradley and Wang, 2005]. Coupled spaces consist typically of two volumes V_1 and V_2 , which are connected through an opening known as the coupling area S (see fig. 2.1). If the volume V_2 exhibits a decay time which is larger than in volume V_1 , then sound energy will be transmitted back from V_2 to V_1 , which will result in a double sloped decay.

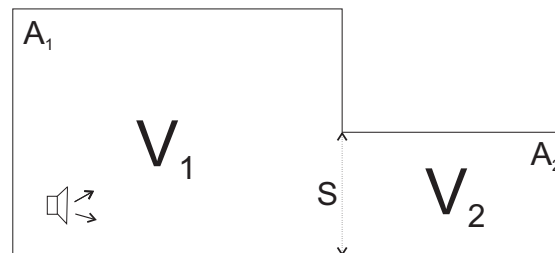


Figure 2.1: Plan view of a coupled space

Eyring investigated and published an article about the reverberation time in coupled spaces already in 1931 [Eyring, 1931]. The decay times of the coupled spaces depend mainly on the volumes, the coupling size, and the absorption of the surfaces in both volumes. Coupled spaces are very common in churches or theatres with lodges but also in concert halls like the Culture and Congress Center in Lucerne (CCL). The CCL was designed by the architect Jean Nouvel and the acoustician Russell Johnson and opened its doors in August 1998. Due to a variable acoustics, it is possible to adjust the reverberation time up to 3 seconds and alter the early and late reflections according to the type of music which is performed. [KKLManagementAG, 2020]

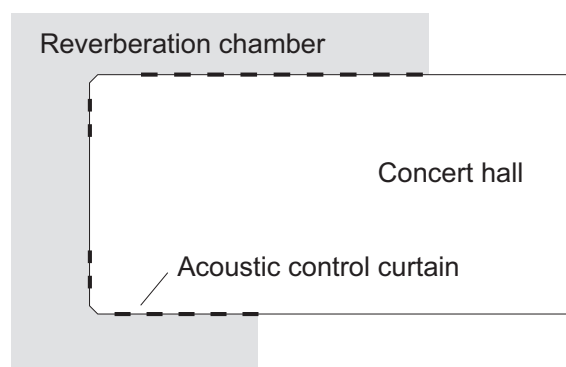


Figure 2.2: Layout of the Culture and Congress Center Lucerne, reverberation chamber surrounding the hall. The openings and thus the additional reverberation can be controlled via an acoustic control curtain.

The variable acoustics is realized with the echo chamber, an U-shaped space which is located in the top surrounding half of the concert hall (see fig. 2.2). Although the constructional effort of such building is enormous, the reputation of the CCL is that it lines up with the top concert

halls of the world [Beranek, 2004]. The volume of the hall (19000 m³) can be increased by 6000 m³ through 52 concrete doors (acoustic control curtains) which are controlled automatically [Kahle, 2001]. Because the echo chamber is sound hard, energy (late reverberation) will be fed back to the main hall while the early reflections remain very clear. Late reverberation (also referred to as room presence) is important to perceive the space and early reverberation (referred to as source presence) is important to clearly perceive the sound sources (instruments and transient events) [Kahle, 2013].

The theory of coupled systems has been derived in detail by [Cremer, 1961] and will be summarized shortly. The power balance equations for the steady state conditions if the sound source is located in volume 1 can be written as:

$$P - \frac{A_1 c E_1}{4} - \frac{S c E_1}{4} + \frac{S c E_2}{4} = 0 \quad (2.1)$$

$$\frac{S c E_1}{4} - \frac{A_2 c E_2}{4} - \frac{S c E_2}{4} = 0, \quad (2.2)$$

where A_i are the equivalent absorption areas in volumes 1 and 2, E_i are the energies, S is the coupling area and c is the speed of sound. The power balance equations in the non steady state condition can be written as:

$$\frac{c}{4} (A_{11} E_1 - \mu S E_2) = -V_1 \frac{dE_1}{dt} \quad (2.3)$$

$$\frac{c}{4} (A_{22} E_2 - \mu S E_1) = -V_2 \frac{dE_2}{dt}, \quad (2.4)$$

where μ is the transmission coefficient, and

$$A_{11} = A_1 + S, \quad A_{22} = A_2 + S. \quad (2.5)$$

The linear equations can be solved with the approach:

$$E_{1,2} = E_{01,02} e^{-2\delta t}, \quad (2.6)$$

where δ is the decay time and $E_{01,02}$ are the initial energies in volumes 1 and 2. The equation for the individual decay times δ_1 in V_1 and δ_2 in V_2 can be written as:

$$\left(1 - \frac{\delta}{\delta_1}\right) \left(1 - \frac{\delta}{\delta_2}\right) - k_1 k_2 = 0, \quad (2.7)$$

with the coupling factors:

$$k_1 = \frac{S}{A_{11}}, \quad k_2 = \frac{S}{A_{22}}. \quad (2.8)$$

If both volumes are not coupled, the decay times of each volume are:

$$\delta_1 = \frac{cA_1}{8V_1}, \quad \delta_2 = \frac{cA_2}{8V_2}. \quad (2.9)$$

For coupled volumes the decay times can be written as:

$$\delta_{I,II} = \frac{1}{2}(\delta_1 + \delta_2) \pm \sqrt{\left(\frac{\delta_1 - \delta_2}{2}\right)^2 + \kappa^2 \delta_1 \delta_2} \quad (2.10)$$

with

$$\kappa = \sqrt{k_1 k_2}. \quad (2.11)$$

The reverberation process in both rooms is a sum of exponentially decaying functions:

$$E_1 = \frac{4P}{cA_1} \left[e^{-2\delta_1 t} + \kappa^2 \frac{\delta_1^2}{(\delta_2 - \delta_1)^2} e^{-2\delta_2 t} \right] \quad (2.12)$$

$$E_2 = \frac{4P\mu S}{cA_1 A_2} \left[\frac{\delta_2}{\delta_2 - \delta_1} e^{-2\delta_1 t} - \frac{\delta_1}{\delta_2 - \delta_1} e^{-2\delta_2 t} \right] \quad (2.13)$$

If $A_1 \geq A_2$, then the energy decay in volume 1 will be double sloped. This results in a high level of perceived clarity and a more lingering late decay. Although the theory is straight forward, estimating the decay times in coupled systems from measurements is highly complex. Due to the multi-exponential decay, estimating a single reverberation time with linear regression is not very useful. It will only give a rough approximation of the slope in a certain decay range. Xiang et al. [Xiang and Goggans, 2001, Xiang and Goggans, 2003, Xiang and Jasa, 2006, Xiang et al., 2011] thoroughly investigated the decay behaviour in coupled spaces and developed a Bayesian framework to calculate multiple decay parameters. The successful application resulted in up to triple-slope detections, showing that the use of conventional methods of linear regression is not valid in those cases.

2.2 Single Spaces

The well-established reverberation theory is based on the assumptions of a diffuse sound field and an exponential sound decay. Derived by Sabine and Eyring, the reverberation formula establishes a connection between reverberation time, the sound absorption by the surfaces and the volume of the space. But already [Eyring, 1931] pointed out that the reverberation formulae may be applied to rooms of simple enclosure with a diffuse sound field, with well distributed absorbing material and an exponential sound decay. Furthermore he stated:

They may not be applied indiscriminately to complex structures for the author has shown that the curves illustrating the decay of the residual sound intensity level may not be straight under certain conditions for coupled rooms of different natural reverberation times or even for a single room with no sound diffusing scheme and non-uniformly distributed absorption.

Energy decays in enclosed spaces of various sizes and shapes have widely been investigated by many researchers in the past. Results indicate that in numerous cases a multi-exponential decay is present in single spaces, also (not just in coupled spaces). Hunt et al. [Hunt et al., 1939] showed that the root-mean-square sound pressure at a given point during the decay is the summation of each excited normal mode of vibration. In reverberation chambers with uneven distribution of absorption, the large number of excited modes within a given frequency band has to be subdivided into groups having common properties, leading to multiple decay parameters. Although restricted to rectangular rooms without any diffusing objects, the proposed method could be validated by various experiments. It was suggested not to use any diffusing elements in the reverberation chamber, since the effect on the sound field cannot be predicted and poses the risk of introducing additional uncertainties. When introducing the backward integration method, Schroeder also pointed out the existence of multi-exponential decays [Schroeder, 1965]. As an example he published measurements carried out in the Boston Symphony Hall exhibiting multiple decay times. Bruel [Bruel, 1978] observed concave sound decays on a logarithmic axis when trying to determine reverberation times for sound power measurements in diffuse-field conditions. He found out that the agreement between the free-field and diffuse-field sound power is much better when the early decay is used. Jacobsen [Jacobsen, 2013] shows that axial and tangential modes exhibit a longer decay time than oblique modes. For the sake of completeness, the individual decay times of axial, tangential and oblique modes are derived in App. D for two different cases (with uniform and non-uniform wall admittances). In small and medium-sized rooms, the decay will, therefore, always be multiple sloped at low frequencies. Furthermore he pointed out that if the initial part of the decay is used for calculating the absorption coefficient, care has to be taken at low frequencies, where the sound field is dominated by axial and tangential modes, as they contribute significantly to the steady state condition in the rooms [Jacobsen, 1982]. Still, he concluded that the systematic error of absorption estimates based on initial decay rates is about two-thirds of the error of usual estimates based on the interval from -5 dB to -35 dB. In [ISO 3382-2, 2008] a parameter for the linearity of the decay is proposed, which estimates the curvature based on the ratio of the reverberation times T_{20} and T_{30} . It has to be pointed out that this gives a rough estimation of whether or not a multi-exponential decay is present, although neglecting the bending point of the curve. Nilsson [Nilsson, 2004b] investigated rectangular rooms with absorbing ceilings like classrooms and offices. He successfully applied a two-system statistical energy analysis model to simulate the double sloped energy decay due to the uneven distribution of absorption. Furthermore the influence of diffusing objects was examined, showing that the curvature can be decreased and the bending point of the decay shifted when introducing irregularities at the boundaries such as boxes on the walls [Nilsson, 2004a].

Previous research, as shown, indicates that multi-exponential decays are ubiquitous: in single and coupled spaces, in concert halls, in small rooms, in rooms with uneven distribution of absorption, in classrooms, and in laboratories. Although it was pointed out that in cases of multi-exponential decays the determination of reverberation times with linear regression can lead to questionable results [Xiang and Goggans, 2001, Xiang and Goggans, 2003, Xiang and Jasa, 2006, Xiang et al., 2011], the standard procedure for calculating absorption coefficients still neglects the curved nature of energy decays which is apparent in the reverberation chamber.

In this thesis a systematic investigation is carried out, analysing the sound decay in various spaces of different sizes and under different diffuse field conditions.

2.3 Double slope indicators

Many attempts have been undertaken to evaluate whether one or more slopes occur within one energy decay. In [Harrison and Madaras, 2001] the “coupling coefficient” (T_{30}/T_{15}) was suggested as an indicator for the double slope effect (DSE), where T_{30} is the reverberation time calculated from the -5 dB to -35 dB drop in the decay curve and T_{15} is the reverberation time calculated from the -5 dB to -20 dB drop. The authors discovered that the shape and the location of the aperture has a less significant effect than the volume of the secondary space and the aperture size. The “coupling constant” (T_{60}/T_{15}) was introduced by [Ermann and Johnson, 2002], where T_{60} is the reverberation time calculated from the -5 dB to -65 dB drop in the decay curve. The value of T_{60} is difficult to measure and often not even possible to calculate. The authors of [Bradley and Wang, 2009] introduced the ratio of the late decay and the early decay (LDT/EDT) as a DSE quantifier. The late decay LDT is defined as the drop in the decay curve from -25 dB to -35 dB, and early decay EDT from 0 dB to -10 dB. In Bradley and Wang, 2010 the authors introduced a modified (LDT/EDT) parameter where the early decay is the drop from -5 dB to -15 dB. Two parameters were introduced in [Bradley and Wang, 2005], the “decay ratio” and the “ ΔL ” as an indicator for the DSE. The decay ratio is defined as the ratio between the slope k_2 of the second decay and the slope k_1 of the first decay within the decay curve. The parameter ΔL is the level difference at $x = 0$ between the two slopes. The double slope indicators use fixed values for evaluation. Those indicators neither consider the time nor the level of the break point of the double slope. Eyring published one of the first papers on the topic of coupled rooms underlining that the conventional reverberation formulae may not be applied under certain conditions, one of them being a coupled system where the single rooms exhibit different reverberation times [Eyring, 1931]. It took 70 years until a group of researchers tackled this problem. In multiple works a Bayesian framework was developed to estimate decay times in coupled room, the successful application resulted in up to triple slope detection [Xiang and Goggans, 2001, Xiang and Goggans, 2003, Xiang and Jasa, 2006, Xiang et al., 2011].

2.4 Multi-exponential decay model

In acoustics, the energy decay curve, which is obtained by applying the Schroeder backwards integration to a measured impulse response, can be written as a sum of exponential functions: [Xiang et al., 2011]

$$EDC(A, T, t_k) = A_0(t_K - t_k) + \sum_{i=1}^N A_i \cdot e^{\frac{-13.8 \cdot t_k}{T_i}}, \quad (2.14)$$

where the linear term $A_0(t_K - t_k)$ denotes the background noise in the room impulse response, t_k is the time parameter, K is the total length of the impulse response, and $k =$

2 Multi-exponential decay model & Bayesian decay time estimation

1, 2, ..., K . A_i denotes the linear amplitude of the i^{th} exponential decay function, T_i is the decay time of the i^{th} decay function, and N corresponds to the total number of slopes. In fig. 2.3 a decay is modelled with two exponentially decaying functions according to eq. 2.14 for the sake of illustration. The figures have been published previously at the Daga Conference in Rostock [Balint and Graber, 2018]. If this decay is considered to be the sum of two decaying modes, then mode one has a starting level of $A_1 = 0$ dB with a reverberation time $T_1 = 1$ s and for mode two $A_2 = -10$ dB and $T_2 = 2$ s. As a result the sum of both exponential function is curved when plotted on a logarithmic axis. If now the reverberation times EDT , T_{20} and T_{30} are calculated with linear regression, a rough estimate of both slopes is given as shown in fig. 2.3. In this case, the EDT is very close to the first slope ($EDT = 1.1$ s instead of $T_1 = 1$ s) and with visual inspection it is not possible to determine weather it is a better fit or not. The parameters $T_{20} = 1.3$ s and $T_{30} = 1.5$ s are an average between the two slopes T_1 and T_2 , even with visual inspection it is clear that the fit is only a rough estimation for the slopes of the curve. If a curved decay is present and one wants to estimate the true decay parameter, a different framework to linear regression should be used. In the following chapter a method to estimate decay parameters is presented.

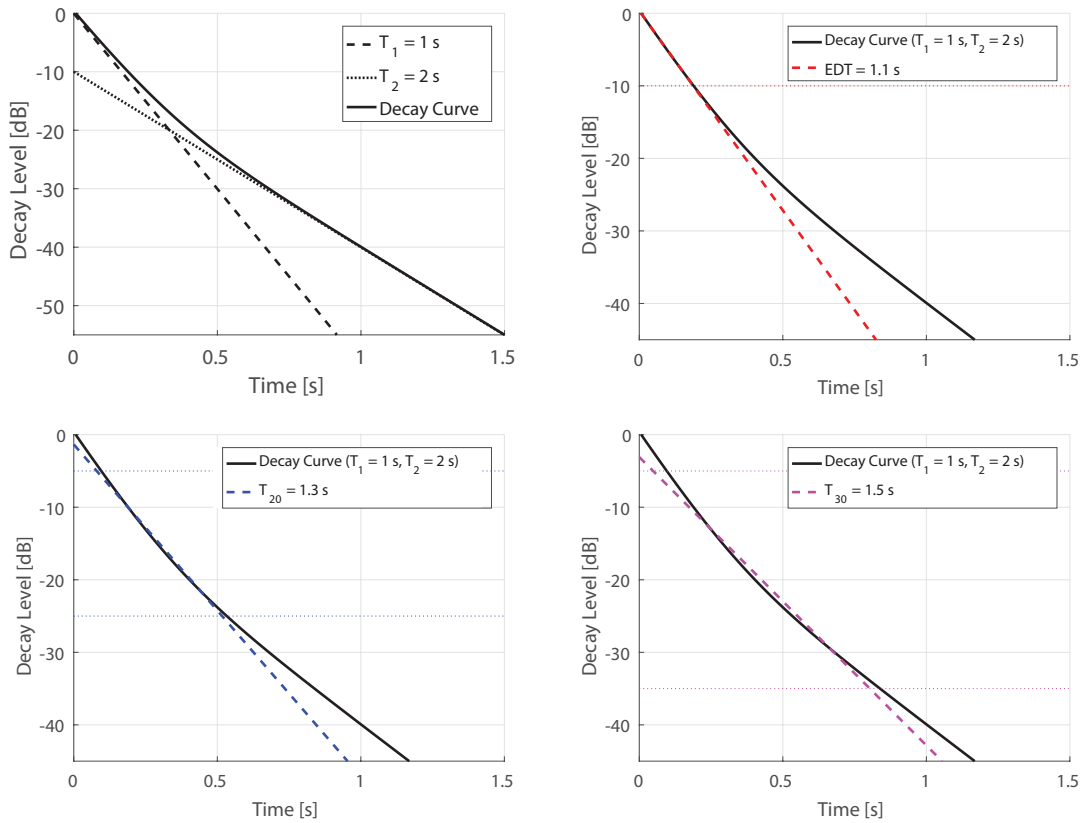


Figure 2.3: Sound decay with $A_1 = 0$ dB, $T_1 = 1$ s and $A_2 = -10$ dB, $T_2 = 2$ s, and the corresponding reverberation parameters EDT , T_{20} and T_{30}

2.5 Bayesian decay time estimation

Bayes' theorem provides a probabilistic framework to solve inverse problems in a variety of fields including acoustics, [Xiang and Jasa, 2006, Xiang et al., 2011, Jeong et al., 2017] image processing, [Gull and Skilling, 1984] and physics [Shukla et al., 1993, Shukla et al., 1995, Shukla et al., 1997]. A recent tutorial was published in [Xiang, 2020] due to the increase in the application of model-based Bayesian analysis in acoustics.

In this work, the aim is to calculate the decay time distribution from a given energy decay function. The method of extracting decay times is based on the algorithm *MELT - Maximum Entropy for LifeTime analysis* [Shukla et al., 1993, Hoffmann et al., 1993, Shukla et al., 1995, Shukla et al., 1997] which was used in the field of positron lifetime analysis. The authors employed the framework to solve the inverse problem of finding the decay times and their intensities resulting from measured multi-exponential decay functions. In acoustics, the energy decay function, which is obtained by applying the Schroeder backward integration to an impulse response, can be regarded as a multi-exponential decay function as well.

The framework in this thesis is taken from the field of physics and has been adapted within the Master Thesis of Florian Muralter [Muralter, 2018]. Different estimation techniques were evaluated and measurements were compared to simulated data [Muralter and Balint, 2019]. The Bayesian decay time estimation is presented in the following chapter, which is used in the present work to estimate decay parameters. This part has been published in [Balint et al., 2019]. Within the peer review process, one of the reviewers did not agree with the name of the framework (Maximum Entropy Method), which was taken from the original work [Shukla et al., 1993]. The name was changed to **Bayesian decay time estimation** according to the reviewer's suggestion.

2.5.1 Framework

Kuttruff suggested, that the decay time distribution can be calculated via the inverse Laplace transform of the energy decay curve. [Kuttruff, 1958] Considering Kuttruff's proposal, the inverse problem can be stated as follows: the causal factors (decay terms with corresponding intensities) have to be calculated from a set of observations (energy decay curve) that produced them. Hence the inverse problem can be written in form of a Fredholm integral as

$$D(y) = \int_a^b K(\tau, t) \Phi(\tau) d\tau + \nu(t), \quad (2.15)$$

where $D(y)$ represents the measured data, $\Phi(\tau)$ is the intensity as a function of decay time (function to be obtained), and $\nu(t)$ denotes the noise in the data. The kernel function follows as:

$$K(\tau, t) = \tau^{-1} e^{-\frac{t}{\tau}}. \quad (2.16)$$

Equation 2.15 can be written as a system of linear algebraic equations:

$$d_j = \sum_{\mu=1}^{n_{mod}} k_{j\mu} \phi_{\mu} + n_j, \quad j = 1 \dots n_{dat} \quad (2.17)$$

and in matrix notation:

$$D = K\Phi + N \quad (2.18)$$

The indices *dat* and *mod* refer to the measured data and the model, respectively.

The proposed algorithm uses a quantified maximum entropy approach, estimating a positive additive distribution (PAD) from noisy and incomplete data. Knowing a number of possible solutions *A*, *B*, and *C*, one can describe them as conditional probabilities $pr(A|D)$, $pr(B|D)$, $pr(C|D)$. If Φ was to represent a particular solution, one needs the probability density $pr(\Phi|D)$ as a function of Φ . This is not directly obtainable from the given dataset *D*. However, the reversed conditioning $pr(D|\Phi)$ - better known as the likelihood function - is obtainable. The likelihood function can be written as

$$pr(D|\Phi) = \prod_{j=1}^{n_{dat}} \frac{1}{\sqrt{2\pi\sigma^2}} e^{\left(-\frac{1}{2\sigma^2} [d_j - \sum_{\mu=1}^{n_{mod}} k_{j\mu} \phi_{\mu}]^2\right)}. \quad (2.19)$$

The model for estimating the unknown function can be found in Bayes' theorem,

$$pr(\Phi|D) = \frac{pr(\Phi)pr(D|\Phi)}{pr(D)} \quad (2.20)$$

with $pr(D)$ being a normalizing factor to ensure that the sum of the probabilities of all possible solutions is equal to one. This formula represents one of the most relevant mathematical fundamentals of data analysis. Considering the $pr(D|\Phi)$ as given and $pr(D)$ being a normalizing constant, the only remaining unknown term is the prior probability distribution of Φ , denoted as $pr(\Phi)$. The pointwise probability

$$pr(\Phi|m, \alpha) \propto e^{(\alpha S(\Phi, m))} \quad (2.21)$$

reflects the most important part of the quantified entropic prior [Skilling, 1990]. The two parameters *m* and α represent a model for Φ and an inverse measure of the expected spread of values of Φ about *m*. The pointwise joint probability distribution is given by

$$pr(\Phi, D|m, \alpha) = \left(\frac{\alpha}{2\pi}\right)^{\frac{\tau}{2}} \prod \frac{1}{\sqrt{2\pi\sigma^2}} e^{(\alpha S(\Phi, m) - \frac{1}{2} C(\Phi, D))}, \quad (2.22)$$

where the function $S(\Phi, m)$ denotes the Shannon-Jaynes entropy. The pointwise joint probability is proportional to the posterior probability by

$$pr(\Phi|m, \alpha, D) = \frac{pr(\Phi, D|m, \alpha)}{pr(D|m, \alpha)}. \quad (2.23)$$

Since the Shannon-Jaynes entropy is a convex function with negative definite curvature and

$C(f)$ has a positive curvature, the posterior probability $pr(\Phi|m, \alpha, D)$ has a unique maximum at

$$\alpha \frac{\partial S}{\partial \Phi} - \frac{1}{2} \frac{\partial C}{\partial \Phi} = 0 \quad \text{at} \quad \Phi = \hat{\Phi} \quad (2.24)$$

The obtained distribution $\hat{\Phi}$ is the single most probable PAD. The choice of a well guessed kick-off solution is essential as it has a stabilizing and regularizing effect. Furthermore it shortens the time needed for the solution to converge. For this particular reason, the algorithm uses a general optimal linear filter to compute a good kick-off solution. Designing a filter in this case means constructing a filter matrix F to solve the inverse problem by satisfying a minimization criterion. This is chosen to be the mean squared error between the "real" Φ and the one extracted by the filter F .

$$\sum_v p_v \langle |F(K\Phi_v - D)|^2 \rangle_N = \min \quad (2.25)$$

Each linear combination corresponds to a Φ_v with a probability p_v . To obtain the coefficients of the filter F the left side of eq. 2.25 has to be differentiated with respect to F and then equated to zero to satisfy the minimization criterion. This leads to a filter F to obtain the regularized solution

$$\Phi_r = FD, \quad (2.26)$$

with

$$F = \frac{C_\Phi K^T}{KC_\Phi K^T + C_N}, \quad (2.27)$$

where

$$C_\Phi = \sum_v p_v \Phi_v \Phi_v^T \quad ; \quad C_N = \langle NN^T \rangle. \quad (2.28)$$

2.5.2 Numerical example

To illustrate how decay times from multi-exponential data can be obtained, artificial energy decay functions (EDFs) are constructed and examples with double and triple slopes are analysed according to the values in tab. 2.1. One EDF is the sum of 100 exponentially decaying functions, where the amplitudes and decay times are normally distributed with mean values at T_i , A_i , a standard deviation of 0.1 and an additive noise term (the amplitude of the noise is set to $A_0 = 5 * 10^{-9}$), resulting in double-slope and triple-slope behaviour.

Table 2.1: Values of the artificial energy decay function: 100 normally distributed, exponentially decaying functions with mean values T_i (decay times) and A_i (amplitudes), and a standard deviation of 0.1.

| | A_1 | T_1 | A_2 | T_2 | A_3 | T_3 |
|-----------|-------|-------|-------|-------|-------|-------|
| Example 1 | 0.7 | 1.4 | 0.3 | 4.6 | | |
| Example 2 | 0.6 | 0.9 | 0.4 | 1.2 | | |
| Example 3 | 0.7 | 1.3 | 0.2 | 2.4 | 0.1 | 4.8 |
| Example 4 | 0.33 | 1.3 | 0.33 | 2.4 | 0.33 | 4.8 |

In example 1 (see fig. 2.4) the decay times are normally distributed with mean values of $T_1 = 1.40$ s and $T_2 = 4.60$ s and a standard deviation of 0.1, resulting in a double slope behaviour. The amplitude of the noise is set to $A_0 = 5e-9$, and the amplitudes of the decays are set to $A_1 = 0.70$ and $A_2 = 0.30$. This data is fed to the algorithm to estimate decay times from the given EDC. Through variation of entropy weights the result with the highest probability is obtained, as shown in fig. 2.4 (a). The result of the estimated decay times with the highest probability is shown in fig. 2.4 (b), where the normalized intensity spectrum (which corresponds to the linear amplitude of the decay process) is represented as a function of decay time. The local maxima of the decay times in fig. 2.4 (b) correspond to the mean values of the normal distributions used to obtain the artificial EDC. Now the peak values of the local maxima (decay times T_i and amplitudes A_i) are summed up to model the artificial EDC. The artificial EDC as well as the EDC obtained with the estimated decay times are shown in fig. 2.4 (c). The decay process is modelled with two exponential functions with the amplitudes $A_1 = 0.72$, $A_2 = 0.28$, the corresponding decay times $T_1 = 1.39$ s and $T_2 = 4.62$ s and an additive noise term.

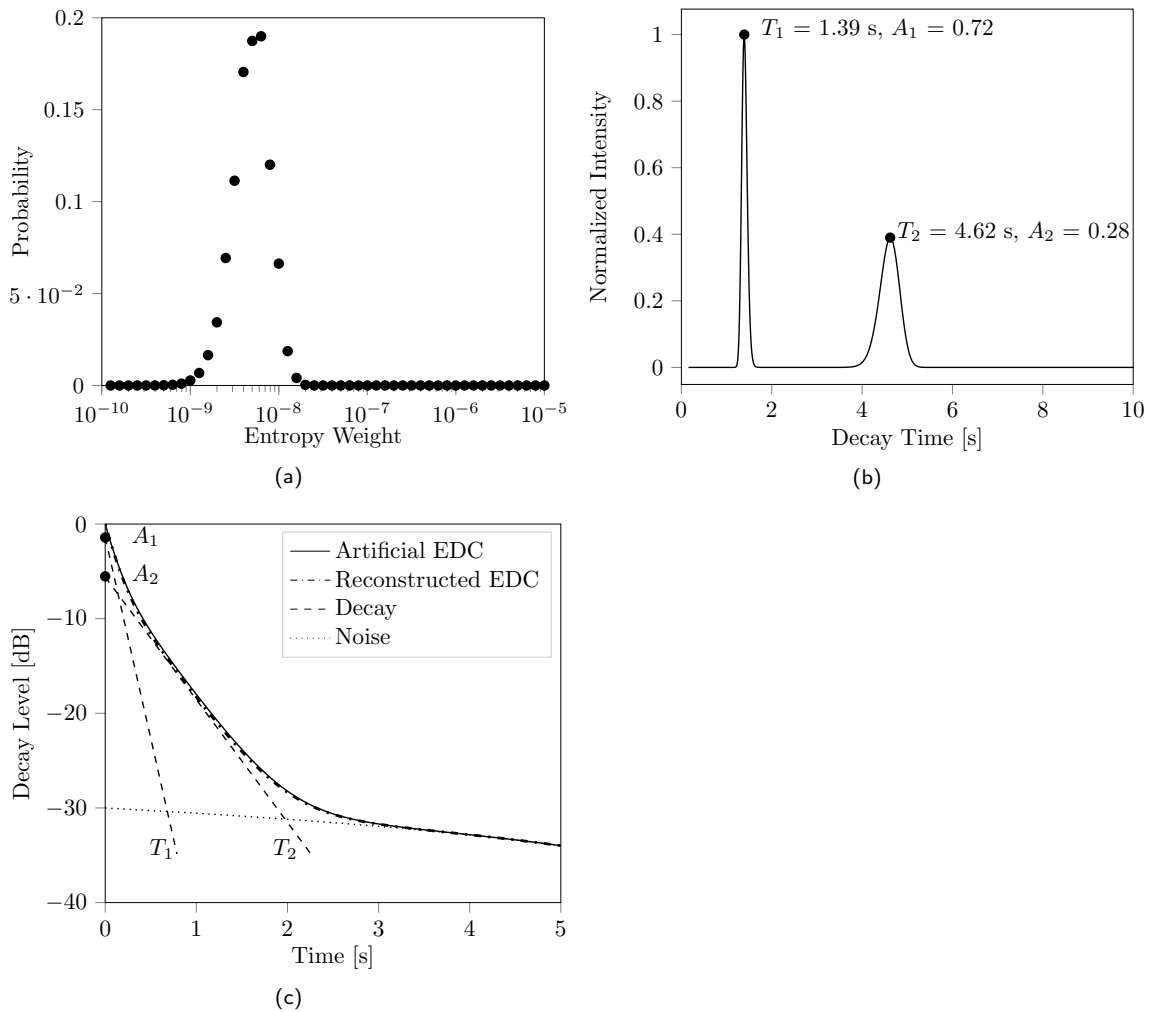


Figure 2.4: Example 1: (A) Variation of the entropy weights, (B) intensity spectrum of the estimated decay times, (C) artificial and reconstructed energy decay curve with the peaks of the intensities $A_1 = 0.72$, $A_2 = 0.28$, $T_1 = 1.39$ s and $T_2 = 4.62$ s and an additive noise term at $A_0 = 5e-9$.

In the following examples (see fig. 2.5 - 2.7) only the decay distribution and the fitted results without the variation of the entropy weights are shown. When both peaks are clearly separated with different amplitudes, already the kick-off solution gives a good estimate of the decay times. With every iteration the peaks are becoming sharper.

In example 2 the decay times are spaced closer together ($T_1 = 0.9$ s, $T_2 = 1.2$ s) and the kick-off solution starts with only one peak in the decay distribution (see fig. 2.5). With every iteration step the result is approaching two peaks, finally estimating $T_1 = 0.91$ s, $T_2 = 1.16$ s.

2 Multi-exponential decay model & Bayesian decay time estimation

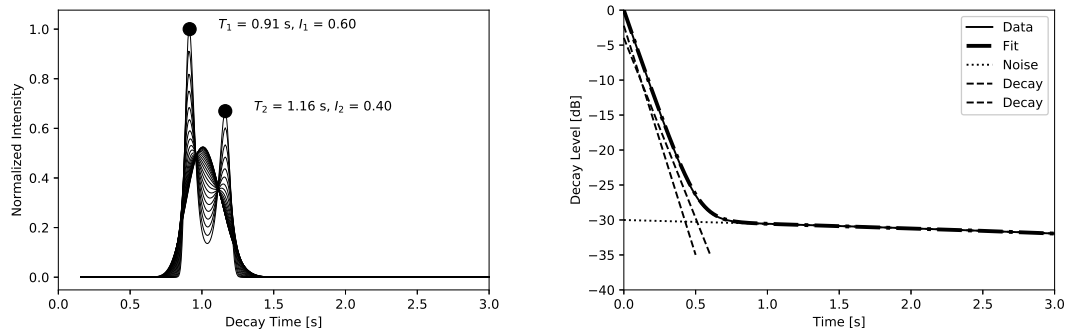


Figure 2.5: Example 2: Two distinct peaks ($T_1 = 0.9$ s, $T_2 = 1.2$ s) which are close together are estimated correctly

Example 3, shown in fig. 2.6 illustrates an EDF with three distinct decay times $T_1 = 1.3$ s, $T_2 = 2.4$ s, $T_3 = 4.8$ s with varying intensities $A_1 = 0.6$, $A_2 = 0.3$, $A_3 = 0.1$. The kick-off solution leads to a rather flat estimate with one peak, with every iteration the prominent decays are approached until the right results are displayed.

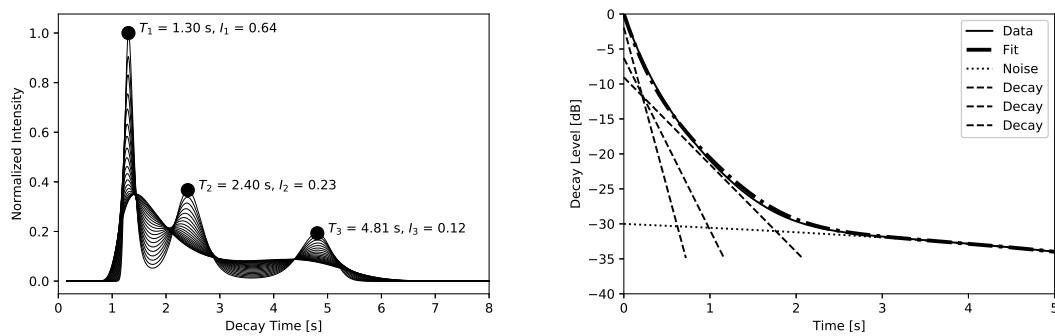


Figure 2.6: Example 3: Three peaks ($T_1 = 1.3$ s, $T_2 = 2.4$ s, $T_3 = 4.8$ s) are estimated correctly

In Example 4 the decay times are equal to Example 3 but the corresponding amplitudes are changed to the same values $A_{1,2,3} = 0.33$. In this case the estimated decay times are very sharp peaks.

In practice, if absorption is concentrated on a single surface, the room modes can be separated into two groups (more attenuated modes and less attenuated modes). [Jacobsen, 2013, Nilsson, 2004b] This is the case in the reverberation chamber, when the sample is mounted on the floor or on the wall according to ISO 354. Although diffusers redirect the sound onto the absorber, in the following chapter it is shown that two peaks are present in the energy decay. The first peak, which corresponds to the shortest decay time, can be regarded as the modes which are attenuated the most. Therefore the smallest decay time is used when calculating the absorption coefficient in the following chapter.

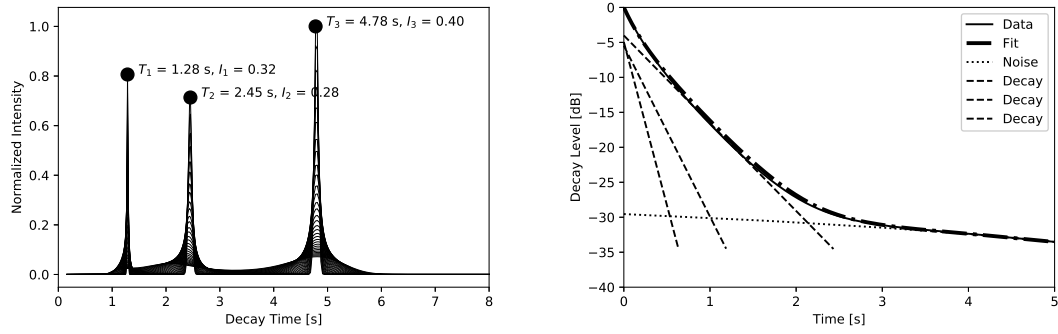


Figure 2.7: Example 4: Three peaks from Ex. 3 ($T_1 = 1.3$ s, $T_2 = 2.4$ s, $T_3 = 4.8$ s) but with different amplitudes are estimated correctly

3

Calculating the absorption coefficient



Die Gestaltung eines guten Hallraumes verlangt in der Tat etwas von der subtilen Arbeit eines Geigenbauers, der auch ein Instrument schaffen soll, das auf alle Töne möglichst gleich gut anspricht.

L. Cremer, [Cremer, 1961]

The main part of this chapter has been published previously in the *The Journal of the Acoustical Society of America* with the title *Bayesian decay time estimation in a reverberation chamber for absorption measurements*. [Balint et al., 2019] The entire journal publication is attached in Appendix A.

The Sabine absorption coefficient can be obtained from measurements in a reverberation chamber. [ISO 354, 2003] The procedure of calculating single reverberation times is based on Sabine's formula [Sabine, 1922], which assumes a diffuse sound field and an exponential energy decay. Yet, when absorption is concentrated on a single surface, the energy decay is not any more exponential but exhibits a double slope, of which the decay rates correspond to those of the grazing and non-grazing waves. [Hunt et al., 1939] This means that different reverberation times will be obtained depending on what portion of the decay function is used for the evaluation, and therefore the decay process cannot be described by a single reverberation time. [Kuttruff, 1958, Nilsson, 2004b] Consequently, absorption coefficients obtained under the conditions specified in the standard might be ambiguous. This poses a major challenge, since results obtained from measurements in the reverberation chamber should be reproducible as they form the basic input parameter for room acoustic simulation tools and acoustic design processes. Yet, numerous investigations have reported a significant problem regarding the reliability and accuracy of the reverberation chamber method. In particular, several round robin tests, in which the same sample of an absorbing material has been tested in a number of laboratories, have revealed a substantial discrepancy in the results. [Davern and Dubout, 1980, ASTM, 2006, Thysell, 2011] This could, to some extent, be attributed to the estimation of the reverberation time from multi-exponential decay functions with the linear regression method.

The measurement standard prescribes specific design criteria for reverberation chambers. [ISO 354, 2003] Especially, adding diffusing elements (in the form of panel or boundary diffusers) is expected to build up diffusion, and thus to minimize the curvature of the sound decays. However, predicting the effect of diffusing elements on the sound field in a reverberation chamber is a challenging task. The use of frameworks like the finite element, the boundary element method or geometrical acoustics simulation depend critically on the boundary conditions, which are often unknown. [Vorländer, 2013] Furthermore, geometrical acoustics simulations cannot take into account wave-based effects. [Savioja and Svensson, 2015]

Uncertainties in standardized reverberation chamber measurements are not only introduced when the absorber is concentrated on a single surface. ISO 354 further stipulates that the evaluation range shall start at 5 dB below the initial sound pressure level. Kuttruff [Kuttruff, 1958] concluded that in the case of a multi-exponential decay, the initial part of the decay contains the mean of all excited modes in the room, and therefore the most relevant information. He derived that the decay function can be seen as the Laplace transform of the damping distribution of the room modes. By calculating the first and second derivatives of the decay distribution, he concluded that the initial slope of a logarithmically plotted decay function is defined by the centroid of the distribution. Therefore the initial slope is the weighted mean

3 Calculating the absorption coefficient

of all decay constants present in the reverberation process, where the weighting function is the frequency distribution of the decay constants. However, the current evaluation procedure [ISO 354, 2003] discards the initial portion of the sound decay and therefore the accurate estimation of reverberation parameters in case of multi-exponential decays may not be possible.

The major contribution of this work is to calculate the Sabine absorption coefficient with accurate decay parameters obtained from multi-exponential energy decay functions (EDFs) measured in a reverberation chamber. In case of multi-exponential decays, a Bayesian framework is used for estimating accurate decay parameters within this investigation. The absorption coefficient is calculated with the decay time obtained from the initial part of the energy decay function. Results are compared to theoretical absorption coefficients calculated with a transfer matrix model [Allard, 1993] combined with Miki's model [Miki, 1990] and Thomasson's size correction [Thomasson, 1980].

3.1 Measurements

This section describes experimental measurements and data obtained to validate the benefit of using a maximum entropy framework for decay time estimation and absorption coefficient measurements. Absorption coefficients obtained with conventional reverberation parameters will be compared to values obtained with the maximum entropy framework. Additionally, a theoretical absorption coefficient serves as a reference value for comparison.

Measurements are carried out in a box-shaped reverberation chamber ($V = 241 \text{ m}^3$) at the Technical University of Denmark. The absorption coefficient of a porous sample is measured according to ISO 354 [ISO 354, 2003] in the chamber with 20 panel diffusers and without diffusers. The porous sample with a flow resistivity of $12.9 \text{ kPa}\cdot\text{s}/\text{m}^2$ has a total area of 10.8 m^2 ($3.6 \text{ m} \times 3.0 \text{ m} \times 0.1 \text{ m}$) and its sides are covered by a wooden frame. Figure 3.1 shows the room setup, with the porous absorber placed on the floor of the chamber and acrylic panel diffusers hung from the ceiling. Impulse responses (IR) are measured at 12 independent source-receiver positions and the EDF is calculated by Schroeder backward integration for each IR [Schroeder, 1965]. EDFs are averaged over all measurement positions to obtain a single function. Conventional reverberation parameters like the early decay time EDT , T_{20} , and T_{30} are calculated by applying linear regression to decay ranges 0 to -10 dB, -5 to -25 dB and -5 to -35 dB, respectively. The initial decay time is obtained with the proposed framework.

The equivalent absorption area A of a porous sample is calculated according to [ISO 354, 2003]:

$$A = \frac{55.3 \cdot V}{c} \cdot \left(\frac{1}{T_a} - \frac{1}{T_e} \right) - 4 \cdot V \cdot (m_a - m_e) \quad (3.1)$$

where V denotes the total volume of the chamber, c is the speed of sound, m is the attenuation coefficient, T_e is the reverberation time in the undamped chamber (empty) and T_a



Figure 3.1: Porous absorber placed on the floor in the reverberation chamber ($V = 241 \text{ m}^3$), absorber with sides covered by a wooden frame and a total area of $S = 10.8 \text{ m}^2$

is the reverberation time in the damped chamber (with the absorber). The Sabine absorption coefficient for octave bands from 125 Hz to 4000 Hz is calculated according to

$$\alpha = \frac{A}{S}, \quad (3.2)$$

where S denotes the total area of the sample.

3.2 Theoretical absorption coefficient

The random incidence absorption coefficient for an infinite absorber can be calculated as follows [Kuttruff, 2016]:

$$\alpha_{random} = \int_0^{\pi/2} \alpha_{inf}(\Theta_i) \sin(2\Theta_i) d\Theta_i, \quad (3.3)$$

where $\alpha_{inf}(\Theta_i)$ is the oblique incidence absorption coefficient at incidence angle Θ_i .

In a reverberation chamber, the measured absorption coefficient is typically overestimated due to diffraction phenomena evoked by the edges of the finite-size sample. This size-effect is particularly marked at low frequencies (below 1 kHz). A size-corrected random incidence absorption coefficient is derived by Thomasson [Thomasson, 1980] as follows,

$$\alpha_{theory} = 2 \int_0^{\pi/2} \frac{4\text{Re}(Z_s)}{|Z_s + \overline{Z_r}|^2} \sin(\Theta) d\Theta, \quad (3.4)$$

where Z_s denotes the surface impedance and $\overline{Z_r}$ the radiation impedance which is a function of shape, size, frequency and is averaged over azimuthal angles from 0 to 2π . The main assumptions are local reaction, infinite baffle, and flush-mounting of the absorber to the infinite baffle. Although the theoretical absorption coefficient is not the perfect truth, it is chosen to be a reference in this paper for the following reasons. Such a coefficient is a comprehensible comparison value as opposed to ISO results. Several round robin tests have shown large deviations in the results from chamber to chamber, hence raising serious doubts regarding

3 Calculating the absorption coefficient

the reliability of the obtained coefficients. [Davern and Dubout, 1980, ASTM, 2006, Thysell, 2011] Besides, the derivation by Thomasson makes it possible to account for the finite size of the sample and has therefore been widely used in the literature. [Jeong, 2010, Jeong, 2013, Brunskog, 2012, Brunskog, 2013]

In the following, α_{theory} in Eq. 3.4 is calculated based on a transfer matrix model for the case of a single layer of porous material with a rigid backing. [Allard, 1993] The surface impedance and complex wave number are calculated with Miki's model, [Miki, 1990] which is a modified version of the Delany and Bazley model, [Delany and Bazley, 1970] and gives improved results at low frequencies. The calculated results for the theoretical absorption coefficients are shown in Tab. 3.5.

Table 3.1: Theoretical absorption coefficient for a porous absorber with flow resistivity $\sigma = 12.9$ Pa s/m calculated with Miki's model and Thomasson's size correction

| f (Hz) | 125 | 250 | 500 | 1000 | 2000 | 4000 |
|-------------------|------|------|------|------|------|------|
| α_{theory} | 0.86 | 1.24 | 1.14 | 1.03 | 0.98 | 0.98 |

Thomasson's size-corrected absorption coefficient by Eq. 3.4 for a finite sample of 3.6 m x 3 m x 0.1 m backed by a rigid wall exceeds unity for the octave bands centered at 250 Hz, 500 Hz, and 1 kHz.

For comparison, the deviation $\Delta\alpha$ of the measured absorption coefficient from the theoretical absorption coefficient α_{theory} is calculated in the following sections with:

$$\Delta\alpha = \alpha_{theory} - \alpha, \quad (3.5)$$

where α is the Sabine absorption coefficient according to Eqs. 3.1 and 3.2 calculated with different reverberation parameters EDT , T_{20} , T_{30} and the decay time T_1 .

3.3 Linear regression

To illustrate how conventional reverberation parameters EDT , T_{20} , and T_{30} vary in case of multi-exponential data, results are shown for one frequency band. In fig. 3.2 the energy decay curve as well as the regression lines for the damped condition at 500 Hz are shown with and without panel diffusers. The reverberation times EDT , T_{20} , and T_{30} vary from 2.9 s to 3.44 s without scattering elements, indicating a multi-exponential decay due to the increase of the reverberation time when the evaluation range is increased. In the case when scattering elements are added to the room, reverberation parameters EDT , T_{20} , and T_{30} vary from 2.12 s to 2.21 s, still indicating a slightly curved decay. The reverberation time is decreased significantly compared to the case without panels, since the sound waves are redirected onto the absorber by the panels. T_{30} is decreased from 3.44 s to 2.12 s when diffusers are added, also EDT is reduced from 2.9 s to 2.12 s. The results are in agreement with investigations carried out in [Nilsson, 2004a].

To investigate how the evaluation range for reverberation parameters influences the absorption coefficient, α is calculated for $f = 500$ Hz with EDT , T_{20} , and T_{30} with and without

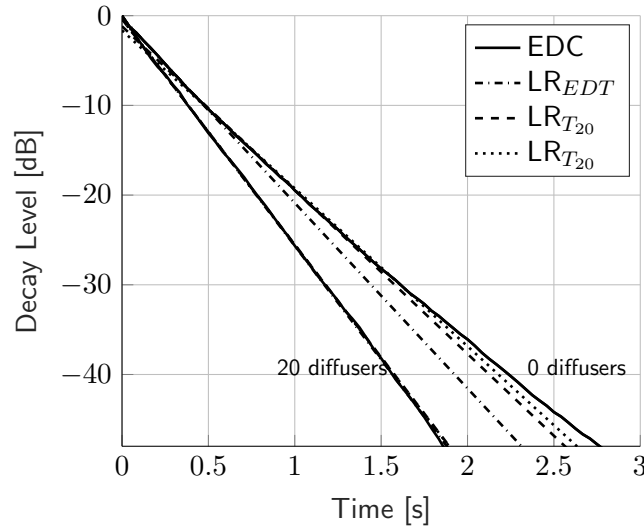


Figure 3.2: Energy decay curve EDC and linear regression LR for $f = 500$ Hz in the damped condition for room acoustic parameter without diffusers $EDT = 2.90$ s, $T_{20} = 3.29$ s, $T_{30} = 3.44$ s, and with diffusers $EDT = 2.12$ s, $T_{20} = 2.21$ s, $T_{30} = 2.21$ s.

scattering elements. Table 3.2 shows the values for the absorption coefficient calculated with EDT , T_{20} , and T_{30} . The absorption coefficient decreases when the evaluation range for decay parameters is increased. Therefore the absorption coefficient is higher when EDT is used instead of T_{20} or T_{30} . This is in agreement with [Kuttruff, 1958], where the author derives that the initial part of the EDC contains the mean of all excited modes and should be used to calculate α rather than the late part of the EDC. Furthermore the author concludes that the late part of the EDC only contains the less attenuated modes, which will lead to questionable results when used to calculate the absorption coefficient. The values vary between 0.7 and 0.86 without scattering elements and from 1.18 to 1.2 with scattering elements.

Table 3.2: Absorptions coefficient for 500 Hz calculated with different reverberation times (RT) EDT , T_{20} , T_{30} , with and without scattering elements present

| RT | EDT | T_{20} | T_{30} |
|-------------------------|-------|----------|----------|
| α / 0 diffusers | 0.86 | 0.80 | 0.7 |
| α / 20 diffusers | 1.20 | 1.18 | 1.18 |

Table 3.3 shows the absorption coefficient without any scattering elements, calculated from 125 Hz to 4 kHz with reverberation parameter T_{20} like suggested in [ISO 354, 2003]. The absorption coefficients are lower than the theoretical values in the entire frequency range. Due to the multi-exponential nature of the EDC, using linear regression to obtain T_{20} will underestimate the absorption coefficient.

Tab. 3.4 shows the reverberation times T_{20} and the absorption coefficient obtained with diffusers. In this case the absorption coefficient is increased and exceeds the theoretical values

3 Calculating the absorption coefficient

Table 3.3: Reverberation times T_{20} in the undamped (T_{empty}) and damped ($T_{absorber}$) condition, and the resulting absorption coefficient without any scattering elements installed, and deviation $\Delta\alpha$ from the theoretical absorption coefficient.

| f (Hz) | 125 | 250 | 500 | 1000 | 2000 | 4000 |
|----------------------|-------|-------|-------|------|------|------|
| $T_{20,empty}[s]$ | 18.59 | 15.04 | 12.22 | 9.84 | 6.19 | 3.69 |
| $T_{20,absorber}[s]$ | 6.79 | 3.64 | 3.29 | 3.25 | 2.83 | 2.08 |
| α | 0.37 | 0.75 | 0.80 | 0.74 | 0.70 | 0.75 |
| $\Delta\alpha$ | 0.49 | 0.49 | 0.34 | 0.29 | 0.28 | 0.23 |

at 500 Hz and above. At 250 Hz the absorption coefficient is significantly increased compared to the case without scattering elements from 0.75 to 1.03. At 125 Hz the absorption coefficient is slightly increased from 0.37 to 0.39. It is expected that the absorption coefficient increases when scattering elements are added to the chamber because the sound waves are redirected onto the absorber by the diffusers. However, at high frequencies the absorption coefficient is overestimated compared to the theoretical values, although the deviation from α_{theory} could be decreased compared to the case without diffusers in the chamber.

Table 3.4: Reverberation times T_{20} in the undamped (T_{empty}) and damped ($T_{absorber}$) condition, and the resulting absorption coefficient, with 20 panel diffusers hung from the ceiling and deviation $\Delta\alpha$ from the theoretical absorption coefficient.

| f (Hz) | 125 | 250 | 500 | 1000 | 2000 | 4000 |
|----------------------|-------|-------|-------|-------|-------|-------|
| $T_{20,empty}[s]$ | 13.93 | 13.27 | 11.12 | 9.06 | 5.82 | 2.39 |
| $T_{20,absorber}[s]$ | 5.59 | 2.77 | 2.39 | 2.37 | 2.08 | 1.62 |
| α | 0.39 | 1.03 | 1.18 | 1.12 | 1.11 | 1.16 |
| $\Delta\alpha$ | 0.47 | 0.21 | -0.04 | -0.09 | -0.13 | -0.18 |

3.4 Use of shortest decay time

The proposed Bayesian framework is applied to estimate the parameters of multiple decays instead of the linear regression as described in Ch. 2. Decay parameters are calculated for each octave band from 125 Hz to 4 kHz. In Fig. 3.3 and 3.4 the results for the decay times and intensities are plotted in the undamped (left) and damped (right) conditions without diffusing elements. In the entire frequency range two distinct peaks are detected, indicating a double slope behaviour (i.e., a multi-exponential decay).

Table 3.5 shows the obtained absorption coefficients calculated in the octave bands with Sabine's equation using the first peak from the estimated decay times in fig. 3.3 and 3.4. Good agreement between the theoretical and estimated absorption coefficients is achieved at the 250 Hz band and above. At the 125 Hz band the absorption coefficient obtained with the initial decay time is increased compared to the values obtained with T_{20} from 0.37 to 0.48. For better illustration, fig. 3.5 shows the absorption coefficient calculated with T_{20}

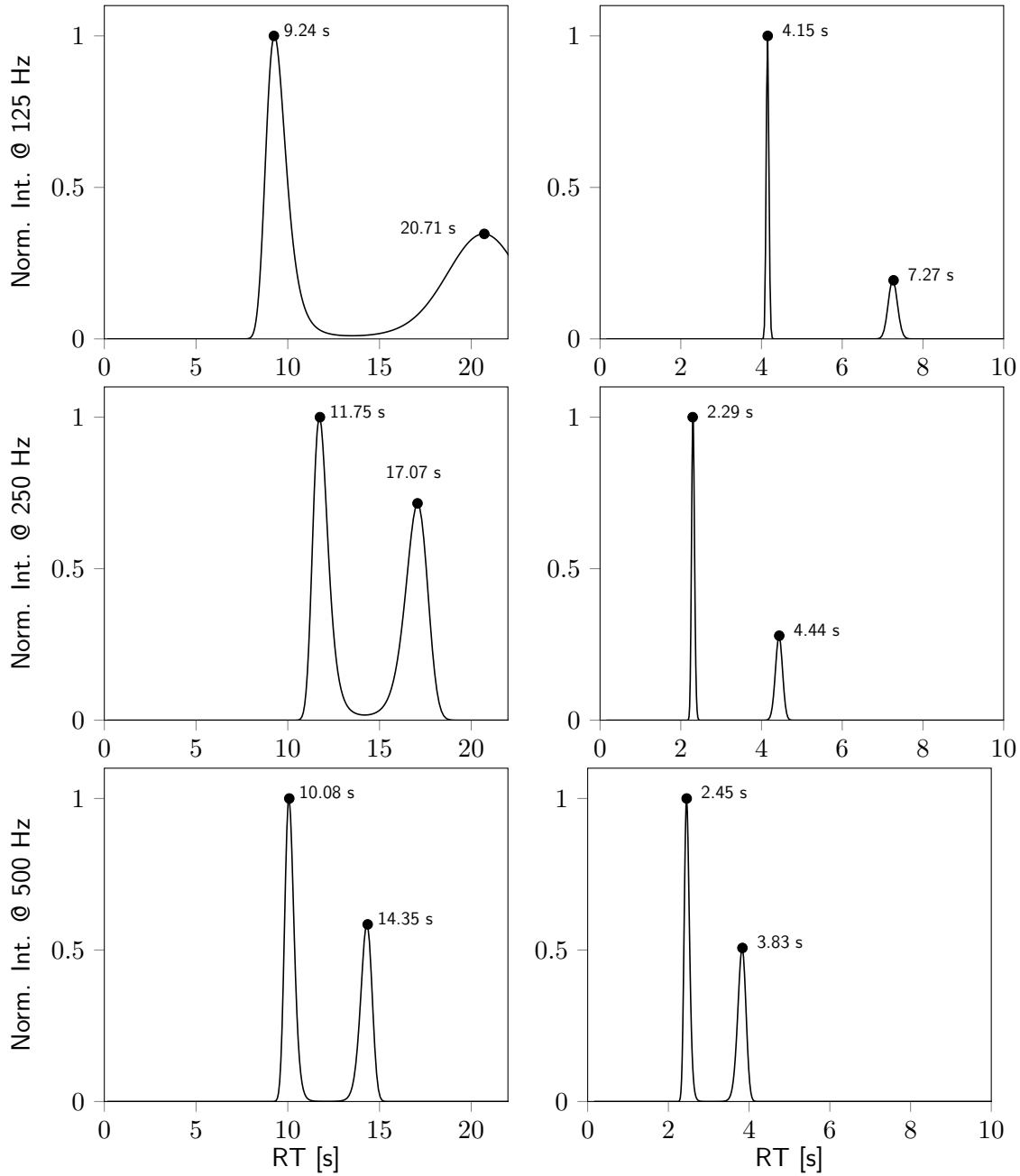


Figure 3.3: Estimated normalized intensities of reverberation times from 125 Hz to 500 Hz for undamped (left) and damped (right) conditions and the corresponding peak values of the reverberation times. The first peak corresponds to the value used for calculating the absorption coefficient.

without diffusers ($\alpha_{T_{20,0dif.}}$), with diffusers ($\alpha_{T_{20,20dif.}}$), calculated with the initial decay time without diffusers (α_{T_1}) and the theoretical value (α_{theory}). Although no diffusers are present, the absorption coefficients obtained with the initial decay time estimated with the proposed method are in very good agreement with α_{theory} above the 250 Hz band. The absorption coefficient obtained with T_{20} without diffusers is underestimated compared to the other values in the entire frequency range. With diffusers the absorption coefficient at the 500 Hz band

3 Calculating the absorption coefficient

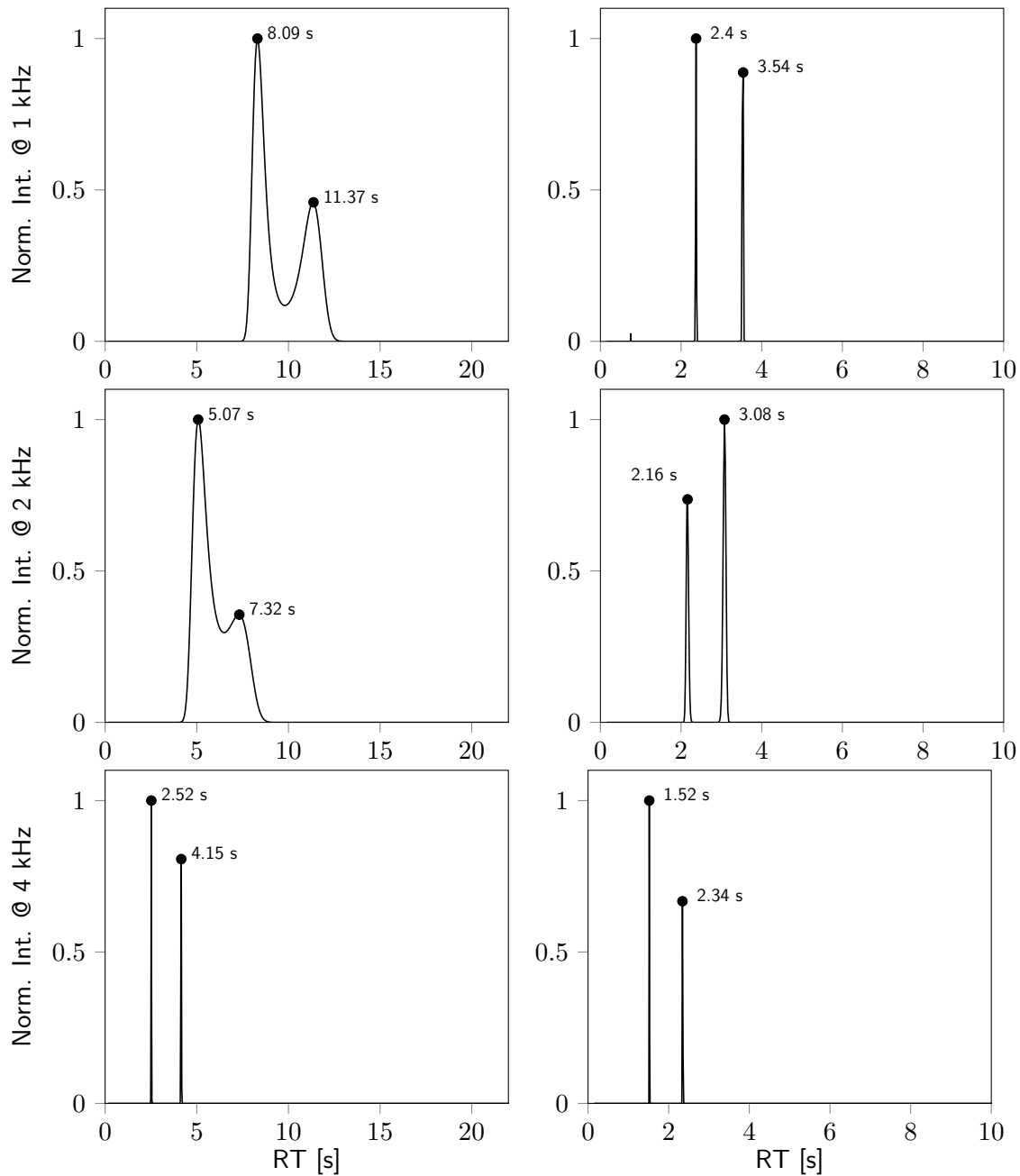


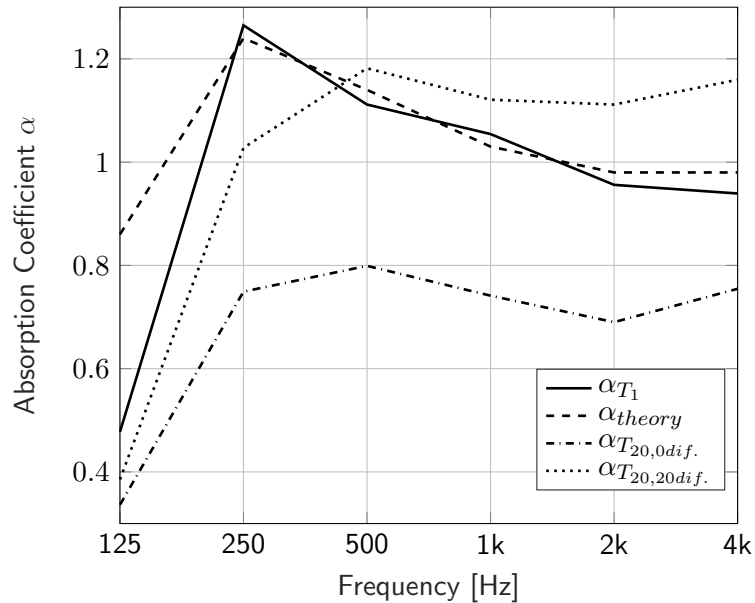
Figure 3.4: Estimated normalized intensities of reverberation times from 1000 Hz to 4000 Hz for undamped (left) and damped (right) conditions and the corresponding peak values of the reverberation times. The first peak corresponds to the value used for calculating the absorption coefficient.

and above is overestimated compared to the theoretical absorption coefficient.

In Tab. 3.6 the relative error between the theoretical absorption coefficient and the calculated absorption coefficients with and without diffusing objects is summarized. The smallest deviation from α_{theory} is obtained with absorption coefficients α_{T_1} calculated with the initial decay time with the proposed framework. The error between α_{T_1} and α_{theory} above the 250

Table 3.5: Initial decay times in the undamped (T_{empty}) and damped ($T_{absorber}$) condition, resulting absorption coefficient α and deviation $\Delta\alpha$.

| f (Hz) | 125 | 250 | 500 | 1000 | 2000 | 4000 |
|--------------------|------|-------|-------|------|------|------|
| T_{empty} [s] | 9.24 | 11.75 | 10.08 | 8.09 | 5.07 | 2.52 |
| $T_{absorber}$ [s] | 4.15 | 2.29 | 2.45 | 2.4 | 2.16 | 1.52 |
| α | 0.48 | 1.26 | 1.11 | 1.05 | 0.93 | 0.94 |
| $\Delta\alpha$ | 0.38 | -0.02 | 0.03 | 0.02 | 0.05 | 0.04 |

Figure 3.5: Absorption coefficient α_{T_1} calculated with the shortest decay time compared to α_{theory} , $\alpha_{T_{20},0dif.}$ and $\alpha_{T_{20},20dif.}$.

Hz band is less than 5%. At the 125 Hz band the theoretical absorption coefficient exceeds the measured value. The deviation at 125 Hz could be due to the fact that the theoretical absorption coefficient is calculated for all angles of incidence, whereas in the reverberation chamber it cannot be assumed that below the Schroeder frequency the incident sound on the absorber is uniformly distributed over all possible directions.

Table 3.6: Relative error ε_α from the theoretical absorption coefficient in %. Absorption coefficient calculated with reverberation parameter T_{20} without (0 dif.) and with (20 dif.) diffusers, as well as with the initial reverberation time T_1 without (0 dif.) diffusers.

| f (Hz) | 125 | 250 | 500 | 1000 | 2000 | 4000 |
|--|-------|-------|-------|-------|-------|-------|
| $\varepsilon_{\alpha_{T_{20},0dif.}}$ [%] | 56.98 | 39.52 | 29.82 | 28.16 | 28.57 | 23.47 |
| $\varepsilon_{\alpha_{T_{20},20dif.}}$ [%] | 54.65 | 16.94 | 3.51 | 8.73 | 13.27 | 26.53 |
| $\varepsilon_{\alpha_{T_1,0dif.}}$ [%] | 44.19 | 1.61 | 2.63 | 1.94 | 5.01 | 4.08 |

3.5 Discussion

In this study, measurements are conducted in a box-shaped reverberation chamber with absorption concentrated on one of its walls, separating the room modes into two groups [Hunt et al., 1939, Jacobsen, 2013] (fast decaying and slow decaying), and thus provides a tractable environment to validate the methodology. Note however that additional mode groups (and therefore, additional decay times) can be considered to achieve higher accuracy, or in more complex environments (chambers with non-parallel walls).

It is widely accepted that without diffusing objects the sound field is not sufficiently diffuse to calculate the Sabine absorption coefficient. The results of this investigation indicate that reasonable absorption coefficients can be estimated without diffusing elements, if the initial decay time is used, which is calculated via the Bayesian framework. This means that the initial part of the decay process contains valuable information that should not be neglected. Care has to be taken at low frequencies, where the geometry of the room and the modal distribution have a great impact on the measured absorption coefficient. In practice, it cannot be assumed that the incident sound on the absorber is uniformly distributed over all possible directions. Therefore the measurement results in chambers of different volumes will differ from each other, depending on the modal distribution and the placement of the sample.

Predicting the influence of diffusing elements on the decay process is a very challenging task. Although it can be assumed that through the use of diffusers the grazing and non-grazing sound fields will be less distinct, the effect of adding diffusers seems to vary over the frequency range. When diffusing elements are introduced, the decay process can be regarded almost linear when plotted on a logarithmic axis at mid and high frequencies, when an absorber is placed on the floor. However, the absorption coefficient is still underestimated in the low frequency range and overestimated in the mid and high frequency range compared to the theoretical absorption coefficient. In this investigation installing diffusers did not provide a solution to obtain reasonable absorption coefficients. As already mentioned in the beginning, other researchers pointed out that diffusing elements introduce uncertainties that cannot be considered or modelled in an accurate way. [Hunt et al., 1939]

Schultz claims that *until we cannot measure diffusion, we will take the extravagant route of trying to provide our test room with all the diffusion we can* [Schultz, 1971]. The author was referring to the many boundary and panel diffusers that are installed in such chambers. It seems that until today this statement is valid and installing many diffusers in laboratories is very common; without improving the interlaboratory reproducibility unfortunately, as many round robin tests in the past have shown [Vercammen, 2010]. In Tab. 3.7 data from 22 reverberation chambers are shown. It demonstrates the variety of sizes, applied measurement techniques and equipment. Maybe the trend should be reversed and instead of building complex oblique-angled laboratories with countless diffusers and irregular shapes, room geometries should be as simple as possible (rectangular). If reverberation parameters are obtained accurately in first place, maybe the question will not be anymore if the sound field is sufficiently

diffuse or not and the mystery of obtaining a *reasonable absorption coefficient* might not be as impossible anymore as it always seemed to be [Cremer, 1961]. Furthermore, installing scattering elements in various sizes in a random manner cannot guarantee a uniform distribution of sound incidence on the sample, nor can it guarantee a linear decay in the chamber.

It is important to point out that this work does not deal with the curvature of decays as a diffuseness measure, since the impulse responses used for the analysis were measured with an omnidirectional microphone which does not contain any directional information of the sound field. Recent work [Berzborn and Vorländer, 2018] focuses on directional energy decay functions as a diffuseness measure. The quantification of the isotropy of the sound field is investigated in [Nolan et al., 2018]. An overview of various diffuseness measures has been given in [Jeong et al., 2018] with considerations on how data and code could be shared in the future for inter-chamber comparisons. Furthermore, this work does not deal with the quantification of double slopes like in [Bradley and Wang, 2009], where ratios were calculated using linear fits with fixed ranges. Those methods are a rough estimation of whether or not a multi-exponential decay is present but they do not provide a solution to calculate accurate decay parameters.

Table 3.7: Data from 22 chambers.

| | |
|------------------------------------|---|
| chamber volume | 123 - 393 m ³ |
| Schröder frequency | 260 - 512 Hz |
| number of diffusers | 1 - 19 |
| size of diffusers | 0.8 - 24 m ² |
| parameter for RT: # chambers | T_{20} : 16 T_{30} : 3 T_{40} : 1 n/s: 2 |
| EDC verifiable | yes: 20 no: 2 |
| interrupted noise method | 19 |
| impulse response method | 3 |

This work has discussed the use of the initial decay time to calculate the absorption coefficient from measurements conducted in the reverberation chamber. Initial decay times as well as multiple decay parameters were estimated with a Bayesian framework from energy decay functions. The need for such a framework to estimate decay parameters from multiple sloped decays as an alternative to linear regression has been argued with the fact that energy decays are not linear in most real world scenarios, especially in reverberation chambers at low frequencies and with uneven distribution of absorption.

Absorption coefficients calculated with the initial decay time were compared to the theoretical absorption coefficients calculated with a transfer matrix model combined with Miki's

3 Calculating the absorption coefficient

model including Thomasson's size correction. Good agreement was achieved in the frequency range from the 250 Hz band and above. In the 125 Hz band the theoretical absorption coefficient exceeded the calculated values due to the assumption of the sound incidence being uniformly distributed over all possible directions, which is not the case in the reverberation chamber. The results presented in this work included measurements without diffusing objects like panel or boundary diffusers, which is in contrast to the well-established approach in the reverberation chamber. The effect of diffusers on the decay process and on the sound field in general still poses a challenging task and such analysis is beyond the scope of this work.

Many round robin tests in the past have proven the poor interlaboratory reproducibility of absorption coefficient measurements. This work raises the question, if the poor reproducibility is to be owed to the evaluation of the decay parameters with linear regression. If a multi-exponential decay is present, using linear regression to obtain decay parameters will lead to questionable results. A future round robin test could evaluate if the method proposed in this paper provides a reliable alternative for measuring the Sabine absorption coefficient in reverberation chambers. The proposed Bayesian method to obtain decay parameters is not restricted to laboratories. It is anticipated that the framework may also find important applications in measuring representative decay parameters in small and mid sized room (e.g. in classrooms or offices, where absorption is concentrated on the ceiling).

4

Experimental investigation of absorber placement



The main part of this chapter has been published previously in the Proceedings of the 23rd Int. Congress on Acoustics, Aachen with the title *The effect of absorber placement on absorption coefficients obtained from reverberation chamber measurements* [Balint and Muralter, 2019]. A discussion and further analysis have been carried out to complement the measurements.

4.1 Absorber placement

This work investigates the influence of the placement of absorbers in a reverberation chamber on the decay rates. The typical test situation according to ISO 354 [ISO 354, 2003] renders the establishment of a diffuse sound field rather difficult because the absorber is placed on a single surface of the chamber. Although diffusing elements like boundary or panel diffusers prove to be very useful in increasing the sound field diffusivity and redirecting the sound onto the absorber, the optimum state of diffusion is rather ambiguous [Bradley et al., 2014]. The use of Sabine's reverberation formula to calculate the absorption coefficient requires a diffuse sound field and an even distribution of absorption in the room. Investigations on the dependence of decay rates on the wall diffusion have been carried out in [Kuttruff and Straßen, 1980], where the author simulated sound decays for various conditions. Simulation results showed that the placement of the absorber on three walls perpendicular to each other provides a test setup in which the decay rates are less sensitive to the state of diffusion than in the case when the absorber is placed on a single wall. Less sensitive means in this case that the decay rates don't change with the state of diffusion and that the energy decay curves are linear, when plotted on a logarithmic axis. Yet, splitting the absorber apart and placing it on three different walls most likely increases the edge diffraction of the absorber. Besides, the energy density in room edges is higher than far away from the walls, which can lead to an increased absorption coefficient at low frequencies. In 1969 Kuttruff investigated the new method from Schroeder to calculate the reverberation time and concluded that the the new method, although much more revealing, points to more open questions than leading to answers [Kuttruff and Jusofie, 1969]. He investigated several sound decays and found out that in many cases the sound decay measured in a reverberation chamber is curved (which was not so obvious before, when the decay was measured with the interrupted noise method). Furthermore he concluded that it would be simply pointless to try to estimate the reverberation time in chambers for absorption coefficient measurements if curved decays are present, therefore they should be eliminated from the analysis. Despite those difficulties, the question remains if an improved absorber placement can lead to more reliable measurements in the reverberation chamber. For the past decades multiple round robin test have pointed out the poor interlaboratory reproducibility of absorption coefficient measurements as mentioned in the introduction.

The aim of this investigation is to analyse five different absorber placements and the influence of three different diffuse field conditions (0, 6, and 20 panel diffusers) on the decay rates experimentally. Measurements are carried out in a rectangular reverberation chamber and impulse responses are measured when the absorber is placed in a typical testing situation as well as split apart and spread in the edges of the room. The amount of diffusion is varied by changing the number of panel diffusers in the chamber.

4.2 Measurements

Measurements are carried out in a box-shaped reverberation chamber ($V = 241 \text{ m}^3$) at the Technical University of Denmark in Lyngby. The box-shape is chosen to compare a sound field

with the least amount of diffusion (where no panel diffusers are installed) to a configuration with increased diffusion with six additional panel diffusers and to a configuration which complies with the current standard [ISO 354, 2003] for absorption measurements (with 20 panel diffusers randomly hung from the ceiling). Figure 4.1 shows the empty chamber as well as five different mounting setups. The setup 'Iso' corresponds to the typical test situation according to ISO 354, where the absorber ($S = 3 \text{ m} \times 3.6 \text{ m} = 10.8 \text{ m}^2$) is placed on the floor with covered side walls. Then the absorber is split apart into three patches (each $S = 1.2 \text{ m} \times 3 \text{ m} = 3.6 \text{ m}^2$, setup 'Split'), which results in an increased edge length. In the next step the three patches are distributed on the floor in the room edges, as shown by setup '1D'. In the next configuration '2D', one of the patches is set upright, so that only two patches remain on the floor. The last setup '3D' shows the three patches distributed on three different walls. Measurement setups were developed during discussions together with Jonas Brunskog and Cheol-Ho Jeong.

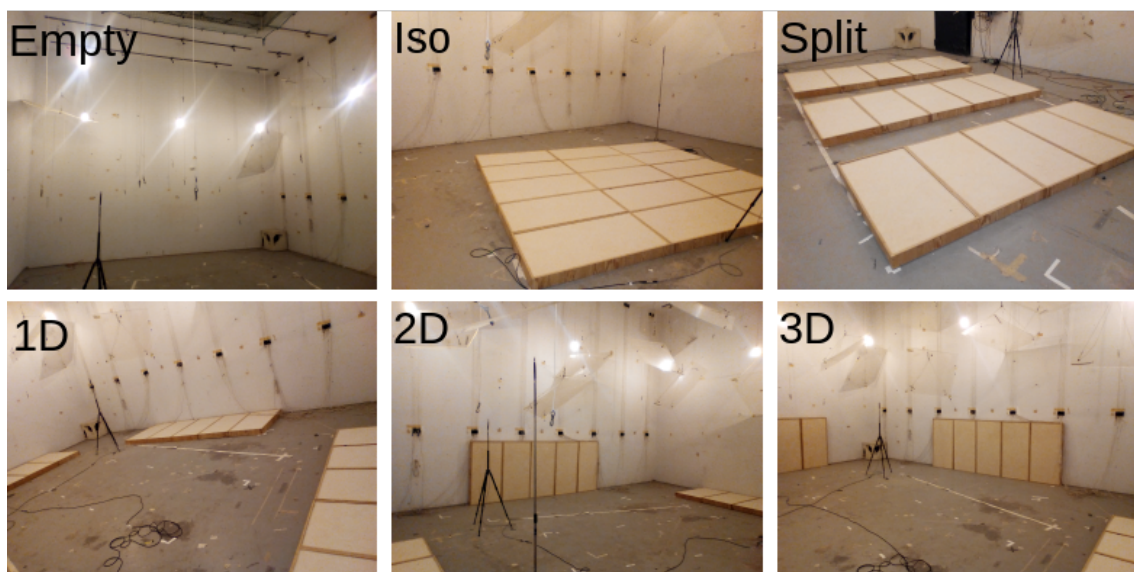


Figure 4.1: Measurement setup, empty chamber and five different configurations of absorber placements.

Impulse responses are measured at twelve independent source receiver positions and energy decay curves are calculated by applying the Schroeder backwards integration to the squared impulse response. Twelve energy decay curves are averaged to obtain a single decay curve.

Figure 4.2 shows the energy decay curves of the empty chamber without the absorber for the octave bands from 125 Hz to 4 kHz for three different diffusers setups (0, 6, and 20 panel diffusers randomly hung from the ceiling). The dotted line shows a linear decay, which indicates if the decay curves are bent when plotted on a logarithmic axis. At low and high frequencies (125 Hz, 250 Hz, 2 kHz, 4 kHz) the energy decay curves are bent, independent from the amount of diffusers installed. At 500 Hz and 1 kHz the energy decay curves are mostly linear, independent from the amount of panel diffusers. With increasing number of diffusers, the decay rates decrease at all frequency bands. Figure 4.3 shows the energy decay curves of the setup 'Iso', where the absorber is placed on the floor according to ISO 354. At 125 Hz, 250 Hz, and 4 kHz the energy decay curves are bent, independent from the amount

4 Experimental investigation of absorber placement

of diffusers installed. At 500 Hz, 1 kHz and 2 kHz the energy decay curves are mostly linear when the amount of diffusers is increased. With increasing number of diffusers, the decay rates decrease at all frequency bands.

Figure 4.4 shows the energy decay curves of the setup 'Split', where the absorber is split into three patches and placed in the middle of the floor. The characteristics of the energy decay curves are similar to the setup 'Iso', but the decay rates are decreased when the absorber is split apart. Figure 4.5 shows the energy decay curves of the setup '1D', where the absorber is distributed on the floor in the edges of the chamber. The characteristics of the energy decay curves are similar to the previous setups. At low frequencies the curves are bent but at 250 Hz the initial decay seem to be less dependent on the amount of diffusers installed. Figures 4.6 and 4.7 show the setups '2D' and '3D', where the three patches are distributed on two and three walls respectively. Again, the decay curves behave similarly. At low frequencies the decay curves are still bent.

In fig. 4.8 to fig. 4.10 different absorber setups are compared for each frequency band and diffuser state. In all configuration the setup '3D' results in the lowest decay rates. Even at high frequencies the decay rates can be decreased when the absorber is distributed on three walls.

4.2.1 Difficulties with comparing absorber setups

The boundary effects due to the increased energy density at the rigid wall, usually referred to as 'Waterhouse effect' [Waterhouse, 1955], takes into consideration that the square of the sound pressure amplitude in front of a rigid wall exceeds its value far from the wall. The same holds for the energy absorbed per unit time and area by the test specimen which perpendicularly adjoins the wall. To account for this effect, the geometrical area S of a test specimen can be corrected with [Kuttruff, 2016]:

$$S_{eff} = S + \frac{1}{8} \cdot L' \cdot \lambda, \quad (4.1)$$

where λ is the wavelength corresponding to the centre frequency of the selected band, L' is the length of the edges adjacent to perpendicular walls. When the absorber patches in this investigation are split into three parts and distributed in the room edges, as it is done in configurations '1D', '2D', and '3D', the total length corresponding to L' is 9 m. The corrected geometrical area is shown in tab. 4.1, where the effect is most prominent at low frequencies.

Table 4.1: Correction of the geometrical area of the specimen ($S = 10.8 \text{ m}^2$) due to the placement in the room edges.

| | 125 Hz | 250 Hz | 500 Hz | 1000 Hz | 2000 Hz | 4000 Hz |
|------------------------|--------|--------|--------|---------|---------|---------|
| $S_{eff} [\text{m}^2]$ | 13.9 | 12.3 | 11.3 | 11.2 | 11.0 | 10.9 |

Another difficulty to deal with, is the finite size of the sample and the diffraction of sound at the edges of the absorber, which can lead to an increase in absorption at certain frequencies. To

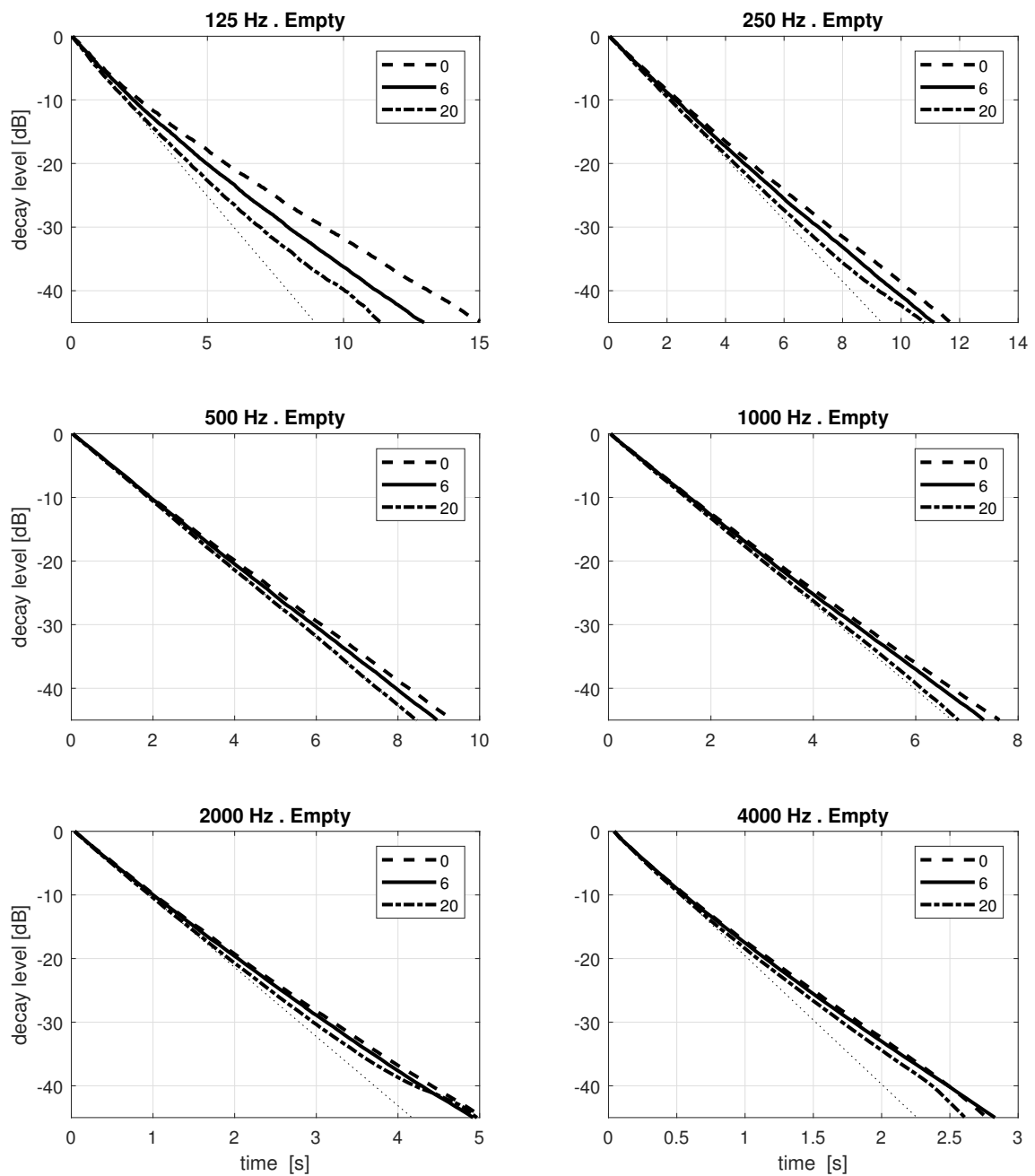


Figure 4.2: Comparison of energy decay curves in the empty reverberation chamber without the absorber. The amount of diffusers is varied between 0, 6 and 20 panel diffusers randomly hung from the ceiling. The dotted line indicates a linear decay.

4 Experimental investigation of absorber placement

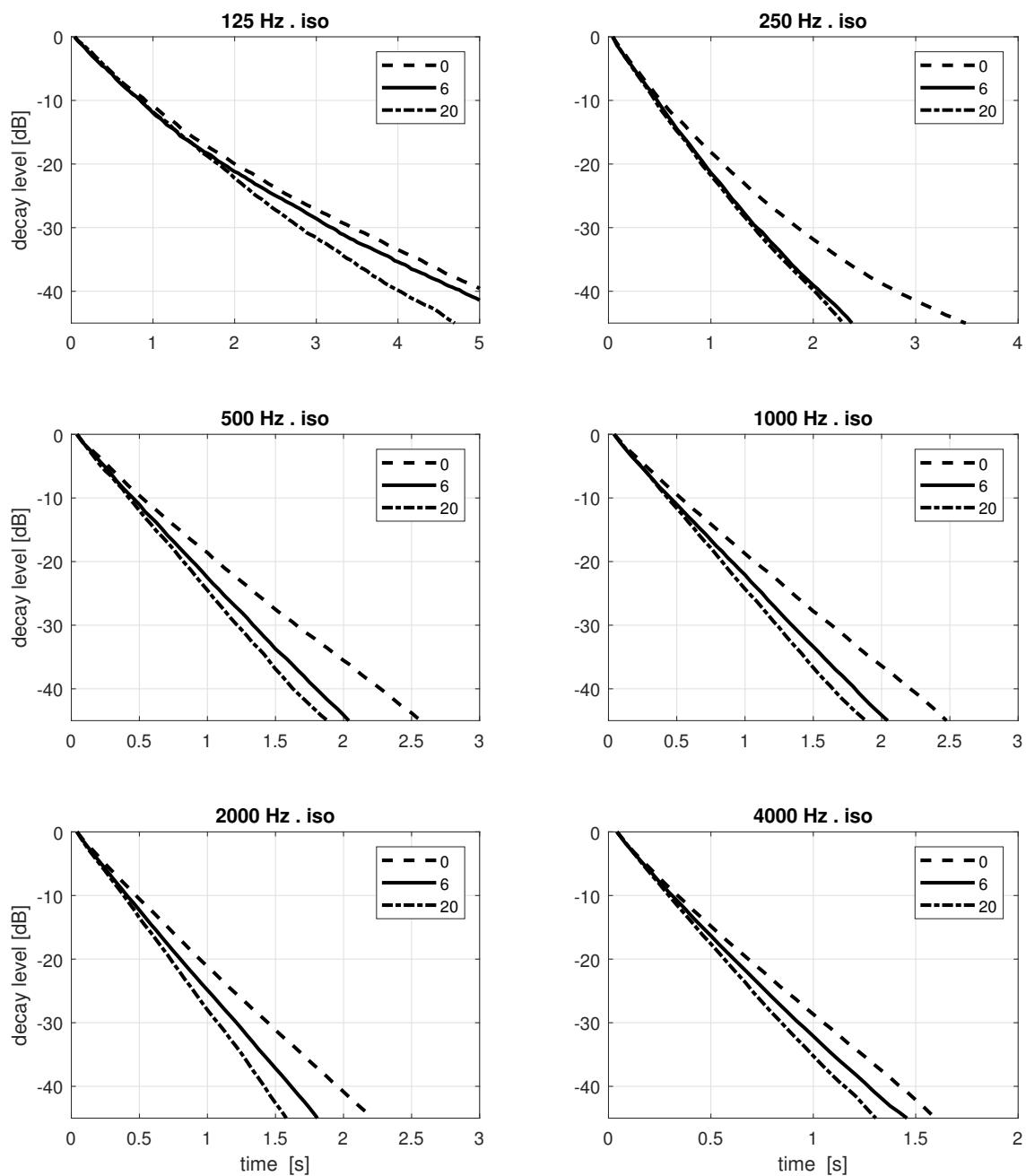


Figure 4.3: Comparison of energy decay curves at setup 'Iso'. The amount of diffusers is varied between 0, 6 and 20 panel diffusers randomly hung from the ceiling.

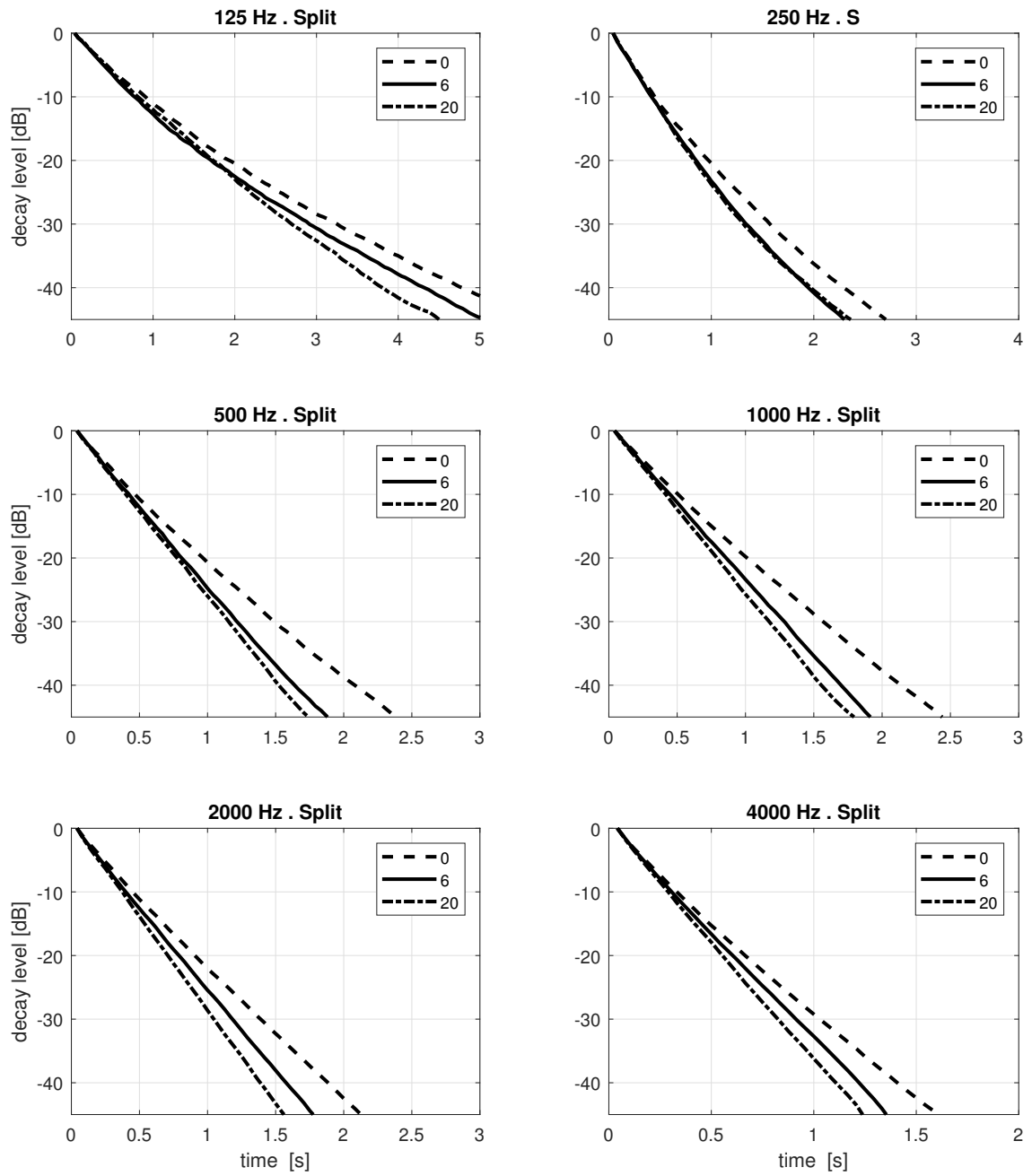


Figure 4.4: Comparison of energy decay curves at setup 'Split'. The amount of diffusers is varied between 0, 6 and 20 panel diffusers randomly hung from the ceiling.

4 Experimental investigation of absorber placement

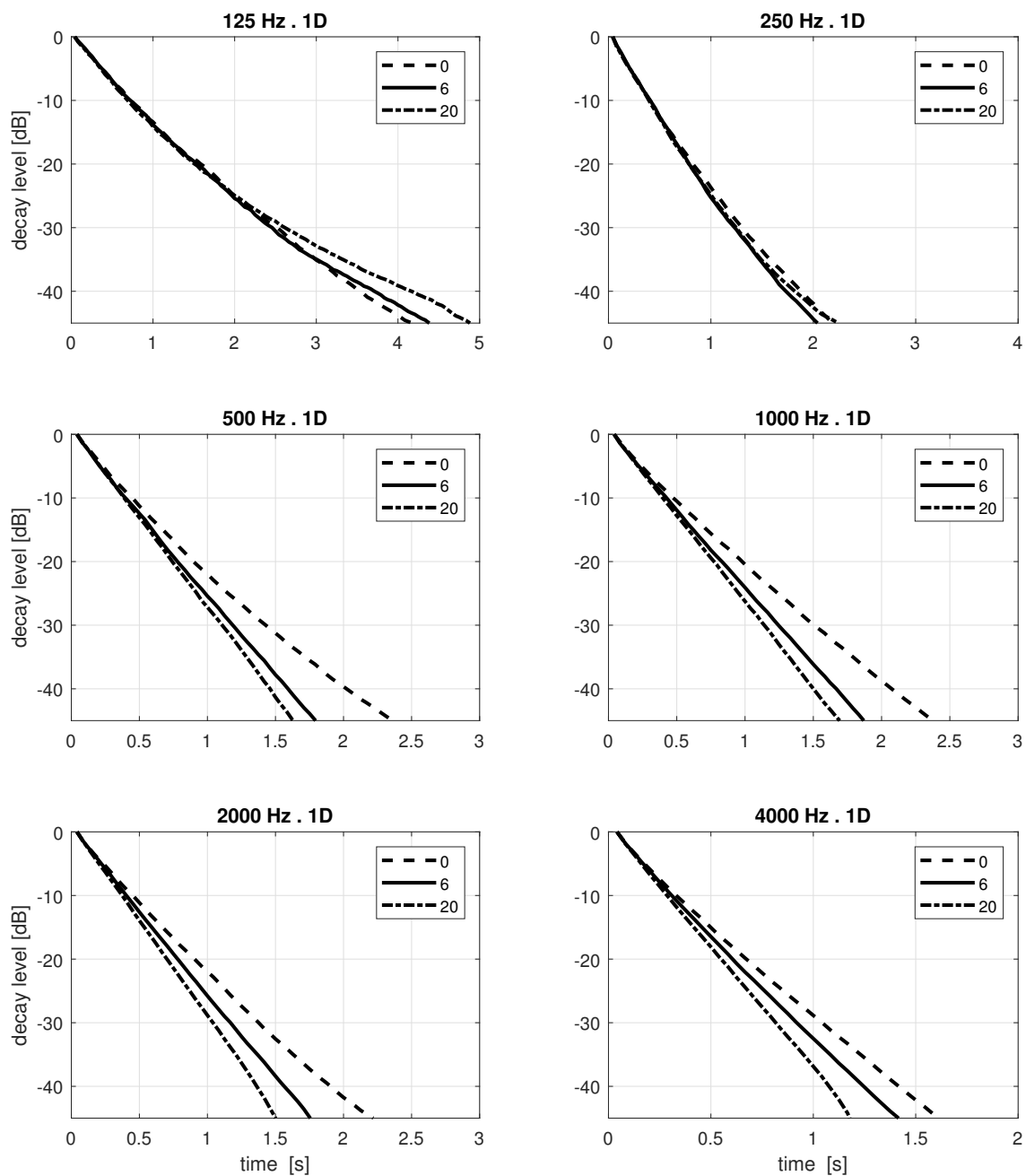


Figure 4.5: Comparison of energy decay curves at setup '1D'. The amount of diffusers is varied between 0, 6 and 20 panel diffusers randomly hung from the ceiling.

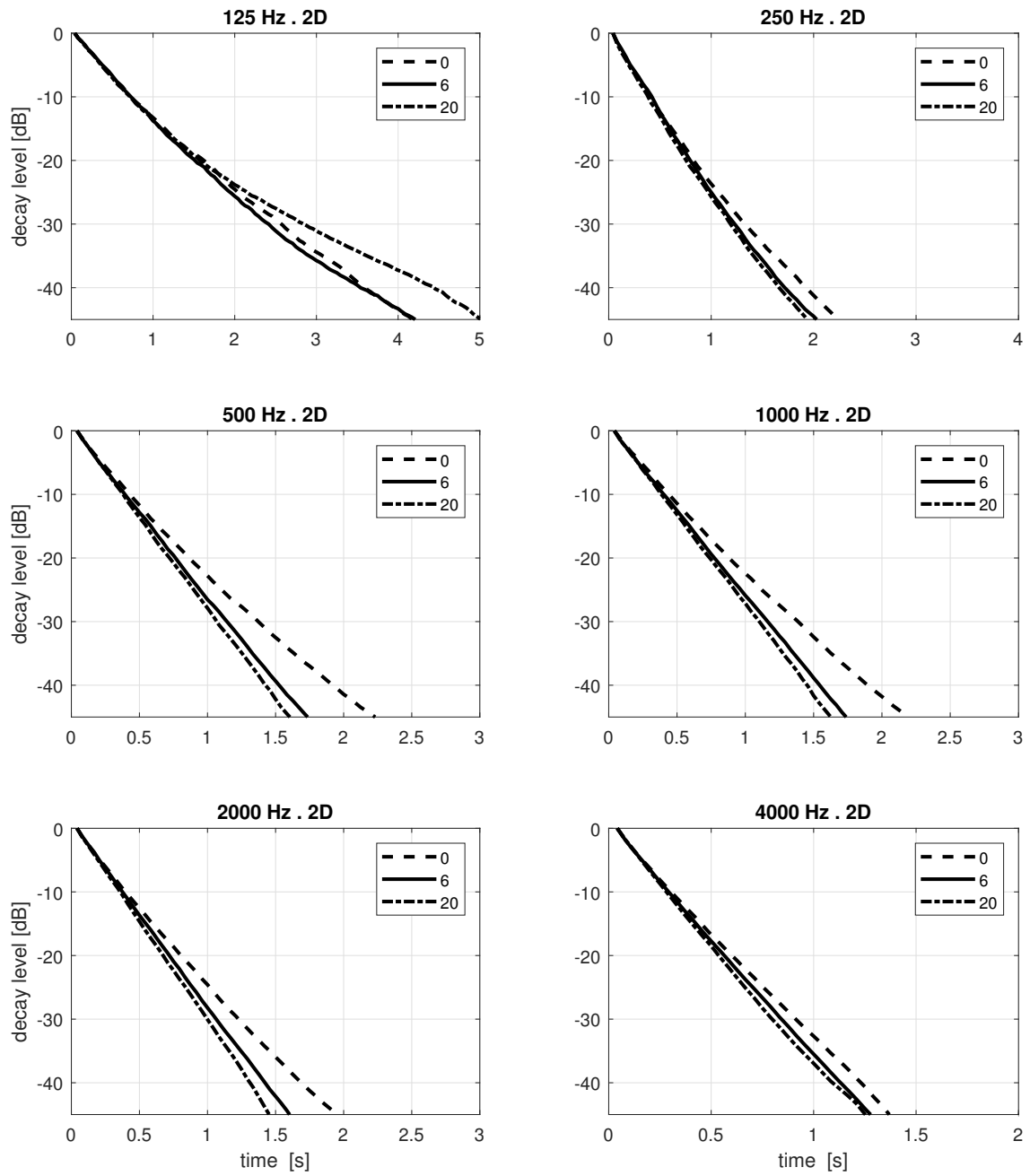


Figure 4.6: Comparison of energy decay curves at setup '2D'. The amount of diffusers is varied between 0, 6 and 20 panel diffusers randomly hung from the ceiling.

4 Experimental investigation of absorber placement

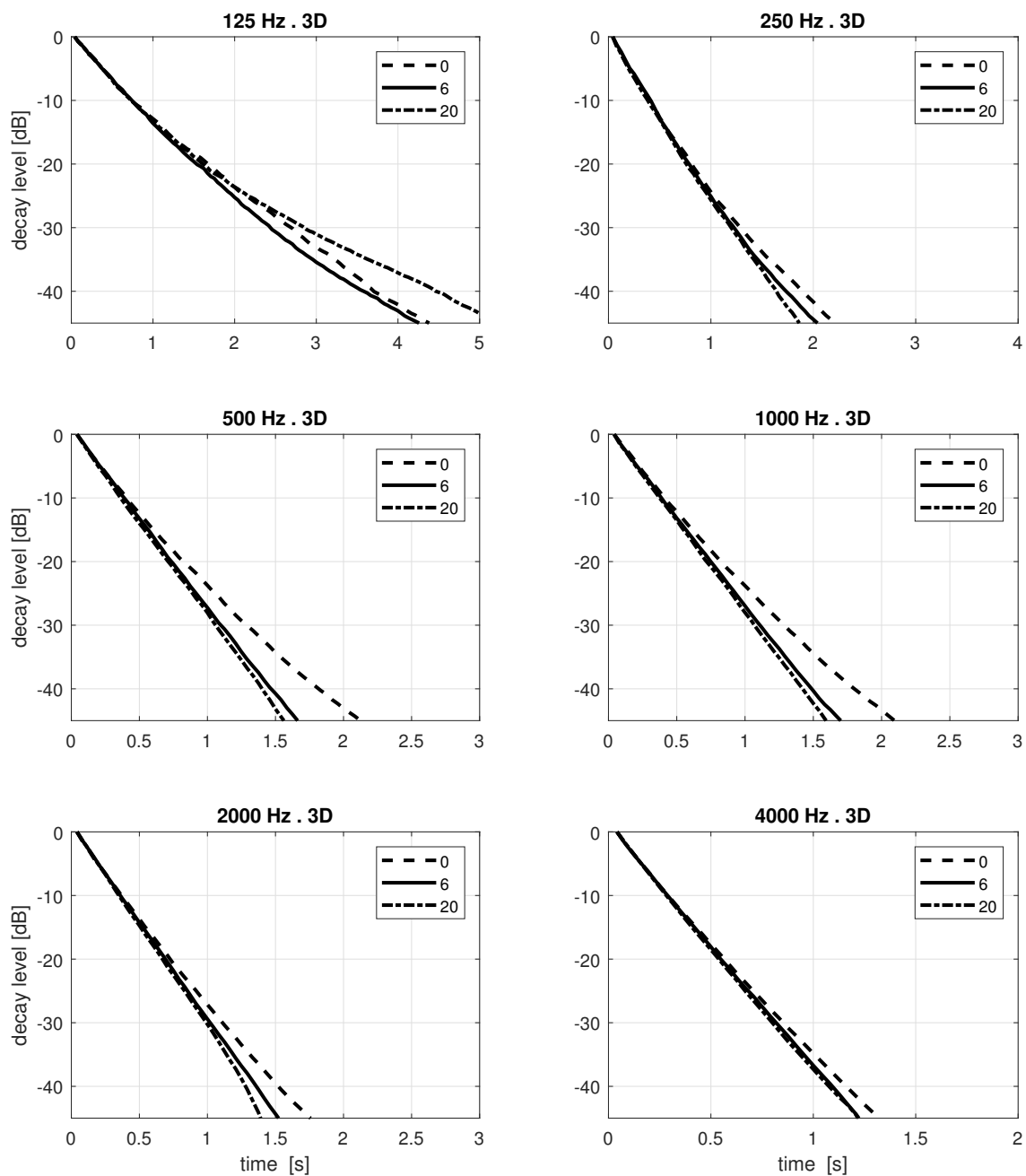


Figure 4.7: Comparison of energy decay curves at setup '3D'. The amount of diffusers is varied between 0, 6 and 20 panel diffusers randomly hung from the ceiling.

account for the finite size of the sample, Thomasson derived a theoretical absorption coefficient which depends on absorber shape, size, and frequency [Thomasson, 1980]. The size correction holds for an absorber which is mounted on an infinite rigid baffle, which cannot be applied if the absorber is placed in the room edges.

4.2.2 Evaluation of decay parameter

As apparent from fig. 4.2 to fig. 4.7, at 125 Hz and 250 Hz the energy decay curves are always bent, even in the empty reverberation chamber. No absorber placement or diffuser setup leads to a straight decay when plotted on a logarithmic axis. Evaluating reverberation parameter T_{20} , as it is required according to ISO 354, leads to questionable results in this case. Therefore it does not seem very rewarding to calculate absorption coefficients for low frequencies with the conventional method. As suggested in [Xiang et al., 2011], if a decay is multiple sloped, a different framework has to be used to calculate decay parameter. For coupled rooms, a Bayesian framework was introduced to estimate multiple decay parameter. In case of a double sloped decay, two decay times could be estimated, namely an initial and a late decay time. For calculating the absorption coefficient, it would be reasonable to take the initial decay time. [Kuttruff, 1958]

The lowest decay rates can be achieved with absorber setup '3D' and 20 panel diffusers, as shown in figs. 4.8 - 4.10 for all frequency bands. Although it requires to split the absorber apart, fig. 4.7 shows that it provides the setup where the initial part of the energy decay seems to be less sensitive to the state of diffusion compared to the typical test situation according to ISO 354. Furthermore, the boundary effects can be corrected according to eq. 4.1, where the geometrical area of the absorber is replaced with the effective area S_{eff} .

In almost every case the shortest decay rates can be achieved when 20 panel diffusers are randomly hung from the ceiling. Although it is expected that this allows for a more uniform distribution of sound incidence on the absorber, additional investigations should be carried out which allow for experimentally characterizing the distribution of sound incidence [Nolan et al., 2019].

Figures 4.11 - 4.13 show the equivalent absorption area A of the setup ISO. It is calculated with the decay parameters EDT , T_{20} , and T_1 (initial decay time calculated with the Bayesian framework described in Ch. 2) for the state when 0 and 20 diffusers are installed. The difference between A in the two states of diffusion is large when calculated with the conventional parameters EDT and T_{20} compared to the case when it is calculated with T_1 . The equivalent absorption area is higher when calculated with EDT compared to T_{20} indicating that EDT is shorter than T_{20} . When no diffusers are installed, the highest values for A can be achieved when calculated with T_1 .

4.3 Discussion

This work investigated different absorber placements and its effect on the decay process in a reverberation chamber. Measurement results suggest that at low frequencies, namely 125 Hz and 250 Hz the energy decay curves are multiple sloped with any absorber placement and diffuser configuration. Also at 4 kHz the energy decays are bent, even when diffusers are installed. At mid frequencies, adding diffusers resulted in many cases in a linear decay, although sometimes already a low number of diffusers was sufficient to produce a linear decay. Regarding absorber placement, spreading the test material on three walls resulted in the lowest decay rates. Also, measurement results suggest that if the absorber is spread on three walls, the initial portion of the energy decay seems to be less sensitive to the state of diffusion in the chamber, which is in accordance with the results in [Kuttruff and Jusofie, 1969].

The equivalent absorption area of the conventional measurement setup (ISO 354) was calculated with different decay parameters and compared in different diffuse field conditions. Results indicate that the initial part of the decay process is less sensitive to the state of diffusion, even in the case when the absorber is concentrated on a single surface. When the equivalent absorption area is calculated with the initial decay time T_1 , the difference between 0 and 20 diffusers (regarding the equivalent absorption area A) is rather small compared to the cases when it is calculated with EDT or T_{20} . In a future round robin test it could be evaluated if the interlaboratory reproducibility can be improved in case of absorption coefficient measurements when the decay times are evaluated with the Bayesian framework and the initial decay parameter T_1 is used to calculate the absorption coefficient.

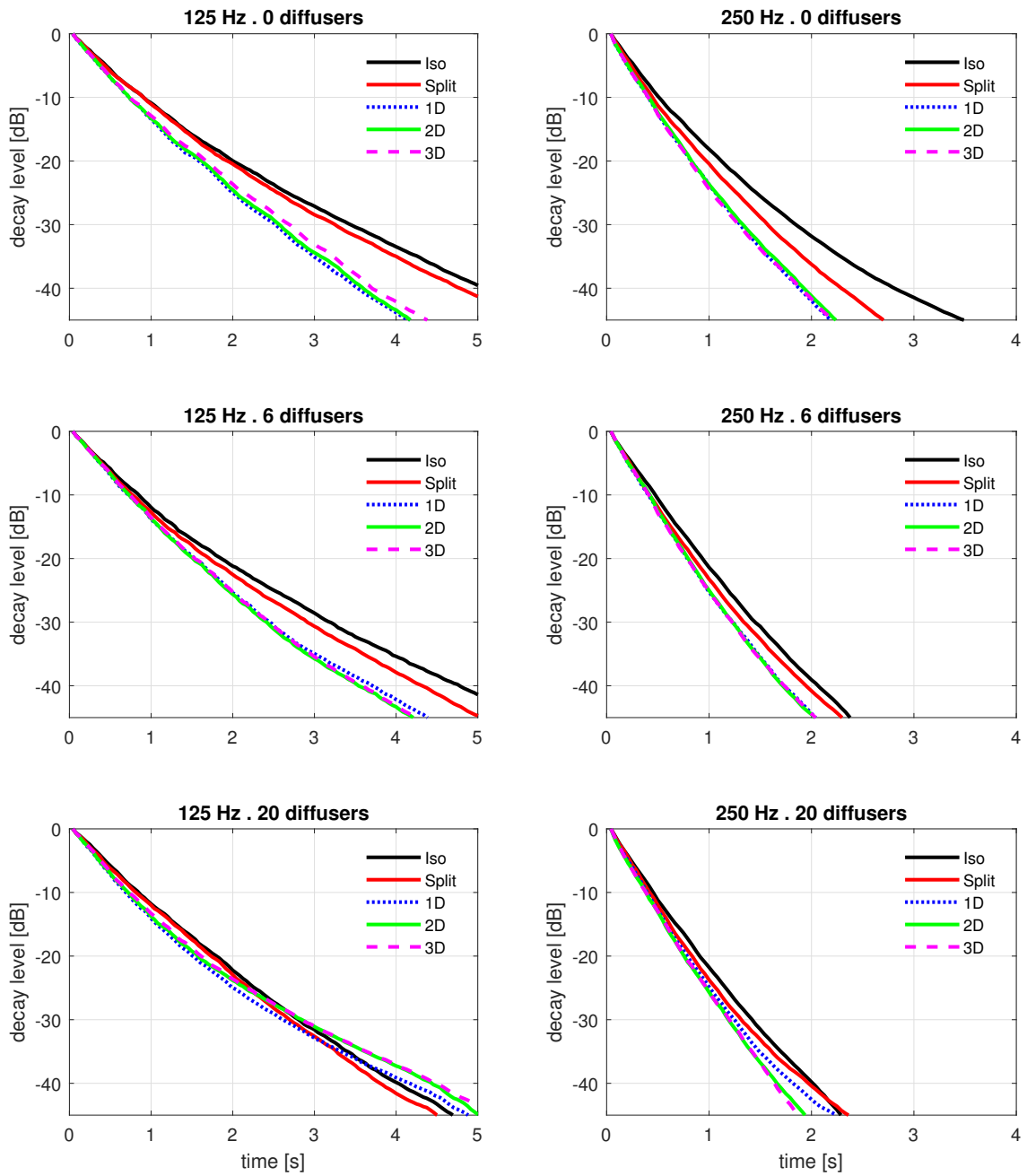


Figure 4.8: Comparison of absorber placements for 125 Hz and 250 Hz, and each diffuser configuration.

4 Experimental investigation of absorber placement

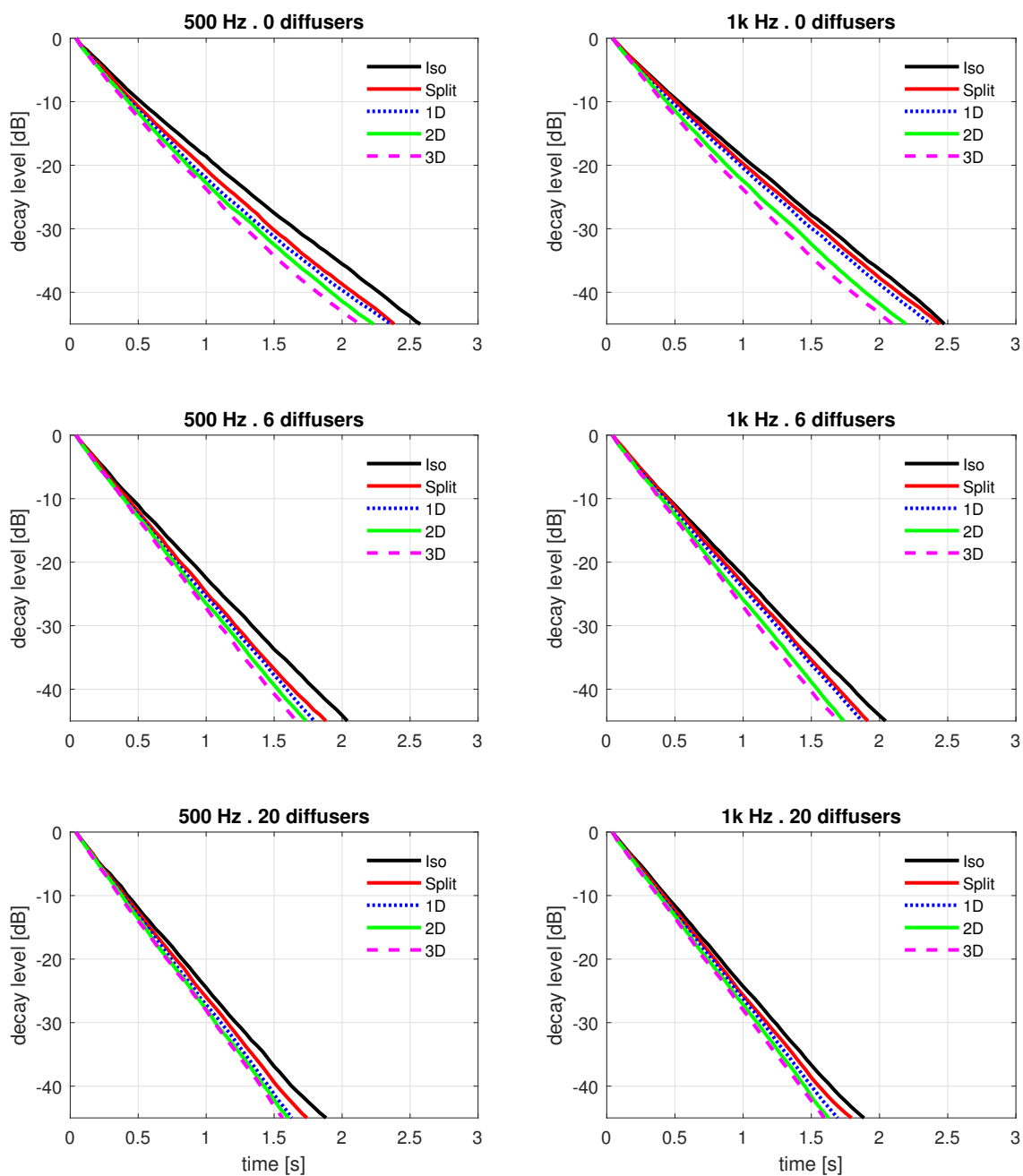


Figure 4.9: Comparison of absorber placements for 500 Hz and 1 kHz, and each diffuser configuration.

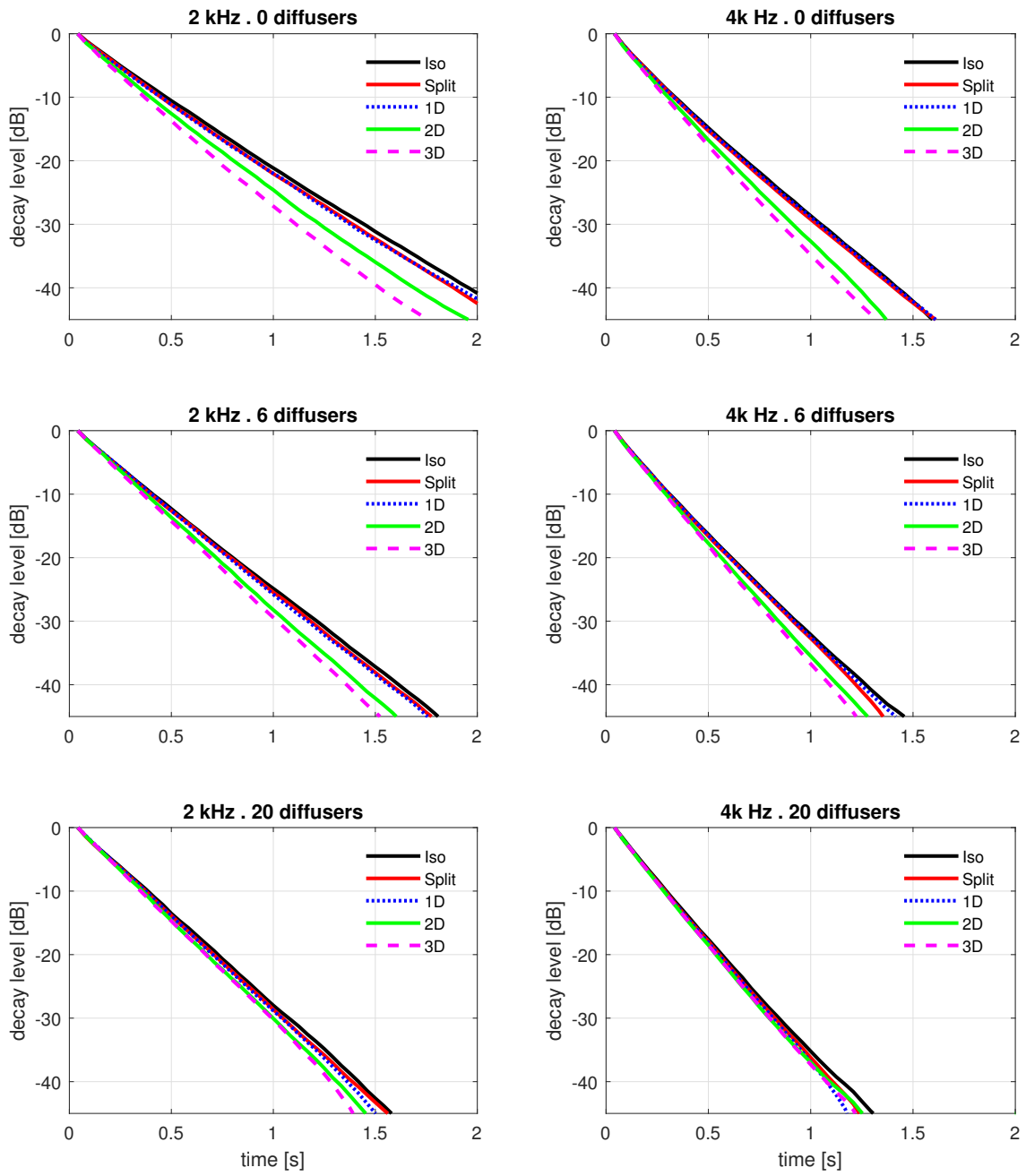


Figure 4.10: Comparison of absorber placements for 2 kHz and 4 kHz, and each diffuser configuration.

4 Experimental investigation of absorber placement

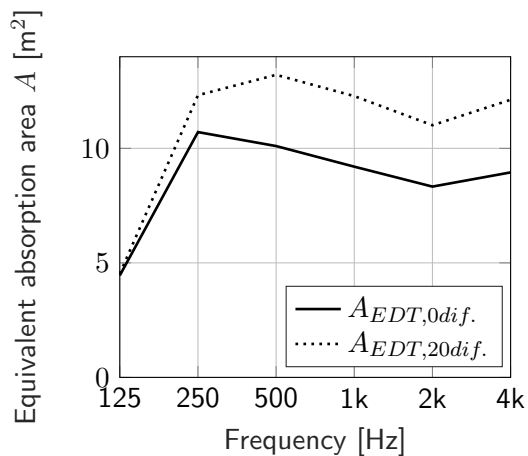


Figure 4.11: Equivalent absorption area A calculated with EDT , with 0 and 20 diffusers.

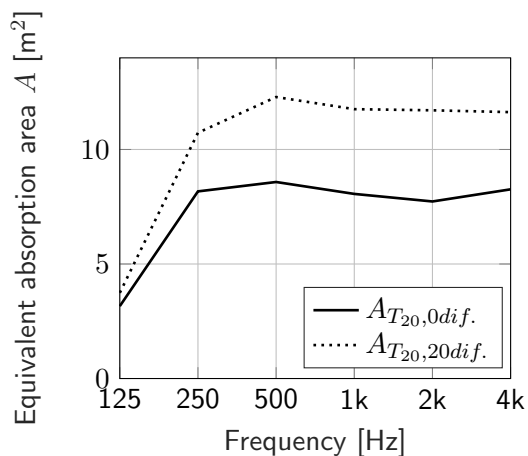


Figure 4.12: Equivalent absorption area A calculated with T_{20} , with 0 and 20 diffusers.

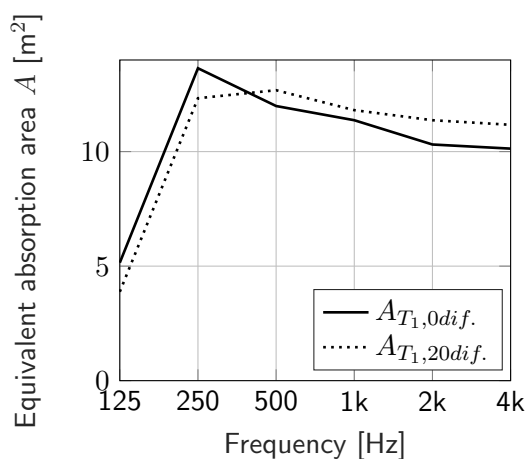
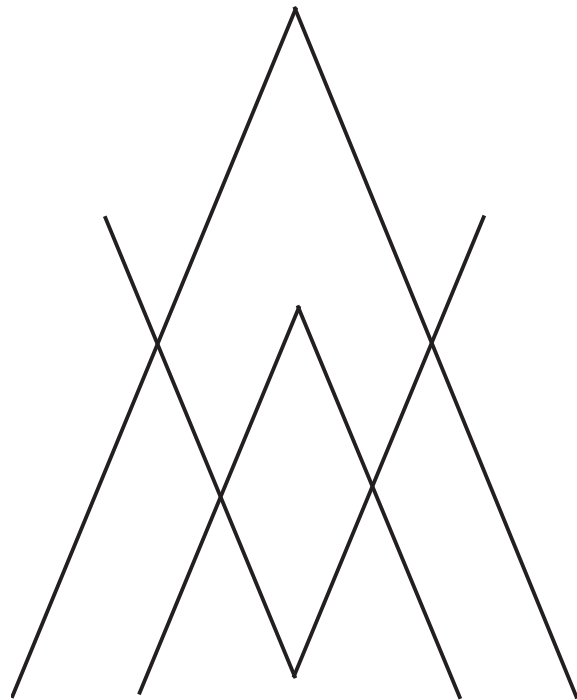


Figure 4.13: Equivalent absorption area A calculated with T_1 , with 0 and 20 diffusers.

5

Experimental investigation of artificial reverberation



This chapter deals with the modification of reverberation times by means of electro-acoustic systems and the analysis of the decay behaviour. This chapter has been published in the Proceedings of the 'Auditorium Acoustics Conference in Hamburg, 2019' with the title *Multi-exponential decay curves in auditoriums* [Balint and Kaiser, 2018]. The work has been carried out jointly with the Co-Author of the article, Fabio Kaiser. He conducted the measurements and made contributions to the section about the active acoustic system.

The acoustic design process for auditoria is usually based on specifying a reverberation time (RT) depending on the application of the hall. To meet the desired RT, the volume and the acoustic properties of the surfaces are determined by Sabine's equation or room acoustic simulation techniques. RT is one of the most common parameters for designing and describing concert hall acoustics. How the objective measure RT is related to the perceived reverberance is still not completely clear but the early decay time (EDT) is considered to relate more closely to perceived reverberance than RT [Barron, 2000]. In most cases the values for EDT are slightly shorter than for RT. Barron [Barron, 1995] presented measurements from 17 concert spaces with a trend for shorter EDT than RT, indicating that the decay process is not linear.

Since Schroeder's method of backwards integrating the impulse response, RT measurements can be carried out very efficiently [Schroeder, 1965]. Schroeder pointed out several advantages, one of them being able to detect multiple sloped energy decays. He showed measurements from the Boston Symphony Hall where the energy decay exhibits a double decay. But as already mentioned, the Boston Symphony Hall is not the only auditorium whose decay process is multiple sloped [Barron, 1995]. Although there is much evidence that in many cases curved decays are present, the conventional method to determine the slope for calculating parameters like *EDT* and RT (T_{20} or T_{30}) is based on linear regression with fixed evaluation ranges. This is due to the reason that in most cases a linear decay is expected. But applying linear regression to a non-linear data set seems highly questionable to obtain representative parameters.

In coupled systems like the Culture and Congress Center in Lucerne (CCL), where energy is fed back from a reverberant auxiliary space to the main hall, curved decays are very common and have been investigated in the past [Luizard et al., 2013]. In those cases a curvature in the decay process is caused by costly constructional measures. If curved decays are well perceived in coupled spaces, the question is if this behaviour is also desired in concert halls without coupled systems. In this chapter, measurements from a multi-purpose auditorium are presented with different room configurations, focusing on the shape of energy decays. Common parameters like *EDT*, T_{20} , and T_{30} are calculated with conventional methods and compared to decay parameters obtained by fitting a sum of exponential decaying functions to the data obtaining decay values independent from the evaluation range. It will be discussed if this method provides an option to linear regression. Additionally, the auditorium is described in detail due to the installation of an active acoustic system. By using an active acoustic system it is possible to shape and enhance the acoustics of a room in various ways. Several different acoustic presets allow for modifying room acoustic parameters like EDT and RT, or even modify early and late reflections from different directions. This makes active acoustics also the ideal tool when investigating the behaviour of energy decay curves.

The causes for multiple sloped energy decays are diverse. Barron [Barron, 1995] discussed three different types of energy decay curves: the cliff-type decay, the plateau-type decay and the sagging decay. Those effects could be related to certain types of geometries or measurement positions within a concert hall: fan-shape in plan, poor diffusion and strong overhead reflection from orchestral reflectors, balcony overhangs, directed reflection design, and low

ceiling above balcony seating.

Energy decays with double slopes are also a common phenomena in coupled spaces. Concert halls like the CCL in Lucern have a reverberation chamber attached to the main space to adapt the late reverberance in the auditory space. The resulting energy decay has a double slope because late energy is fed back to the auditory space from the much more reverberant auxiliary space. Eyring [Eyring, 1931] thoroughly investigated coupled rooms pointing out that the sound decay may not be straight in coupled or single rooms with uneven distribution of absorption. He pointed out that although he omitted the first few dB of the decay in his analysis because the reverberation meter was not able to record that portion accurately, it did not mean that it had no significance. Strong early reflections produce steps in the integrated impulse response, this is cited as one of the most common reasons for omitting the first 5 dB when evaluating the energy decay curve for calculating T_{20} or T_{30} . By calculating EDT it is possible to estimate a parameter that is important for the perceived reverberance, in those cases the first 5 dB are not omitted. Jordan [Jordan, 1970] proposed in 1970 that the first 10 dB drop of the decay matched most closely the subjective reverberation. Before him it was Schroeder [Schroeder, 1966] who defined the initial reverberation time as the RT corresponding to the first 15 dB or 160 ms of the decay. According to ISO 3382 [ISO 3382-2, 2008] the *EDT* is obtained by using linear regression within the first 10 dB drop of the decay multiplied by six. But due to the fixed evaluation range, the obtained parameter can be questionable in case of multiple sloped data as well.

5.1 Measurements

The auditorium in the Congress Center Alpbach (CCA) is used for lectures and conference sessions as well as for acoustic and amplified concerts. Therefore an active acoustic system was installed to vary the reflections and reverberance of the space. Without the active acoustic system the hall should exhibit a suitable reverberation time for adequate speech intelligibility.

The auditorium (see fig. 5.1) has a total volume of $V = 3800 \text{ m}^3$ (configuration A) with a rectangular ground floor ($23.5 \times 28.9 \text{ m}$) and varying heights between $h = 4 - 6 \text{ m}$. It can be subdivided into four halls if desired. The rear third of the hall can be separated from the main hall resulting in one elongated auditorium ($23.5 \times 11.7 \times 4 \text{ m}$, $V = 1090 \text{ m}^3$, configuration B) or it can be split in three rectangular conference rooms ($V = 350\text{-}380 \text{ m}^3$ each, configuration C). The remaining volume of the main space is $V = 2710 \text{ m}^3$ (configuration D).

The ceiling in the front half of the hall is partly covered by the HVAC system and partly with an acoustic plaster. The entire front wall (gypsum board) serves as a screen, the side walls in the first two third of the hall are covered by a special panelling system containing wood and felt. The back third of the hall has sound hard wooden walls which can be used to split the hall. The back of the auditorium has a glass front, the ceiling in the back third of the hall is



Figure 5.1: Auditorium of the Congress Center Alpbach, $V = 3800 \text{ m}^3$, ©CCA

a perforated gypsum board filled with glass wool and an air gap.

The challenges in this project were the different requirements concerning the reverberation time. According to national standards [OENORM B 8115-3, 2005] a target reverberation time between $RT = 1.1 - 1.4 \text{ s}$ for adequate speech intelligibility is required in configuration A + D, whereas target values of $RT = 1 - 1.2 \text{ s}$ were demanded by the active acoustics system. On the one hand the acoustics should not be too dry, on the other hand too much reverberation reduces the function of the active acoustic system due to feedback issues.

Active Acoustics is the term comprising several techniques to influence the sound field in rooms in order to achieve goals like speech and acoustic enhancement. This comprises the generation and distribution of early reflections, the generation and shape of late reverberation and the generation and projections of 3D audio scenes. The idea for such an approach to room acoustic enhancement exists since the 1950's - starting out in the Royal Festival Hall in London – and different variants of such systems are commercially available ever since [Kaiser, 2009, Werner, 2008]. An Active Acoustics system always consist of microphones, pre-amplifiers, A/D and D/A converters, a signal processing unit, amplifiers and loudspeakers. Figure 5.2 shows a schematic drawing of an Active Acoustics system.

Basically, there are two different approaches to active acoustics: In-Line and regenerative (or non in-line). The difference lies mainly in the way feedback is handled – or, more technically spoken, in the way the transfer function $H_{LM}(\omega)$ is handled. The In-Line approach uses directive microphones positioned rather closely to the sound sources, usually within their critical distance. Reverberance is added to the microphone signals either by algorithms or by convolution of synthesized or measured impulse responses. Typically, 4-8 microphones are placed in the stage area and many loudspeakers are placed in the audience area. Feedback is avoided by the directive characteristic and the spatial separation of microphones and loudspeakers. Hence, the loop gain is inherently low and the focus of system design lies on the reverberation generation.

5 Experimental investigation of artificial reverberation

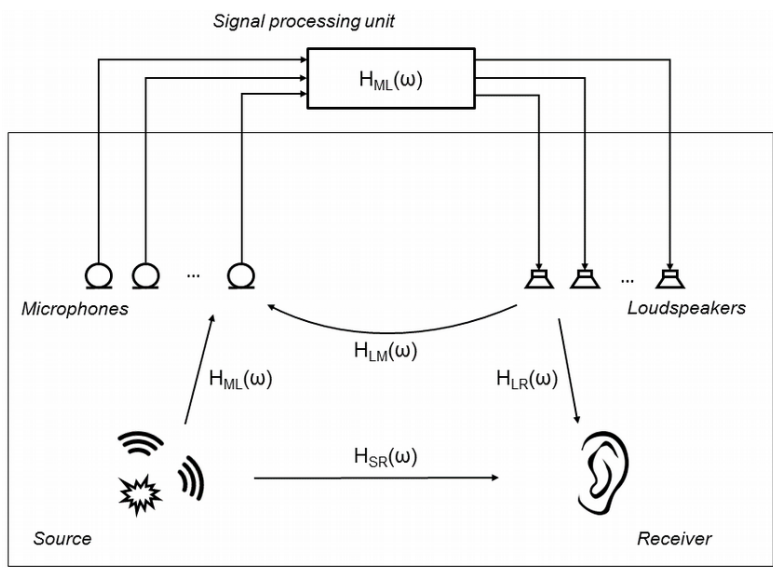


Figure 5.2: Schematic drawing of an active acoustic system [Svensson, 1994].

On the other hand, the regenerative approach uses signal loops in between loudspeakers and microphones to generate reverberation. Microphones are placed outside the critical distance of sound sources and loudspeakers. The basic idea is that the picked-up signals are directly given back via the loudspeakers, however, usually a reverberation stage is added to the signal chain. The loop gain is therefore higher and audible artefacts like ringing tones are likely to occur. In order to increase stability a very high number of microphones and loudspeakers has to be used. A combination of both approaches is typically called a hybrid system (e.g. Amadeus Active Acoustics). In the Congress Center Alpbach the main requirement for the active acoustic system was the uniform performance across the whole hall. There should be no preferred spots for the stage, performers and musicians can be positioned at any point in the hall. A special feature of this hall is that the rear third of the hall can be separated from the main hall and be split in three small conference rooms. This needed to be considered in the process of developing the system. The active acoustic system in the Congress Center consists of altogether 44 loudspeakers and 17 microphones. In the front two thirds of the hall a hexagonal grid was used at the ceiling (17 microphones, DPA, 18 loudspeakers + 4 subwoofer, Renkus-Heinz). The microphones had to be hung from the ceiling ranging from $h = 4 - 6$ m above floor level and following the line of projection. On the walls 22 loudspeakers (Renkus-Heinz) were installed at a height of $h = 2$ m. The system was tuned to five different acoustic presets dedicated to different applications like solo concert, chamber music, orchestra, or choir music. A special challenge was that every acoustic preset had to be tuned for two cases, the open hall with $V = 3800$ m³ (configuration A) and the separated hall with $V = 2710$ m³ (configuration D).

The system can be remotely controlled via a web interface using an iPad or a regular computer. Using the web interface, the technical team is able to turn the system on/off,

select presets, get status information about the components, and playback 3D audio-content or select virtual speaker setups for motion picture playback. Figure 5.3 shows the reverberation times T_{30} measured in the hall (configuration A, $V = 3800 \text{ m}^3$) with different acoustic presets, averaged over eight independent microphone-source positions. The measurement results were provided by Fabio Kaiser.

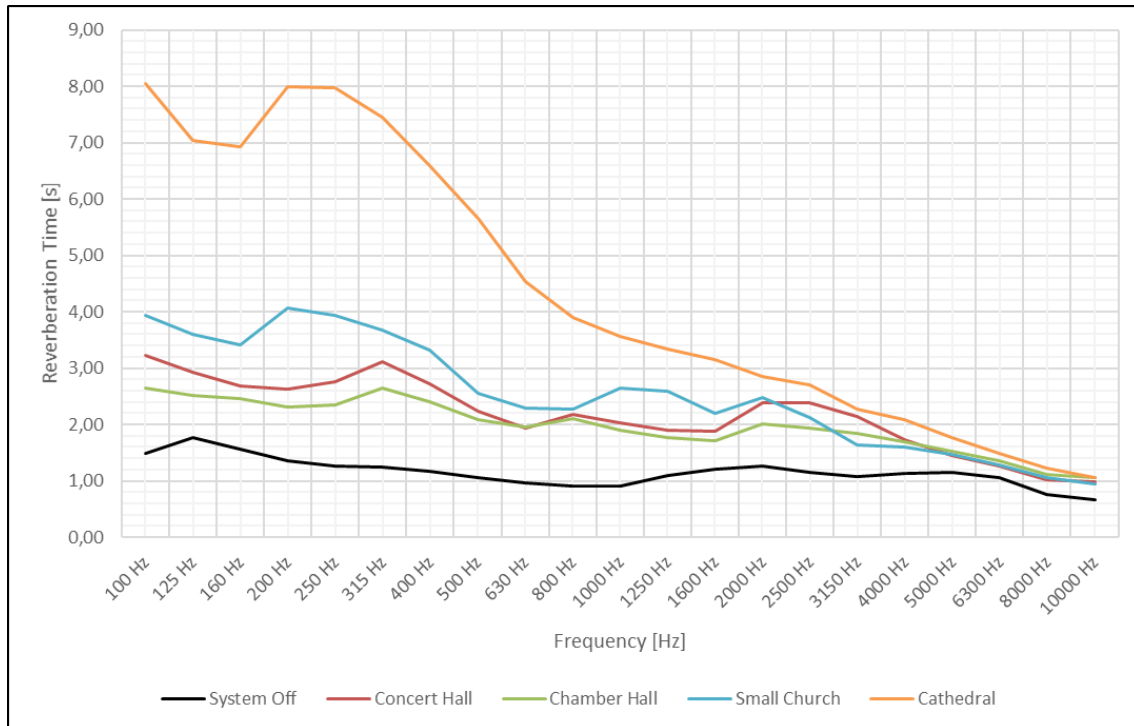


Figure 5.3: Reverberation time T_{30} if different acoustic presets of the active acoustic system measured in the auditorium of the CCA Alpbach.

5.2 Discussion

Figure 5.4(a) shows the EDC for the octave band $f = 250 \text{ Hz}$ for configuration A ($V = 3800 \text{ m}^3$). The EDT is shorter than the reverberation times T_{20} and T_{30} , clearly indicating that the decay process is not linear. When a sum of exponential functions is fitted to the data (the Bayesian framework from Ch. 2 is used), the resulting decay times are $T_1 = 0.70 \text{ s}$ and $T_2 = 1.53 \text{ s}$. With this method the initial reverberation time T_1 is shorter than the EDT. The late part of the decay curve seems to be underestimated by the reverberation times, since the late decay parameter T_2 is greater than T_{30} . In the case when the active acoustic system is turned on (see fig. 5.4(b)), the early as well as the late decay can be altered in various ways. In the following case reverberance was added to both the early and late part. Again the reverberation parameters EDT, T_{20} , and T_{30} differ from each other. In this case the results for the decay times when a sum of exponential functions is fitted to the data are $T_1 = 0.76 \text{ s}$, $T_2 = 2.31 \text{ s}$, $T_3 = 4.16 \text{ s}$. The initial decay time T_1 is much shorter than EDT, indicating that the curvature

5 Experimental investigation of artificial reverberation

already effects the evaluation with linear regression.

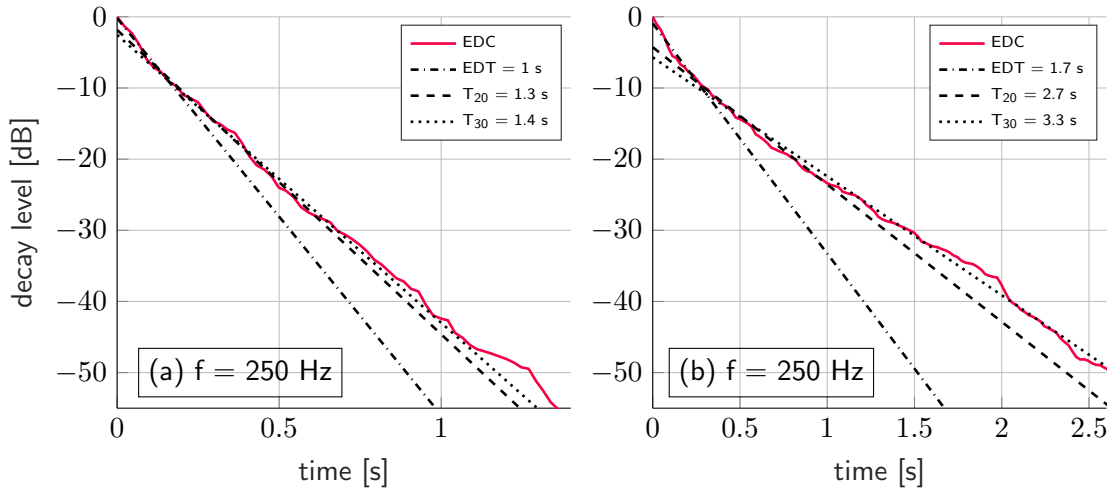


Figure 5.4: EDC for $f = 250$ Hz and conventional reverberation parameter for configuration A, (a) without and (b) with the active acoustic system.

The case for the octave band $f = 500$ Hz is similar to the lower octave band, although the EDC is almost straight over the first 30 dB drop (see fig. 5.5), the parameters EDT , T_{20} , and T_{30} are almost equal. But it is clear already by visual inspection that the late part of the decay is underestimated also by T_{30} . The results for the fitting procedure are $T_1 = 0.96$ s, $T_2 = 1.61$ s. In this case the initial decay time T_1 corresponds well with EDT but the late decay parameter T_2 is greater than T_{20} and T_{30} .

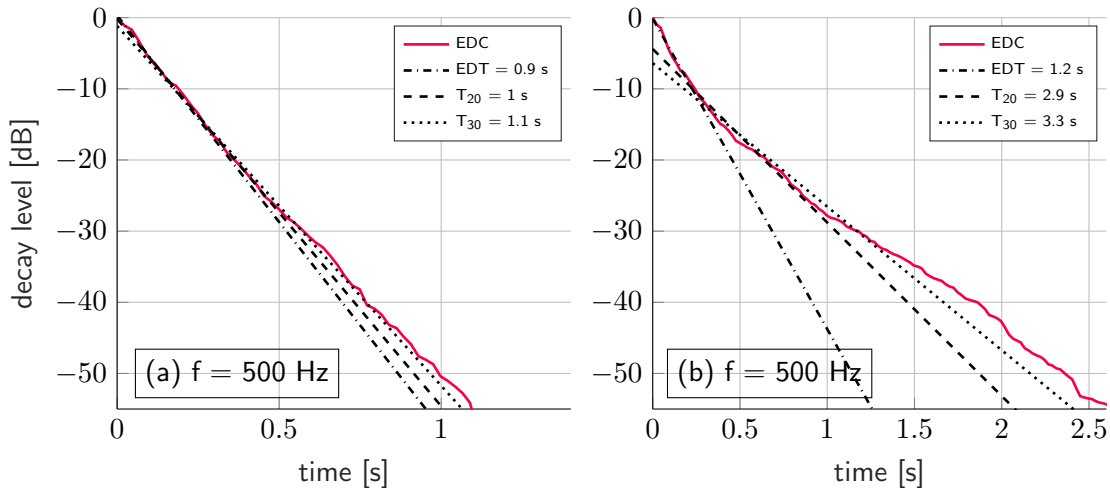


Figure 5.5: EDC for $f = 500$ Hz and conventional reverberation parameter for configuration A, (a) without and (b) with the active acoustic system.

When a sum of exponential function is fitted to the data in the case when the active acoustic

system is turned on, the resulting decay times are $T_1 = 0.99$ s, $T_2 = 2.38$ s, $T_3 = 3.76$ s. In this case the early and the late part of the decay curve is underestimated by EDT , T_{20} , and T_{30} . In fig. 5.6 (a) the energy decay curve of the separated hall with a total volume of $V = 1090$ m³ (config. B) for $f = 1$ kHz is shown. Because only the ceiling is absorbing and the rest of the surfaces are sound hard, the decay is curved. The reverberation times EDT , T_{20} , and T_{30} differ from each other. In fig. 5.6 (b) the energy decay curve for a single seminar room (config. C) with a total volume of $V = 380$ m³ for $f = 1$ kHz is shown. Although the volume is one third of the previous volume, the reverberation parameter stay almost the same. In this case the uneven distribution of absorption is responsible for the curved decay process. In those cases the late part of the decay is highly underestimated.

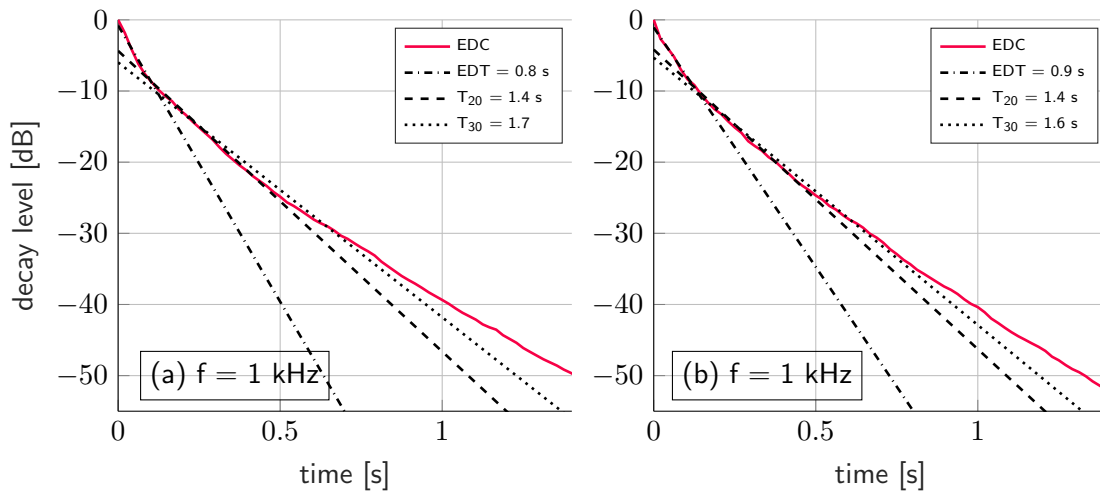


Figure 5.6: EDC for $f = 1$ kHz and conventional reverberation parameter for (a) config. B and (b) config. C without the active acoustic system.

Table 5.1 shows the reverberation times T_1, T_2, T_3 estimated with the Bayesian framework as well as the conventional parameters EDT, T_{20}, T_{30} for configuration A ($V = 3800$ m³) with the active acoustics system turned on. In all octave bands (except for $f = 125$ Hz) three decay times were estimated, whereby the initial decay time T_1 is smaller than EDT in every frequency band. The late decay parameter T_3 is significantly larger when compared to T_{30} . The results indicate that with conventional parameters it is not possible to estimate multiple decay processes properly. It is possible to alter the initial, mid, or late part of an impulse response with electro-acoustic enhancement systems, therefore the clarity or the speech intelligibility can be modified in certain ways, too. The Bayesian framework yields the opportunity to estimate decay parameters which could help to understand the relations between certain parts of the decay process in a space and aforementioned room acoustic parameters.

It is evident that in all configurations curved decays are present. The reason for the curvature can be various. At lower and mid frequencies the various decay times of modes within one frequency band can cause a curvature. In fig. 5.6 the uneven distribution of absorption causes the non linear decay process. But it is possible also to create curved decays like in

5 Experimental investigation of artificial reverberation

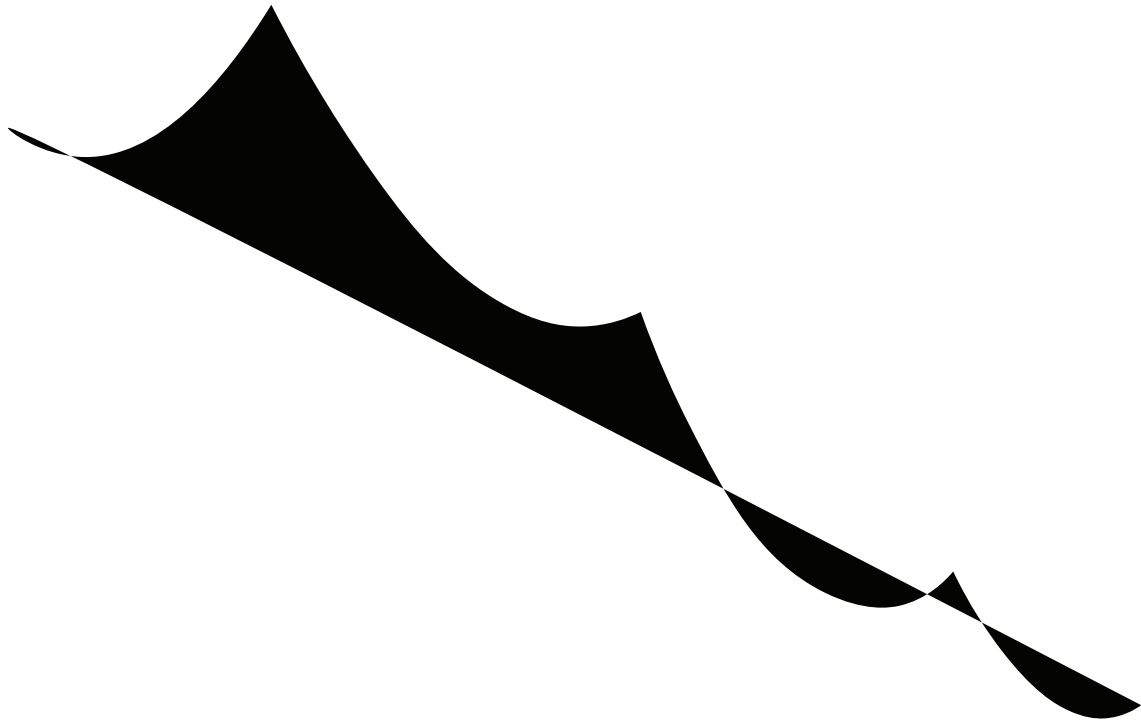
Table 5.1: Reverberation times $T_1, T_2, T_3, EDT, T_{20}, T_{30}$ with the active acoustic system turned on, configuration A: $V = 3800 \text{ m}^3$.

| f (Hz) | 125 | 250 | 500 | 1000 | 2000 | 4000 |
|--------------|------|------|------|------|------|------|
| T_1 [s] | 1.01 | 0.76 | 0.99 | 0.74 | 0.59 | 0.58 |
| T_2 [s] | 4.08 | 2.31 | 2.38 | 1.58 | 1.70 | 1.40 |
| T_3 [s] | - | 4.16 | 3.76 | 3.09 | 3.25 | 2.61 |
| EDT [s] | 1.85 | 1.70 | 1.21 | 1.07 | 1.60 | 1.34 |
| T_{20} [s] | 2.60 | 2.73 | 2.92 | 1.72 | 2.21 | 1.79 |
| T_{30} [s] | 3.15 | 3.34 | 3.32 | 2.24 | 2.54 | 2.10 |

coupled volumes with active acoustics systems on purpose. With conventional reverberation parameters it is not possible to evaluate decay times that correspond to the early or late part of the decay in many cases as shown in this section. The values are either underestimated or overestimated. With the Bayesian framework it is possible to properly quantify initial and late decay parameters. This could be a helpful tool to analyse the sound field in spaces with electro-acoustic enhancement systems, which are usually set up by experienced audio engineers by ear. Otherwise the room acoustic parameters like EDT , T_{20} , and T_{30} will only be an approximation of the decay process in a room.

6

Conclusion



Wir empfinden unseren Raum mit unserem ganzen unteilbaren Ich, zugleich mit Seele, Verstand und Leib und also gestalten wir ihn mit allen leiblichen Organen.

W. Gropius [Gropius, 1923]

The purpose of this thesis was to investigate the poor interlaboratory reproducibility of absorption coefficient measurements. Due to the fact that the fundamental assumptions for the laboratory procedures are not met, namely a completely diffuse sound field and uniform sound incidence on the sample, the following topics have been addressed within this work:

- 1) Evaluating the decay of sound in different spaces under different diffuse field conditions.
- 2) Developing a Bayesian framework to estimate decay parameters based on the assumption of a multi-exponential decay model.
- 3) Proposing a method to use that model and framework to calculate the absorption coefficient from measurements in the reverberation chamber.

The first point was assessed in the reverberation chamber with different diffuser and absorber configurations and in a multi-purpose auditorium. In all cases it could be validated experimentally that the fundamental assumption of a single exponential sound decay is not valid. Instead, a multi-exponential decay model formed the basis for the investigations carried out within this thesis. This led to the second topic, the development of a Bayesian framework to estimate multiple decay parameters from measurements. The common evaluation procedure regarding reverberation times (T_{20} , T_{30}) is based on a single-exponential decay model and is therefore not suited to quantify the decay process in a room. Furthermore, the initial part of the decay process is neglected when T_{20} and T_{30} are calculated. The initial part contains valuable information not just for the human perception but also about the interaction of the sound field in the room with the absorber. It has been found that it is less sensitive to the state of diffusion than the late part of the sound decay. Although the *EDT* regards the first 10 dB of the sound decay, in many cases it is only a rough approximation because it neglects the curvature of the decay. Subsequently the third topic was addressed by using the initial decay time T_1 estimated with the Bayesian framework to calculate absorption coefficients from reverberation chamber measurements. Good agreement could be achieved between measured values compared to theoretical values. In a future round robin test it could be evaluated, if the interlaboratory reproducibility of absorption coefficient measurements can be improved when the initial decay time is used to calculate the absorption coefficient.

Nevertheless, this work is not a collection of novel findings rather than an accumulation of evidence supporting the need for rethinking common views. It is not sufficient just to present research results but to convey the knowledge so it can be questioned again in K. H. Popper's sense.¹

¹ From [Popper and Lorenz, 1985]: *Meine Wissenschaftstheorie ist also ungeheuer einfach. Es sind wir, die die wissenschaftlichen Theorien schaffen, es sind wir, die die wissenschaftlichen Theorien kritisieren. Das ist die ganze Wissenschaftstheorie. Wir erfinden die Theorien, und wir bringen unsere Theorien um. Wir schaffen damit neue Probleme und kommen in die Situation, in der wir, wenn wir können, neue Theorien erfinden. Das ist in kurzem die Wissenschaft und die Wissenschaftsgeschichte.*

6.1 Rethinking reverberation time

It is not the basic definition of the reverberation time that needs to be questioned but the procedure of how the parameter is obtained that we then call *reverberation time* in order to calculate the Sabine absorption coefficient. Usually it is claimed that the RT is measured but actually the impulse response or a sound decay are measured and the RT is then calculated. This step is crucial in understanding that in between a standardized, deterministic procedure and the final result lies a step that is open to interpretation. Even when it is clear that a certain range from a decay process should be evaluated and the mathematical process behind is unambiguous (for instance performing linear regression), there is still enough freedom that can lead to results which are inconclusive. Round robin test have been performed in the past to evaluate the influence of the person who performs the measurements and the calculations [Thysell, 2011]. Even when the standard states clearly that the evaluation range for obtaining RT should start at -5 dB and end at -25 dB, the results from tab. 3.7 indicate that six technicians out of 22 did not comply with the standard and chose their own evaluation range.

When RT is determined, we want to know how much time passes until the sound level drops 60 dB (the volume range which an average person can perceive). The only reason why a linear regression is performed to sound decays is the fact that only in a few cases a sufficient SNR can be obtained. The assumption of a single exponential decay allows then to evaluate a certain part of the decay followed by an extrapolation. Although the first part of the decay is the most important for the human perception [Jordan, 1970], it is neglected in the calculation for two reasons: (a) when the decay process is measured with the interrupted noise method, the first part of the decay can be difficult to evaluate [Schroeder, 1965] and (b) usually the first part of the decay exhibits a shorter decay time than the rest. Although the EDT is often used as a parameter to quantify the perceived reverberation in the room, in most measurement standards for laboratory procedures T_{20} or T_{30} is used, and the initial part is neglected.

Even in the case of an ideal diffuse sound field, the energy decay in a reverberation chamber will not be linear and reverberation times cannot be estimated with and without the sample by applying linear regression to the decay curve. When decay times vary within a frequency band, the resulting decay will be curved (see Appx. D). Applying linear regression to obtain decay parameter is highly questionable in those cases. As a result, obtained absorption coefficients will be questionable, too. Especially for the case of measuring the Sabine absorption coefficient of a sample in the reverberation chamber, it is of utmost importance to obtain accurate decay parameters. Otherwise absorption coefficients measured in different settings and different laboratories will deviate from each other. The accuracy with which reverberation times can be determined from decay curves is crucial for precisely measuring several quantities used in acoustics.

Recent developments in the field of directional decay analysis give insight into the topic of isotropy and diffuseness of sound fields during the decay process [Nolan et al., 2020]. Visualizing measurements is in that case a crucial step in understanding the physics of sound

propagation in rooms. The authors observed that isotropy is higher in the early part of the decay process if an absorber is placed in the chamber (non-uniform absorption) and when following the standard this portion is discarded when estimating the reverberation time T_{20} . Although these were the first results and a systematic study with additional experiments is required, the work of Nolan et al. highlights the argument that we might have to rethink how we evaluate the reverberation time that we use to calculate the absorption coefficient in the reverberation chamber.

6.2 The process of standardization

Although with the new evaluation method presented in Chapter 2, the interlaboratory reproducibility for absorption coefficient measurements could be improved for certain frequencies, or at least a more realistic absorption coefficient for the respective chamber could be obtained, the process of adapting an international standard (in this case ISO 354) poses a major challenge. The revision of ISO 354 has been an ongoing process for the last decade and it still has not come to a reasonable compromise. The new draft allows for a reference absorber to be measured in the chamber [Nolan et al., 2014]. The resulting absorption coefficient has to be within a certain range, to achieve such values the chamber has to be modified accordingly (for instance with diffusers) to meet the target values. The new ISO draft has drawn a lot of attention to the changes, and the harsh criticism still prevents the draft to become published. Although the majority agrees that the standard needs to be revised, no agreement can be reached on the final changes.

In my personal opinion, I agree that the standard needs to be revised, otherwise the measured values of absorption coefficient measurements in the reverberation chamber will not serve as reliable input parameter for room acoustic simulations and design processes. The way of improving the reliability of the measurement procedure is still an open question. Several issues are still not resolved, and the basic principles of diffuseness and isotropy of (decaying) sound fields need to be investigated further. If the interests from the practical application cannot be merged with the findings from the latest research output, the revision will not be based on scientific principles but on experimental investigations which are not suited for the laboratory work. It is of utmost importance that the procedures are well understood, based on scientific results and provide a framework for reproducible measurement results. In [Nolan et al., 2020] the debate surrounding the revision of ISO 354 is mentioned. Through new findings regarding the isotropy of decaying sound fields, the authors hope that the results can clarify some issues involved in the debate.

6.3 Further thoughts on (architectural) acoustics

Acoustics is considered to be a part of (electrical) engineering, a field which is quantified through measurements, numbers and parameters. Although this work has the aim to make a

6 Conclusion

small contribution to that field of numbers and parameters, it became very clear during the process of research that there is much more to acoustics than pure measurements. As Walter Gropius stated, *the perception of a space is an experience with the whole inseparable Me, with the soul, the mind and the body, therefore it has to be designed with all bodily senses*. Just because we know the reverberation time or other acoustic parameter from a space, it does not mean that we know that it is the best concert hall in the world. As it was stated in the introduction, the design of a space should please all senses. To quantify the acoustics of a room just by some parameters seems like a sheer impossibility, it fails repeatedly at the complex process of perception [von Fischer, 2013].

Fischer [von Fischer, 2013] and Thompson [Thompson, 2004] gave an overview about the development of architectural acoustics in Germany, Switzerland and the United States beginning with the findings of W. C. Sabine. At the Swiss Federal Institute of Technology in Zurich it was always a struggle to incorporate the field of acoustics into an existing research area. The faculty of architecture was not quite interested in acoustics and the faculty of physics did not acknowledge acoustics as a research discipline. It was a struggle until the time of loudspeakers and electro-acoustic systems paved the way for acoustics to become a part of electrical engineering. Until now acoustics is integrated in the faculty of electrical engineering and a great part of architectural acoustics (namely building acoustics) is outsourced to civil engineering. I always asked myself why architectural acoustics is not a fundamental part of architecture, also? With the experience we gained over the last years, where acoustics is considered a burden in the design process and usually an acoustician is only introduced to the project after the damage has been done and the space is not fit for the purpose. In my opinion, to make a difference in the evolving design process of architecture and acoustics, both parts need to benefit from each other's viewpoints and integrate a holistic approach to design a space.

The introductory quote is taken from the transcript which describes the fundamental ideas of the Bauhaus school, written by the architect Walter Gropius. The idea behind the Bauhaus school was a comprehensive and broad education which should enable young individuals to design and enhance their surroundings in harmony obeying the natural laws of structural engineering, mechanics, optics and acoustics.² According to Gropius, the holistic approach to design an environment should be incorporated within an education to create a better world. He understood the need for an aesthetic form to function at various levels for the people living and working in it. In my work as a research and teaching associate I tried to understand how education and research can be combined to create knowledge and stress critical thinking. Teaching the fundamentals of acoustics many times and trying to convey knowledge helps to first understand the topics and then to take it one step further to question the common views in acoustics. In App. C I included some of the work of students that I accompanied,

² From [Gropius, 1923]: *Der schöpferische Vorgang einer Raumvorstellung und -gestaltung ist jedoch immer ein gleichzeitiger, nur die Einzelentwicklung der Organe des Individuums für das Fühlen, das Wissen und das Können ist wechselreich und verschieden im Tempo. Den bewegten lebendigen künstlerischen Raum vermag nur der zu erschaffen, dessen Wissen und Können allen natürlichen Gesetzen der Statik, Mechanik, Optik, Akustik gehorcht und in ihrer gemeinsamen Beherrschung das sichere Mittel findet, die geistige Idee, die er in sich trägt, leibhaftig und lebendig zu machen. Im künstlerischen Raum finden alle Gesetze der realen, der geistigen und der seelischen Welt eine gleichzeitige Lösung.*

which I thought succeeded in understanding the fundamentals of acoustics, interpreting the results and questioning traditional views. Additionally I tried to summarize my thoughts on the incorporation of acoustics into other disciplines to point out the potential of joint work between different scientific fields.

To explore the potential of interdisciplinary work, a collaboration between architecture and acoustics was started with a joint teaching project with Assoc. Prof. Milena Stavic. The mutual interaction and inspiration paved the way for several projects where students from architecture and audio engineering could benefit from each others' curiosity [Stavic and Balint, 2019b, Stavic and Balint, 2019a, Stavic and Balint, 2020, Blöcher and Sattler, 2019]. The first project report *Architectural Acoustics Extended - Between two languages new space is discovered* summarizes the interdisciplinary collaboration and points out the potential for future work. Selected pages are shown in App. A. The italic section is taken from the introduction of the project report jointly written together with Milena Stavic: *The course 'Methods of Presentation' at the faculty of architecture, held in the winter term 2018/19, addressed the topic of architectural acoustics. Students were assigned to develop new, unique and innovative designs for acoustic panels and to build a 1:1 scale prototype. The key challenge was the application of two dimensional standard materials, which through cutting, bending, folding or layering should provide an ideal solution in the acoustic and aesthetic sense. At the beginning the students were introduced to different acoustic topics such as speech intelligibility, noise pollution, sound insulation, sound absorbing measures for low, mid and high frequencies as well as measures for an ideal 'architecture for listeners'. The question was raised: How can we design our surroundings and workplaces taking into account the acoustic components of a space, leading to a concept for a holistic approach? Students began their work with research on acoustic panels in architecture, followed by a detailed documentation of the examples. Inspired by different designs, students created and developed their own unique ideas and solutions for a novel acoustic panel design. From a geometric point of view, students could develop their designs within the given geometric themes, such as 'Linear Geometry', 'Ornamental Structures', 'Folding Surfaces' or 'Modular Design'. With the provided material (light gray felt with a thickness of 3mm), the students produced prototypes which were then processed with the help of a laser cutter. Each student either designed two 45cm x 45cm panels by themselves or was working in a group of two in which they designed and presented four panels together. The development of the idea to a finished product was accompanied by students studying audio engineering at the faculty of electrical engineering and information technology. They advised on how to improve the acoustic properties and helped measuring the absorption coefficient of each design. Together they created the basis for further studies and opened up an interdisciplinary research topic. The absorption coefficient of each element was measured in the impedance tube for normal sound incidence. Due to the different structures like folded design, resulting air gaps and multi-layered elements a various amount of different absorbing specimens were produced. The absorption coefficient is shown for each element in a table. The designed elements were applied onto a 25 mm hard felt and measured with 0 mm and 100 mm air gap behind the structure. At the end of the course the students presented their acoustic designs in an architectural context, such as dividing walls, facades, ceilings etc. The book 'Architectural*

6 Conclusion

Acoustics ext.' is composed of all the student works as well as the measured data, providing architects, designers and acousticians with numerous ideas for further applications. The students carrying out the work were studying architecture in their first semester, therefore I think the benefit of planting the seed of curiosity beyond classical topics of architecture paved the way for future collaborations with acoustics, mainly due to the fact that students are sensitized to a different topic.

When audio engineers were asked to evaluate the collaboration with students from architecture, they honestly commented that although the goal seems to be same, namely to design a space which is comforting to all senses, the way to get there and the importance of acoustics diverges greatly³. Nevertheless, despite all the circumstances an attempt was undertaken to collaborate in an interdisciplinary field and merge all the knowledge, visions, expectations, and even the vocabulary to extend the views and to design a space in a holistic sense.

6.3.1 W. C. Sabine, a lecture hall, and TU Graz

When I read the *Collected Papers on Acoustics*, written by W.C.Sabine, one topic immediately caught my attention. It was the acoustics of a lecture hall which brought Sabine to the fields of acoustics. He carefully measured the reverberation time during the night (so there were no disturbing sounds from cars or students) and emphasized the importance of precision when giving lectures to his students. After discovering the fact that his clothes had a small impact on the reverberation time, he threw away over 3000 measurements and decided to always wear the same outfit when conduction experiments (*blue winter coat and vest, winter trousers, thin underwear, high shoes*) [Thompson, 2004]. Almost exactly 100 Years later, together with student from audio-engineering we carried out measurements and tried to evaluate the acoustics of the lecture halls at Graz University of Technology [Frischmann et al., 2019, Mülleder et al., 2019]. One would expect that such a long time after laying the foundation for designing lecture halls not just from a visual but also from an acoustic point of view that every single lecture hall should fulfill the basic requirements (sufficient speech intelligibility among other things). The scope of both Bachelor Theses was to investigate the acoustic condition of the majority of the lecture halls (from an objective and subjective point of view) and if necessary, suggest improvements. The students should apply their knowledge from the lectures and laboratories which they attended for three years and then try to interpret the measurement results as well as compare them to their own personal impression as an acoustician. Although the skills are being acquired during the Bachelor studies which are necessary to carry out basic measurements, the challenge lies in understanding and interpreting the data in a meaningful way. The students generated data sheets for 26 lecture halls, acoustic parameter with visual representation are shown, including the subjective perception of the students who carried out the investigation

³ From [Mülleder et al., 2019], Über die Zusammenarbeit mit den Architekten: Es war sowohl für uns Toningenieure als auch für die ArchitektInnen interessant, einmal mit der jeweils anderen Sichtweise konfrontiert zu werden. Obwohl beide Seiten im Grunde das Ziel haben, einen Raum zu entwerfen in dem man sich gerne aufhält, legen sie eher wenig Wert auf die anderen Ansprüche. So lernten wir andere Sichtweisen kennen und so manch angehende ArchitektInnen machten sich das erste Mal ernsthafte Gedanken über die Akustik eines Raumes und dessen subjektiven Eindruck.

(in App. B two exemplary data sheets are shown). The results are alarming, 14 out of 26 halls are recommended for an acoustic refurbishment. Future student projects and courses could be devoted to the refurbishment of their own lecture halls with novel design and innovative acoustic concepts.

6.3.2 Why concert halls should please the ear AND the eye

This paragraph is a short comment on T. Lokki's and J. Paetynen's contribution *Concert halls should primary please the ear, not the eye* [Lokki and Pätynen, 2018] at the Auditorium Acoustics Conference in Hamburg in 2018, which was located in the Elbphilharmonie. The grand hall in the Elbphilharmonie is a vineyard hall which was heavily criticized by the authors. Although they admit that architectural features influence the sound, at the same time they claim that recently *acousticians tend to design halls that serve mainly the sense of sight and do not optimally support the music*. The purpose of the paper was, according to the authors, to spark a discussion. Six points are addressed in the following paragraphs, where the opinion of the authors is shortly summarized at the beginning of each paragraph followed by a comment.

1) Users: Lokki and Paetynen mention different users, for which different aspects of a concert hall are important. Conductors' (people with strong egos and even narcissistic traits)⁴ attitudes would often be biased, nevertheless they have a strong opinion on the acoustics of the halls. Although they would not say anything bad about their resident hall, based on their outstanding hearing ability they make pronounced statements about acoustics. One outcome of their findings was that conductors want to hear every instrument in a good balance and want to be able to easily communicate with the orchestra. As a conclusion, one could say that the speech intelligibility should be very high in both directions but the acoustics should not be too dry so that the orchestra sound does not fall apart. Nevertheless, the reputation of a hall does have a significant impact on the opinion of a conductor. Recording engineers prefer dry halls where they can post-process the recordings and even vineyard halls due to the missing reflections from the side walls. Audience members, the great part of the users, would not care so much about perfect acoustic conditions. They would value the interaction with people, the architecture, being part of a crowd and seeing the musicians. The overall conclusion of the authors is that despite the fact that it is very important to design halls for different users with different expectations, *acoustics should be the main focus in design*.

Comment: In my opinion, their findings can be interpreted in a different way, too. It is impossible to detach acoustics from every other aspect which is inherent to the perception, the prepossession, or the marked preferences of human beings. Instead of separating acoustics from the rest, a multi-modal approach could benefit all instead of only one group of people, namely acousticians. Even if this leads to a compromise between aesthetics and acoustics, I believe that the result in the end is much far-reaching than from every single discipline by itself. In a collaborative teaching project (Grenadier Acoustics, see App. C), a compromise

⁴ Although no reference is given for this correlation, it might be possible that a personal discussion between one of the authors and a conductor led to this comment. They did not agree on the quality of two halls and in the end the conductor concluded that *there must be something wrong with the author's hearing*. [Lokki and Pätynen, 2018]

was found between the optimum amount of absorbing panels and the demand for aesthetic perfection. It only worked because both parties agreed that one would not work without the other. Although the starting point was the aim to improve the acoustics, the collaboration led to the benefit of innovative acoustics paired with impressive aesthetics.

2) Perception: The authors are leading experts in the field of concert hall acoustics and have published many findings regarding the quality of halls around the world [Pätynen and Lokki, 2016a, Pätynen and Lokki, 2016b, Lokki and Pätynen, 2011, Lokki et al., 2016]. Findings on the positive and negative aspects of architectural features are based on two evaluation methods: first, listening to halls in-situ, and second (for the main part), auralizations without any visual influence. The authors mention that this might introduce a bias from the complete audio-visual and physical/societal experience. Nevertheless, they make pronounced statements on architectural features.

Comment: Concerning auralizations, although highly advanced measurement and reproduction techniques provide a controllable laboratory environment, limitations still exist which make them differ from 'real-world' experiences. Furthermore, a visual cue can change what is perceived in the auditory context. Based in the field of speech perception, the McGurk effect demonstrates the connection between visual cues and auditory perception [McGurk and MacDonald, 1976]. Even if we want to disconnect visual and auditory cues, our brain tries to make the most sense of what we see by combining both information for our perception.⁵ Future research could be devoted to the question on how we can support the perception of music to be able to see good acoustics and hear outstanding architecture.

3) Scattering: A new approach of concert hall design stresses the importance of flat surfaces to avoid high frequency attenuation [Kahle, 2018]. This is in contrast to the well-established approach that the small diffusing elements are responsible for outstanding acoustics; the more diffusion the better the hall (e.g. the Vienna Musikverein is usually referred to as one of the best halls, among other things due to the scattering caused by the gold statues). Recent findings include the fact that if someone looks really carefully, the Vienna Musikverein actually has more flat surfaces than scattering elements, creating a clear acoustic signature.

Comment: For architects this should come as a gift from heaven, since modern buildings tend to be rather flat than full with ornaments. Maybe the acoustic design process takes a step towards architectural design preferences without recognizing it. The authors of the paper in discussion highlight the negative effect of small diffusing elements while standing in the grand hall of the Elbphilharmonie with its *white skin*. The surface of the hall is highly structured on the micro and macro level, thus providing excessive diffusion in the context of contemporary acoustics. On the contrary, the white skin was specially designed to guarantee that the acoustics are perfect, developed by internationally renowned acoustics specialist Yasuhisa Toyota [ArchitonicAG, 2020]. Despite the discussion on diffusion, when entering the grand hall one steps into this overwhelming white space designed by Swiss Architects Herzog & de Meuron. It is just an assumption but it is hard to believe that anyone wants to close their eyes

⁵ For a short demonstration of the McGurk effect, a BBC video can be accessed here: <https://www.youtube.com/watch?v=G-1N8vWm3m0>

and not look at this stunning architecture (and just listen to the music).

4) Late reverb: Another interesting aspect in the paper highlights the importance of high ceilings to support late reverberation. Early and late reverberation is mentioned in the context of 'source presence' and 'room presence' [Kahle, 2013]. This is important to clearly perceive the sound sources (instruments and transient events) and the room (reverberation and sustained events).

Comment: When talking about an early and late decay in 'good' concert halls, Schroeder immediately has to be cited within this context when he introduced his new method of measuring reverberation time and showed a double sloped energy decay from measurements in the Boston Symphony Hall [Schroeder, 1965]. As already mentioned throughout this thesis, double or triple sloped sound decays are ubiquitous in acoustics. With the new evaluation method described in Ch. 2, future research could be devoted to calculating early and late reverberation parameters for concert halls and analysing the perceived preferences in certain halls.

5) Stages and auditorium: A preference for relatively high stages and flat audience areas are supported by the authors, giving examples of excellent concert halls where such environment can be found (Boston Symphony Hall, Amsterdam Concertgebouw, Vienna Musikverein). Among other reasons for the excellent acoustics, indeed one might be the high stage and the flat audience. This would be a simple design criteria which can be implemented by architects easily.

Comment: Nevertheless, every one of those concert halls need an additional comment: 1) The Boston Symphony Hall was originally designed by W. C. Sabine himself. When entering the hall, an acousticians mind cannot not think about this fact. Only the slight sense suffices that one of the pioneers of acoustics once stood in this hall and carried out acoustic measurements to stand in awe of this space. 2) The Vienna Musikverein is a hall with a long tradition in the heart of Europe. Austria has excellent orchestras and therefore it is hard not to be overwhelmed when entering this state hall with all the gold and crystal chandeliers and listening to the Viennese Philhamonic orchestra. A comment by architect Adolf Loos [Loos, 1912] about the *Mystery of Acoustics* sets up the hypothesis that good acoustics comes from good music and nothing else. The article suspects that Loos knew the fundamentals of acoustics and that he had a strong opinion about that topic. For him it was obvious that concert halls with a long tradition like the Vienna Bösendorfersaal had good acoustics because the sound of Liszt vibrated through the halls a long time ago and the walls are filled with good music. On the other hand, one can destroy the acoustics with bad music. Therefore building the same hall somewhere else did never work, like in the case when the great concert hall in Bremen was rebuilt in Manchester. Although the article from Loos cannot be taken completely seriously, it shows that also architects acknowledge the fact that a concert hall is more than just the optics or its acoustics. 3) The Concertgebouw Amsterdam is a very beautiful building, too. With a long tradition, it can also be queued in line with halls where the walls have heard good music. Furthermore, beverages are being served for free in the breaks which might influence the positive experience during the recital.

6) Vineyard halls: A fourth concert hall, which is worth mentioning and which is in contrast to the opinion of the authors is the Berlin Philharmony. It was the first vineyard type concert hall ever built, designed by another acoustic pioneer, Lothar Cremer. It is one of the few buildings, where the architect Hans Scharoun built the facade of the hall after Cremer designed the form and the interior of the concert hall. The idea behind the seating arrangement was that every seat should provide good sight to the orchestra and good acoustic conditions equally. Maybe this type of hall should not be erased from future concert hall drafts like the authors of the paper suggest. As Y. Toyota commented on the diverse reviews on the Elbphilharmony, a concert hall is never finished at the opening. It always needs some work after all. And he is used to the critical voices, just like it was at the opening of Paris Philharmony. The material keeps working and after one or two years the people in Paris swear that they love their concert hall. Maybe somehow Adolf Loos was right after all.

Comment: From 1897 until 1900, W.C. Sabine was asked to consult on the manner of acoustics of the Boston Symphony Hall. When he was consulted regarding a small piece of wood lining on the stage area, he replied that it would have no significant effect on the acoustics. However, *subjectively this small piece of wood would increase the acceptability of the hall to the public by gratifying a long established – and not wholly unreasonable – prejudice* [Thompson, 2004]. Even in the early beginnings of architectural acoustics, it was evident that without some kind of visual confirmation, it is very hard for human beings to believe something they cannot see. Fischer [von Fischer, 2013] devoted one chapter of her doctoral thesis to the visualisation of sound, which helped to make acoustics more tangible for architects and to find a common language where both can communicate. Instead of disconnecting the disciplines, the potential of innovative acoustics and architectural design lies in the interdisciplinary collaboration. As supported by selected examples throughout this chapter, future research in acoustics and architecture should incorporate both fields and exploit the possibilities of joint innovation. In that sense, concert halls should please the ear and the eye, equally!

6.3.3 Sonic environment

In the introduction of this thesis two listening examples were provided. The first one was recorded in the completely empty reverberation chamber from Ch. 3 ($V = 240 \text{ m}^3$). In a more philosophical way, it can be interpreted as the white cube of acoustics. The second example was recorded in the reverberation chamber as well, just with 10.8 m^2 of highly absorbing material on the floor (setup 'ISO' from Ch. 4). In that sense the sonic environment can be used as an augmented design tool in architecture [Castillo-Rutz et al., 2019]. By placing a certain kind of material in the room, the whole perception can change due to the auditory impression. For architects and acousticians, this adds another dimension to the design process which can be used to create a holistic concept for the space.

6.3.4 Y. Toyota and why he prays a lot

To conclude the work, a little anecdote about acoustics will be given. A couple of acousticians came together in Hamburg at the conference called *Auditorium Acoustics* and spend three days in the Elbphilharmonie to listen to the novel developments in the field of concert hall acoustics and to the sound of the surrounding spaces. Mr. Toyota was the guest of honour since he was involved in the design of the main hall as the lead acoustician. Meeting him at the conference was very inspiring. At the conference I presented my findings which were described in Ch. 5 and one question Mr. Toyota asked me when he looked at my poster was: *Are curved decays good or bad?* It took me a while to understand the question. During my research I always wanted to find an explanation to the mystery of absorption coefficient measurements in reverberation chambers. When I finally found an answer that was acceptable to me, I realized that taking it one step further and just evaluating the research outcome in a more philosophical way never occurred to me. So when I met Mr. Toyota and he asked, if curved decays are good or bad for concert halls, I could not answer the question. Until now it is a topic that accompanies me every day but I do not believe that it is a single answer that one can give to tackle the questions that go one step beyond. At the same time I am sure that future research in the field of concert hall acoustics should be devoted to Mr. Toyota's question.

In the evening at the conference dinner a good friend asked Mr. Toyota what his secret was to design a good concert hall. He laughed and honestly said that there would be no secret. He never knows how a concert hall will turn out in the end. There are so many factors that contribute to the final result that it is impossible to know if something will be good or bad. And there would be so much more to it than carrying out simulations, building scale models, calculating room acoustic parameters or trying to translate the architect's acoustic visions to reality. So the only thing left is praying. One can pray that in the end the acoustics will be good.

Now I think that I understand a little bit what he was saying.

Appendix A - Contributions

Journal Contribution

- Title: Bayesian decay time estimation in a reverberation chamber for absorption measurements
- Authors: Jamilla Balint, Florian Muralter, Mélanie Nolan, Cheol-Ho Jeong
- Published in J. Acoust. Soc. Am. 146 (3), September 2019
- The measurements were carried out during a research stay at the Denmark Technical University from January 2017 until July 2017. The adaptation of the algorithm to calculate decay times was part of the Master Thesis written by Florian Muralter under the supervision of Jamilla Balint and Gerhard Graber.

Bayesian decay time estimation in a reverberation chamber for absorption measurements

Jamilla Balint^{a)}

Signal Processing and Speech Communication Laboratory, Department of Electrical Engineering,
Graz University of Technology, Inffeldgasse. 16c, A-8010 Graz, Austria

Florian Muralter

Computing, Electronics and Communication Technologies, Faculty of Engineering, University of Deusto,
Bilbao, Spain

Mélanie Nolan^{b)} and Cheol-Ho Jeong

Acoustic Technology, Department of Electrical Engineering, Technical University of Denmark (DTU),
Building 352, Ørstedsgade, DK-2800 Kongens Lyngby, Denmark

(Received 20 April 2019; revised 13 August 2019; accepted 19 August 2019; published online 19 September 2019)

This work investigates the use of the initial decay time to obtain the Sabine absorption coefficient from measurements conducted in a reverberation chamber. Due to non-uniform distribution of sound absorption in the test chamber, measured energy decay functions exhibit multiple slopes, which cannot be evaluated unambiguously using linear regression as prescribed in the current standard (ISO 354, International Organization for Standardization, Geneva, Switzerland, 2003). As an alternative, this study proposes a Bayesian framework that allows estimating multiple decay parameters, hence capturing more accurately the energy decay features. Measurements are carried out in a reverberation chamber with and without diffusing elements to investigate the influence of diffusers on the absorption coefficient and on the decay process. Measured absorption coefficients of a porous sample are compared to theoretical values estimated with a transfer matrix model. The results show that the Sabine absorption coefficient calculated using the shortest decay time agrees well with the size-corrected theoretical absorption coefficient.

© 2019 Acoustical Society of America. <https://doi.org/10.1121/1.5125132>

[LS]

Pages: 1641–1649

I. INTRODUCTION

The Sabine absorption coefficient can be obtained from measurements in a reverberation chamber.¹ The procedure of calculating single reverberation times (RTs) is based on Sabine's formula,² which assumes a diffuse sound field and an exponential energy decay. Yet, when absorption is concentrated on a single surface, the energy decay does not decay exponentially but exhibits a double slope (in the logarithmic presentation), of which the decay rates correspond to those of the grazing and non-grazing waves.³ This means that different RTs will be obtained depending on what portion of the decay function is used for the evaluation, and therefore the decay process cannot be described by a single RT.^{4,5} Consequently, absorption coefficients obtained under the conditions specified in the standard might be ambiguous. This poses a major challenge, since results obtained from measurements in the reverberation chamber should be reproducible as they form the basic input parameter for room acoustic simulation tools and acoustic design processes. Yet, numerous investigations have reported significant doubts regarding the reliability and accuracy of the reverberation chamber method. In particular, several round robin tests, in which the same sample of an absorbing material has been tested in a number of

laboratories, have revealed a substantial discrepancy in the results.^{6–8} This could, to some extent, be attributed to the estimation of the RT from multi-exponential decay functions with the linear regression (LR) method.

The measurement standard prescribes specific design criteria for reverberation chambers.¹ Especially, adding diffusing elements (in the form of panel or boundary diffusers) is expected to build up diffusion, and thus to minimize the curvature of the sound decays. However, predicting the effect of diffusing elements on the sound field in a reverberation chamber is a challenging task. Frameworks like the finite element method, the boundary element method, or geometrical acoustics simulation tools depend critically on the boundary conditions, which are often unknown.¹⁰ Furthermore, geometrical acoustics simulation tools cannot take into account wave-based effects.⁹

Uncertainties in standardized reverberation chamber measurements are not only introduced by uneven distribution of absorption. ISO 354 (Ref. 1) further stipulates that the evaluation range shall start at 5 dB below the initial sound pressure level. Kuttruff⁴ concluded that in the case of a multi-exponential decay, the initial part of the decay contains the mean of all excited modes in the room, and therefore the most relevant information. He derived that the decay function can be seen as the Laplace transform of the damping distribution of the room modes. By calculating the first and second derivatives of the decay distribution, he

^{a)}Electronic mail: balint@tugraz.at

^{b)}Also at: Saint-Gobain Ecophon, 265 75 Hyllinge, Sweden.

concluded that the initial slope of a logarithmically plotted decay function is defined by the centroid of the distribution. Therefore the initial slope is the weighted mean of all decay constants present in the reverberation process, where the weighting function is the frequency distribution of the decay constants. However, the current evaluation procedure¹ discards the initial portion of the sound decay and therefore the accurate estimation of reverberation parameters in case of multi-exponential decays may not be possible.

The major contribution of this work is to calculate the Sabine absorption coefficient with accurate decay parameters obtained from multi-exponential energy decay functions (EDFs) measured in a reverberation chamber. In case of multi-exponential decays, a Bayesian framework is used for estimating accurate decay parameters within this investigation. The absorption coefficient is calculated with the decay time obtained from the initial part of the EDF. Results are compared to theoretical absorption coefficients calculated with a transfer matrix model¹¹ combined with Miki's model¹² and Thomasson's size correction.¹³

This paper is organized as follows: Sec. II gives an overview of previous research and underlying ideas of the present work. The Bayesian framework to obtain multiple decay parameters is presented in Sec. III. Experimental results are described in Sec. IV and discussed in Sec. V. Finally, Sec. VI summarizes the work and gives an outlook for future research on the presented topic.

II. PREVIOUS RESEARCH

EDFs in enclosed spaces of various sizes and shapes have widely been investigated in the past. Results indicate that in numerous cases a multi-exponential decay is present. Hunt *et al.*³ showed that the root-mean-square sound pressure at a given point during the decay is the summation of each excited normal mode of vibration. In reverberation chambers with uneven distribution of absorption, the large number of excited modes within a given frequency band has to be subdivided into groups having common properties, leading to multiple decay parameters. Although restricted to rectangular rooms without any diffusing objects, the proposed method could be validated by various experiments. It was suggested not to use any diffusing elements in the reverberation chamber since the effect on the sound field cannot be predicted and poses the risk of introducing additional uncertainties. When introducing the backward integration method, Schroeder also pointed out the existence of multi-exponential decays.¹⁴ As an example, he published measurements carried out in the Boston Symphony Hall exhibiting multiple decay times. Bruel¹⁵ observed concave sound decays when trying to determine RTs for sound power measurements in diffuse-field conditions. He found out that the agreement between the free- and diffuse-field sound powers is much better when the early decay is used. Jacobsen¹⁶ derived decay times of each mode group and showed that axial and tangential modes exhibit a longer decay time than oblique modes. In small and medium-sized rooms, the decay will therefore always be multiple-sloped at low frequencies. Furthermore he pointed out that if the initial part of the decay is used for calculating the

absorption coefficient, care has to be taken at low frequencies where the sound field is dominated by axial and tangential modes, as they contribute significantly to the steady-state condition in the room.¹⁷ Still, he concluded that the systematic error of absorption estimates based on initial decay rates is about two-thirds of the error of usual estimates based on the interval from -5 to -35 dB. In ISO 3382-2,¹⁸ a parameter for the linearity of the decay is proposed, which estimates the curvature based on the ratio of the RTs T_{20} and T_{30} . It has to be pointed out that this gives a rough estimation of whether or not a multi-exponential decay is present, although neglecting the bending point of the curve. Nilsson⁵ investigated rectangular rooms with absorbing ceilings like classrooms and offices. He successfully applied a two-system statistical energy analysis model to simulate the double-sloped energy decay due to the uneven distribution of absorption. Furthermore the influence of diffusing objects was examined, showing that the curvature can be decreased and the bending point of the decay shifted when introducing irregularities at the boundaries such as boxes on the walls.¹⁹ Preliminary studies^{20,21} to the present manuscript were carried out, where the influence of different amounts of diffusing objects on the bending point of the EDF has been investigated in reverberation chambers. Xiang *et al.*^{22–25} thoroughly investigated the decay behaviour in coupled spaces and developed a Bayesian framework to calculate multiple decay parameters. The successful application resulted in up to triple-slope detections, showing that the use of conventional methods of LR is not valid in those cases.

Previous research, as shown, indicates that multi-exponential decays are ubiquitous: in single and coupled spaces, in concert halls, in small rooms, in rooms with uneven distribution of absorption, in classrooms, and in laboratories. Although it was pointed out that in cases of multi-exponential decays the determination of RTs with LR can lead to questionable results,^{22–25} the standard procedure for calculating absorption coefficients still neglects the curved nature of energy decays which is apparent in the reverberation chamber.

III. FRAMEWORK

This section describes the Bayesian framework used to calculate the decay time distribution of a given EDF. Bayesian frameworks were already successfully applied to estimate multiple decay parameters by Xiang *et al.*^{22–25} in the field of acoustics and by Shukla *et al.*^{26–28} and Hoffmann *et al.*²⁹ in the field of physics.

A. Bayesian decay time estimation

Bayes' theorem provides a probabilistic framework to solve inverse problems in a variety of fields including acoustics,^{25,30,31} image processing,³² and physics.^{26–28} In this work, the aim is to calculate the decay time distribution from a given EDF. The method of extracting decay times is based on the algorithm MELT—Maximum Entropy LifeTime Analysis,^{26–29} which was used in the field of positron lifetime analysis. The authors employed the framework to solve the inverse problem of finding the decay times and their intensities resulting from measured multi-exponential decay functions. In acoustics, the EDF, which is obtained by applying the Schroeder backward integration to

an impulse response (IR), can be regarded as a multi-exponential decay function as well,²⁵

$$\text{EDF}(A, T, t_k) = A_0(t_K - t_k) + \sum_{i=1}^N A_i \cdot e^{-13.8 \cdot t_k / T_i}, \quad (1)$$

where the linear term $A_0(t_K - t_k)$ is associated with the noise in the room IR, t_k is the time parameter, t_K is the total length of the IR, and $k = 1, 2, \dots, K$. A_i denotes the linear amplitude of the i th exponential decay function, T_i is the decay time of the i th decay function, and N corresponds to the total number of slopes. The algorithm *MELT* is modified to directly extract decay times T_i and corresponding intensities A_i from an EDF. Detailed mathematical formulations are presented in the [Appendix](#), following the derivations of Shukla *et al.*²⁶⁻²⁸ and Hoffmann *et al.*²⁹

B. Numerical example

To illustrate how decay times from multi-exponential data can be obtained, an artificial EDF is constructed. The decay process is modelled according to Eq. (1) and consists

of 100 exponentially decaying functions and an additive noise term. The decay times are normally distributed with mean values of $T_1 = 1.40$ s and $T_2 = 4.60$ s and a standard deviation of 0.1, resulting in a double-slope behaviour. The amplitude of the noise is set to $A_0 = 5 \times 10^{-9}$, and the amplitudes of the decays are set to $A_1 = 0.70$ and $A_2 = 0.30$. This data are fed to the algorithm to estimate decay times from the given EDF. Through variation of the entropy weights the result with the highest probability is obtained [see Fig. 1(A)]. The result of the estimated decay times with the highest probability is shown in Fig. 1(B), where the normalized intensity spectrum (which corresponds to the linear amplitude of the decay process) is represented as a function of decay time. The local maxima of the decay times in Fig. 1(B) correspond to the mean values of the normal distributions used to obtain the artificial EDF. The peak values of the local maxima (decay times T_i and amplitudes A_i) are summed up to model the artificial EDF. The artificial EDF as well as the EDF obtained with the estimated decay times are shown in Fig. 1(C). The decay process is modelled with two exponential functions with the

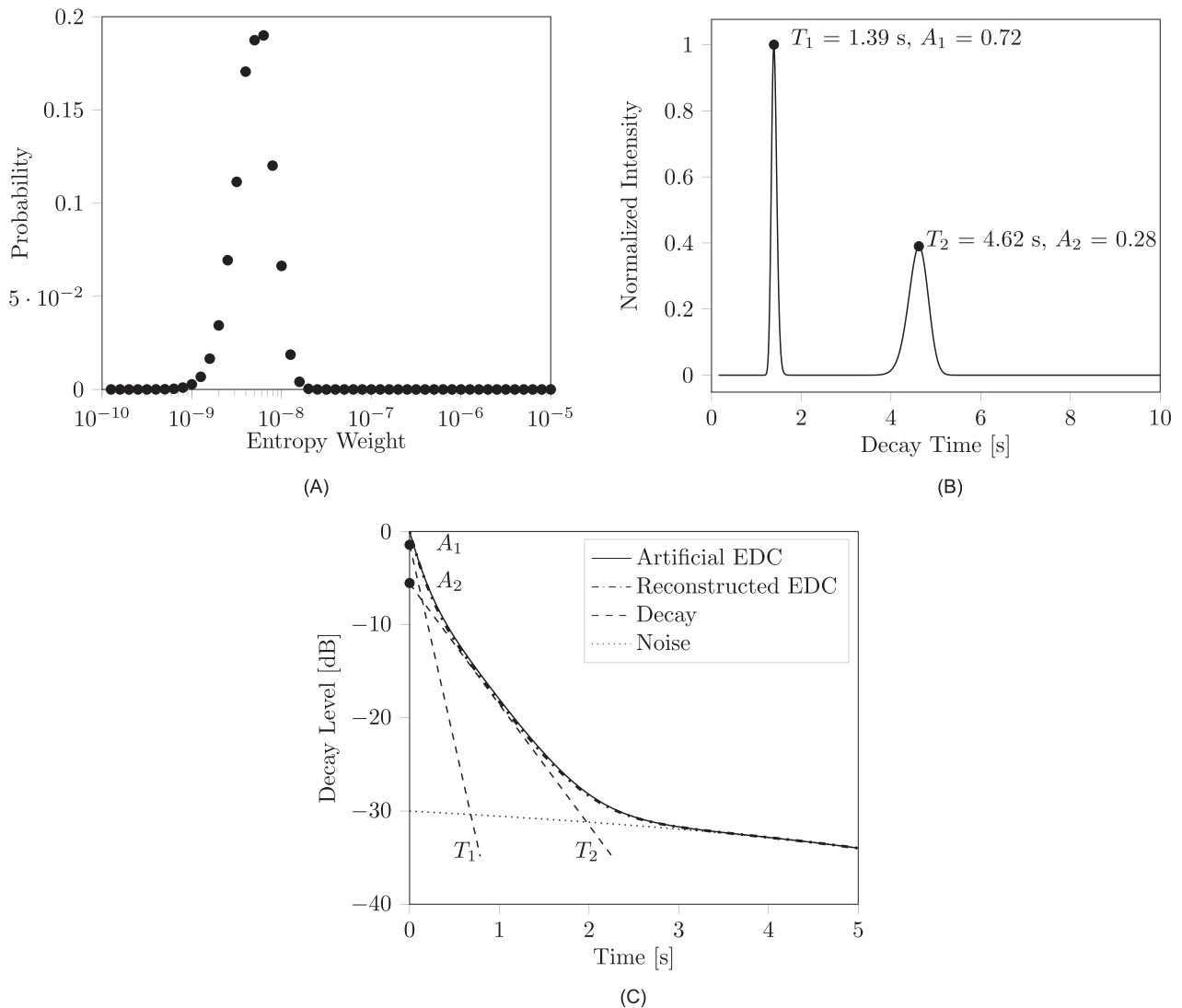


FIG. 1. (A) Variation of the entropy weights, (B) intensity spectrum of the estimated decay times, (C) artificial and reconstructed energy decay curve with the peaks of the intensities $A_1 = 0.72$, $A_2 = 0.28$, $T_1 = 1.39$ s, $T_2 = 4.62$ s, and an additive noise term at $A_0 = 5 \times 10^{-9}$.

amplitudes $A_1 = 0.72$, $A_2 = 0.28$, the corresponding decay times $T_1 = 1.39$ s and $T_2 = 4.62$ s, and an additive noise term. In practice, if absorption is concentrated on a single surface, the room modes can be separated into two groups^{5,16} (more attenuated modes and less attenuated modes). The first peak, which corresponds to the shortest decay time, can be regarded as the modes which are attenuated the most. Therefore the shortest decay time is used when calculating the absorption coefficient in Sec. IV.

IV. EXPERIMENTAL RESULTS

This section describes experimental measurements conducted to validate the benefit of using the proposed Bayesian framework for decay time estimation and absorption coefficient measurements. Absorption coefficients obtained with conventional reverberation parameters will be compared to values obtained with the Bayesian framework. Additionally, a theoretical absorption coefficient serves as a reference value for comparison.

A. Measurements

Measurements are carried out in a box-shaped reverberation chamber ($V = 241$ m³) at the Technical University of Denmark. The absorption coefficient of a porous sample is measured according to ISO 354 (Ref. 1) in the chamber with 20 panel diffusers and without diffusers. The porous sample with a flow resistivity of 12.9 kPa s/m² has a total area of 10.8 m² (3.6 m × 3.0 m × 0.1 m) and its sides are covered by a wooden frame. Figure 2 shows the room setup, with the porous absorber placed on the floor of the chamber and acrylic panel diffusers hung from the ceiling. IRs are measured at 12 independent source-receiver positions and the EDF is calculated by Schroeder backward integration for each IR.¹⁴ EDFs are averaged over all measurement positions to obtain a single function. Conventional reverberation parameters like the early decay time (EDT), T_{20} , and T_{30} are calculated by applying LR to decay ranges 0 to -10 dB,



FIG. 2. Porous absorber placed on the floor in the reverberation chamber ($V = 241$ m³), absorber with sides covered by a wooden frame and a total area of $S = 10.8$ m².

-5 to -25 dB, and -5 to -35 dB, respectively. The initial decay time is obtained with the proposed framework.

The equivalent absorption area A of a porous sample is calculated according to¹

$$A = \frac{55.3 \cdot V}{c} \cdot \left(\frac{1}{T_e} - \frac{1}{T_a} \right) - 4 \cdot V \cdot m, \quad (2)$$

where V denotes the total volume of the chamber, c is the speed of sound, m is the attenuation coefficient, T_e is the RT in the undamped chamber (empty), and T_a is the RT in the damped chamber (with the absorber). The Sabine absorption coefficient for octave bands from 125 to 4000 Hz is calculated according to

$$\alpha = \frac{A}{S}, \quad (3)$$

where S denotes the total area of the sample.

B. Theoretical absorption coefficient

The random incidence absorption coefficient for an infinite absorber can be calculated as follows:^{33,34}

$$\alpha_{\text{random}} = \int_0^{\pi/2} \alpha_{\text{inf}}(\Theta_i) \sin(2\Theta_i) d\Theta_i, \quad (4)$$

where $\alpha_{\text{inf}}(\Theta_i)$ is the oblique incidence absorption coefficient at incidence angle Θ_i .

In a reverberation chamber, the measured absorption coefficient is typically overestimated due to diffraction phenomena evoked by the edges of the finite-size sample. This size-effect is particularly marked at low frequencies (below 1 kHz). A size-corrected random incidence absorption coefficient is derived by Thomasson¹³ as follows:

$$\alpha_{\text{theory}} = 2 \int_0^{\pi/2} \frac{4\text{Re}(Z_s)}{|Z_s + \bar{Z}_r|^2} \sin(\Theta) d\Theta, \quad (5)$$

where Z_s denotes the surface impedance and \bar{Z}_r the radiation impedance which is a function of shape, size, frequency, and is averaged over azimuthal angles from 0 to 2π . The main assumptions are local reaction, infinite baffle, and flush-mounting of the absorber to the infinite baffle. Although the theoretical absorption coefficient cannot be regarded as the “true” absorption coefficient of the sample, it is chosen to be a reference in this paper for the following reasons. Such a coefficient is a comprehensible comparison value as opposed to ISO results. Several round robin tests have shown large deviations in the results from chamber to chamber, raising serious doubts regarding the reliability of the obtained coefficients.⁶⁻⁸ Besides, the derivation by Thomasson makes it possible to account for the finite size of the sample and has therefore been widely used in the literature.³⁵⁻³⁸

In the following, α_{theory} in Eq. (5) is calculated based on a transfer matrix model for the case of a single layer of porous material with a rigid backing.¹¹ The surface impedance and complex wave number are calculated with Miki’s model,¹² which is a modified version of the Delany and Bazley

TABLE I. Theoretical size-corrected absorption coefficient for a porous absorber with a flow resistivity of 12.9 kPa s/m² calculated with Miki's model and Thomasson's size correction.

| f (Hz) | 125 | 250 | 500 | 1000 | 2000 | 4000 |
|--------------------------|------|------|------|------|------|------|
| α_{theory} | 0.86 | 1.24 | 1.14 | 1.03 | 0.98 | 0.98 |

model,³⁹ and gives improved results at low frequencies. The calculated results for the theoretical absorption coefficients are shown in Table I. Thomasson's size-corrected absorption coefficient for a finite sample of 3.6 m × 3 m × 0.1 m backed by a rigid wall exceeds unity for the octave bands centered at 250 Hz, 500 Hz, and 1 kHz.

For comparison, the deviation $\Delta\alpha$ of the measured absorption coefficient from the theoretical absorption coefficient α_{theory} is calculated with

$$\Delta\alpha = \alpha_{\text{theory}} - \alpha, \quad (6)$$

where α is the Sabine absorption coefficient calculated according to Eqs. (2) and (3) with different reverberation parameters: EDT, T_{20} , T_{30} , and the decay time T_1 .

C. Linear regression (LR)

To illustrate how conventional reverberation parameters EDT, T_{20} , and T_{30} vary in case of multi-exponential data, results are shown for one frequency band. In Fig. 3 the energy decay curve, as well as the regression lines for the damped condition at 500 Hz, are shown with and without panel diffusers. The decay times EDT, T_{20} , and T_{30} vary from 2.90 to 3.44 s without diffusing elements, indicating a multi-exponential decay due to the increase of the RT when the evaluation range is increased. When diffusing elements are added to the room, the reverberation parameters EDT, T_{20} , and T_{30} vary from 2.12 to 2.21 s, still indicating a slightly curved decay but much less than in the case without

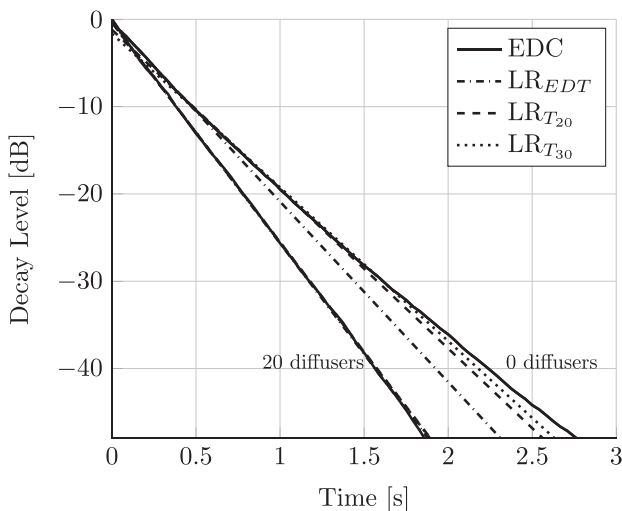


FIG. 3. Energy decay curve and LR for $f=500$ Hz in the damped condition for room acoustic parameter without diffusers EDT = 2.90 s, $T_{20} = 3.29$ s, $T_{30} = 3.44$ s, and with diffusers EDT = 2.12 s, $T_{20} = 2.21$ s, $T_{30} = 2.21$ s.

TABLE II. Absorption coefficient α for the 500 Hz band calculated with different RTs: EDT, T_{20} , and T_{30} , with and without diffusers.

| RT/ α | EDT | T_{20} | T_{30} |
|----------------------------|------|----------|----------|
| α with 0 diffusers | 0.86 | 0.8 | 0.7 |
| α with 20 diffusers | 1.20 | 1.18 | 1.18 |

diffusers. The RT is decreased significantly compared to the case without panels, since the sound waves are redirected onto the absorber by the panels. T_{30} is decreased from 3.44 to 2.12 s when diffusers are added, also EDT is reduced from 2.90 to 2.12 s. The results are in agreement with investigations carried out in Ref. 19.

To investigate how the evaluation range for reverberation parameters influences the absorption coefficient, α is calculated for $f=500$ Hz with EDT, T_{20} , and T_{30} with and without diffusing elements. Table II shows the absorption coefficients calculated with EDT, T_{20} , and T_{30} . The values for α vary between 0.70 and 0.86 without diffusing elements and from 1.18 to 1.20 with diffusing elements. The absorption coefficient decreases when the evaluation range for the decay parameters is increased. Therefore the absorption coefficient is higher when EDT is used instead of T_{20} or T_{30} . This is in agreement with results in Ref. 4, where the author shows that the initial part of the EDF contains the mean of all excited modes and should be used to calculate α rather than the late part of the EDF. Furthermore the author concludes that the later part of the EDF only contains the less attenuated modes, which will lead to questionable results when used to calculate the absorption coefficient.

Table III shows the absorption coefficients without any diffusing elements, calculated from 125 Hz to 4 kHz with the reverberation parameter T_{20} (ISO 354 stipulates to use T_{20}) and the deviation from the theoretical values. The absorption coefficients are lower than the theoretical values in the entire frequency range. Due to the multi-exponential nature of the EDF, using LR to obtain T_{20} will underestimate the absorption coefficient.

Table IV shows the RTs T_{20} and the absorption coefficient obtained with diffusers. In this case the absorption coefficient is increased and exceeds the theoretical values at the 500 Hz band and above. At the 250 Hz band the absorption coefficient is significantly increased compared to the case without diffusing elements from 0.75 to 1.03. At the 125 Hz band the absorption coefficient is slightly increased from 0.37 to 0.39. It is expected that the absorption coefficient increases when diffusing elements are added to the chamber because the sound waves are redirected onto the absorber by the

TABLE III. RT T_{20} in the undamped ($T_{20,\text{empty}}$) and damped ($T_{20,\text{absorber}}$) conditions, resulting absorption coefficient and deviation $\Delta\alpha$. No diffusers are installed.

| f (Hz) | 125 | 250 | 500 | 1000 | 2000 | 4000 |
|--------------------------|-------|-------|-------|------|------|------|
| $T_{20,\text{empty}}$ | 18.59 | 15.04 | 12.22 | 9.84 | 6.19 | 3.69 |
| $T_{20,\text{absorber}}$ | 6.79 | 3.64 | 3.29 | 3.25 | 2.83 | 2.08 |
| $\alpha_{T_{20}}$ | 0.37 | 0.75 | 0.8 | 0.74 | 0.70 | 0.75 |
| $\Delta\alpha$ | 0.49 | 0.49 | 0.34 | 0.29 | 0.28 | 0.23 |

TABLE IV. RTs T_{20} in the undamped ($T_{20,\text{empty}}$) and damped ($T_{20,\text{absorber}}$) conditions, resulting absorption coefficient and deviation $\Delta\alpha$. 20 panel diffusers are hung from the ceiling.

| f (Hz) | 125 | 250 | 500 | 1000 | 2000 | 4000 |
|--------------------------|-------|-------|-------|-------|-------|-------|
| $T_{20,\text{empty}}$ | 13.93 | 13.27 | 11.12 | 9.06 | 5.82 | 2.39 |
| $T_{20,\text{absorber}}$ | 5.59 | 2.77 | 2.39 | 2.37 | 2.08 | 1.62 |
| $\alpha_{T_{20}}$ | 0.39 | 1.03 | 1.18 | 1.12 | 1.11 | 1.16 |
| $\Delta\alpha$ | 0.47 | 0.21 | -0.04 | -0.09 | -0.13 | -0.18 |

diffusers. However, at high frequencies the absorption coefficient is overestimated compared to the theoretical values, although the deviation from α_{theory} is decreased compared to the case without diffusers in the chamber.

D. Use of shortest decay time

The proposed Bayesian framework is applied instead of the LR to estimate multiple decay parameters as described in Sec. III. Decay parameters are calculated for each octave band from 125 Hz to 4 kHz. In Fig. 4 the results for the decay times and intensities are plotted in the undamped (left) and damped (right) conditions without diffusing elements. In the entire frequency range two distinct peaks are detected, indicating a double-slope behaviour (i.e., a multi-exponential decay).

Table V shows the obtained absorption coefficients calculated in octave bands with Sabine's equation using the first peak from the estimated decay times. A good agreement between the theoretical and estimated absorption coefficients is achieved at the 250 Hz band and above. At the 125 Hz band the absorption coefficient obtained with the initial decay time is increased compared to the values obtained with T_{20} from 0.37 to 0.48. For better illustration, Fig. 5 shows the absorption coefficient as a function of frequency, calculated with T_{20} with and without diffusers, and with the initial decay time T_1 without diffusers. The theoretical values are superimposed. Although no diffusers are present, the absorption coefficients obtained with the initial decay time estimated with the proposed method are in very good agreement with α_{theory} above the 250 Hz band. The absorption coefficient obtained with T_{20} without diffusers is underestimated compared to the other values in the entire frequency range. With diffusers the absorption coefficient at the 500 Hz band and above is overestimated compared to the theoretical absorption coefficient.

In Table VI the relative error between the theoretical absorption coefficient and the calculated absorption coefficients with and without diffusing objects is summarized. The smallest deviation from α_{theory} is obtained with absorption coefficients calculated with the initial decay time with the proposed framework. The error between α_{T_1} and α_{theory} above the 250 Hz band is less than 5%. At the 125 Hz band the theoretical absorption coefficient exceeds the calculated value. The deviation at 125 Hz could be due to the fact that the theoretical absorption coefficient is calculated by giving equal weights to all angles of incidence, whereas in the reverberation chamber it cannot be assumed that below the Schroeder frequency the incident sound on the absorber is uniformly distributed over all possible directions.

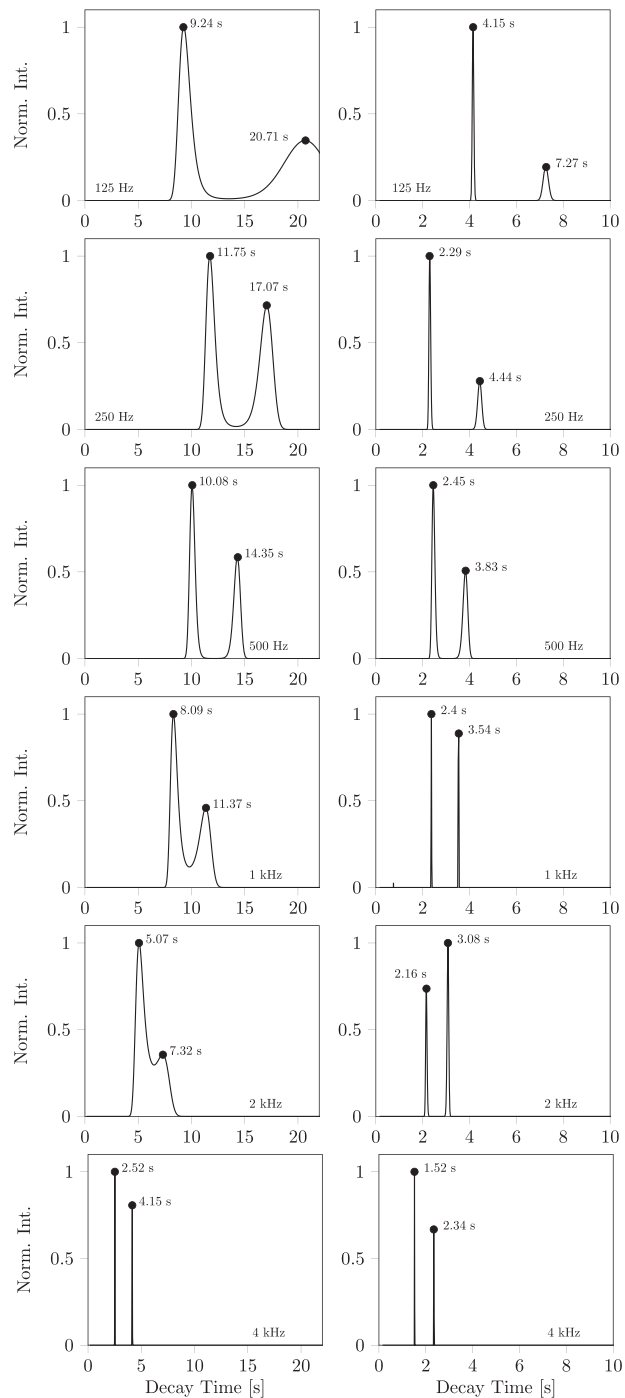


FIG. 4. Estimated normalized intensities of decay times from 125 to 4000 Hz for undamped (left) and damped (right) conditions and the corresponding peak values of the decay times. The first peak corresponds to the value used for calculating the absorption coefficient.

V. DISCUSSION

In this study, measurements are conducted in a box-shaped reverberation chamber with absorption concentrated on one of its walls, as such sound field allows separating the room modes into two groups^{3,16} (fast decaying and slow decaying), and thus provides a tractable environment to validate the methodology. Note however that additional mode groups (and therefore, additional decay times) can be considered to achieve higher accuracy, or in more complex environments.

TABLE V. Initial decay times in the undamped (T_{empty}) and damped (T_{absorber}) conditions, resulting absorption coefficient α , and deviation $\Delta\alpha$. No diffusers are installed.

| f (Hz) | 125 | 250 | 500 | 1000 | 2000 | 4000 |
|-----------------------|------|-------|-------|------|------|------|
| T_{empty} | 9.24 | 11.75 | 10.08 | 8.09 | 5.07 | 2.52 |
| T_{absorber} | 4.15 | 2.29 | 2.45 | 2.4 | 2.16 | 1.52 |
| α | 0.48 | 1.26 | 1.11 | 1.05 | 0.96 | 0.94 |
| $\Delta\alpha$ | 0.38 | -0.02 | 0.03 | 0.02 | 0.05 | 0.04 |

It is widely accepted that without diffusing objects the sound field is not sufficiently diffuse to calculate the Sabine absorption coefficient. The results of this investigation indicate that reasonable absorption coefficients can be estimated without diffusing elements if the initial decay time, calculated via the Bayesian framework, is used. This means that the initial part of the decay process contains valuable information that should not be neglected. Care has to be taken at low frequencies, where the geometry of the room and the modal distribution has a great impact on the measured absorption coefficient. In practice, it cannot be assumed that the incident sound on the absorber is uniformly distributed over all possible directions. Therefore the measurement results in chambers of different volumes will differ from each other, depending on the modal distribution and the placement of the sample.

Predicting the influence of diffusing elements on the decay process is a very challenging task. Although it can be assumed that through the use of diffusers the grazing and non-grazing sound fields will be less distinct, the effect of adding diffusers seems to vary over the frequency range. When diffusing elements are introduced, the decay process can be regarded almost linear at mid and high frequencies, when an absorber is placed on the floor. However, the absorption coefficient is still underestimated in the low frequency range and overestimated in the mid and high frequency range compared to the theoretical absorption coefficient. In this investigation installing diffusers did not provide a solution to obtain reasonable absorption coefficients. As already

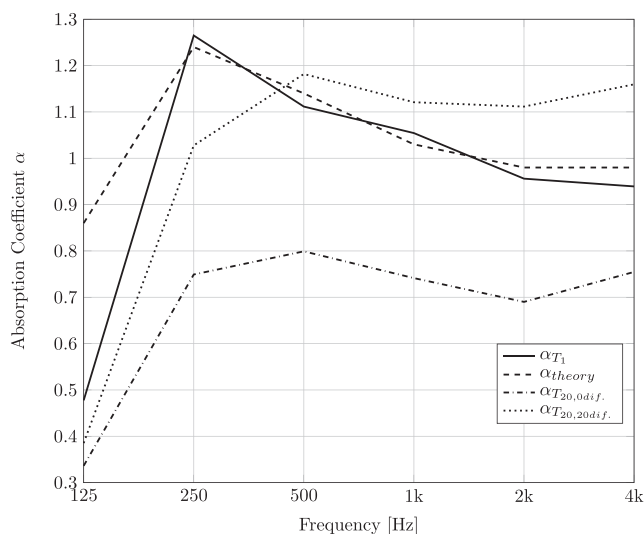


FIG. 5. Absorption coefficient α_{T_1} calculated with the shortest decay time compared to α_{theory} , $\alpha_{T_{20,0\text{dif.}}}$, and $\alpha_{T_{20,20\text{dif.}}}$.

TABLE VI. Relative error ε in % between the theoretical absorption coefficient and the absorption coefficient calculated with reverberation parameter T_{20} without (0 dif.) and with (20 dif.) diffusers, as well as with the decay time T_1 without (0 dif.) diffusers.

| f (Hz)/ ε (%) | 125 | 250 | 500 | 1000 | 2000 | 4000 |
|---|-------|-------|-------|-------|-------|-------|
| $\varepsilon_{\alpha_{T_{20,0\text{dif.}}}}$ | 56.98 | 39.52 | 29.82 | 28.16 | 28.57 | 23.47 |
| $\varepsilon_{\alpha_{T_{20,20\text{dif.}}}}$ | 54.65 | 16.94 | 3.51 | 8.73 | 13.27 | 18.37 |
| $\varepsilon_{\alpha_{T_1,0\text{dif.}}}$ | 44.19 | 1.61 | 2.63 | 1.94 | 2.04 | 4.08 |

mentioned in the beginning, other researchers pointed out that diffusing elements introduce uncertainties that cannot be considered or modelled in an accurate way.³

It is important to point out that this work does not deal with the curvature of decays as a diffuseness measure, since the IRs used for the analysis were measured with an omnidirectional microphone which does not contain any directional information of the sound field. Recent work⁴⁰ focuses on directional EDFs as a diffuseness measure. The quantification of the isotropy of the sound field is investigated in Ref. 41. Furthermore, this work does not deal with the quantification of double slopes like in Ref. 42, where ratios were calculated using linear fits with fixed ranges. Those methods are a rough estimation of whether or not a multi-exponential decay is present but they do not provide a solution to calculate accurate decay parameters.

VI. CONCLUSION

This work has discussed the use of the initial decay time to calculate the absorption coefficient from measurements conducted in the reverberation chamber. Initial decay times as well as multiple decay parameters were estimated with a Bayesian framework from EDFs. The need for such a framework to estimate decay parameters from multiple-sloped decays as an alternative to LR has been argued with the fact that energy decays are not linear in most real world scenarios, especially in reverberation chambers at low frequencies and with uneven distribution of absorption.

Absorption coefficients calculated with the initial decay time were compared to the theoretical absorption coefficients calculated with a transfer matrix model combined with Miki's model including Thomasson's size correction. A good agreement was achieved in the frequency range from the 250 Hz band and above. In the 125 Hz band the theoretical absorption coefficient exceeded the calculated values due to the assumption of the sound incidence being uniformly distributed over all possible directions, which is not the case in the reverberation chamber. The results presented in this work included measurements without diffusing objects like panel or boundary diffusers, which is in contrast to the well-established approach in the reverberation chamber. The effect of diffusers on the decay process and on the sound field in general still poses a challenging task and such analysis is beyond the scope of this work.

Many round robin tests in the past have proven the poor interlaboratory reproducibility of absorption coefficient measurements. This work raises the question, if the poor

reproducibility is to be owed to the evaluation of the decay parameters with LR. If a multi-exponential decay is present, using LR to obtain decay parameters will lead to questionable results. A future round robin test could evaluate if the method proposed in this paper provides a reliable alternative for measuring the Sabine absorption coefficient in reverberation chambers.

The proposed Bayesian method to obtain decay parameters is not restricted to laboratories. It is anticipated that the framework may also find important applications in measuring representative decay parameters in small and mid-sized room (e.g., in classrooms or offices, where absorption is concentrated on the ceiling).

APPENDIX: BAYESIAN DECAY TIME ESTIMATION

The mathematical formulations follow the derivations of Shukla *et al.*^{26–29} Brief parts of the acoustic application of the method have been published in Ref. 43, where different approaches for calculating decay parameters from multi-exponential EDFs were compared.

The aim is to calculate the causal factors (decay terms with corresponding intensities) from a set of observations (EDFs) that produced them. The inverse problem can be written in the form of a Fredholm integral as

$$D(y) = \int_a^b K(\tau, t)\Phi(\tau)d\tau + \nu(t), \quad (\text{A1})$$

where $D(y)$ represents the measured data, $\Phi(\tau)$ is the intensity as a function of decay time (function to be obtained), and $\nu(t)$ denotes the noise in the data. The kernel function follows as:

$$K(\tau, t) = \tau^{-1}e^{t/\tau}. \quad (\text{A2})$$

Equation (A1) can be written as a system of linear algebraic equations:

$$d_j = \sum_{\mu=1}^{n_{\text{mod}}} k_{j\mu}\phi_{\mu} + n_j, \quad j = 1, \dots, n_{\text{dat}} \quad (\text{A3})$$

and in matrix notation

$$D = K\Phi + N, \quad (\text{A4})$$

where the indices *dat* and *mod* refer to the measured data and the model, respectively.

The proposed algorithm uses a quantified maximum entropy approach, estimating a positive additive distribution (PAD) from noisy and incomplete data. Knowing a number of possible solutions A , B , and C , one can describe them as conditional probabilities $pr(A|D)$, $pr(B|D)$, $pr(C|D)$. If Φ was to represent a particular solution, one needs the probability distribution $pr(\Phi|D)$ subject to Φ . This is not directly obtainable from the given dataset D . However, the reversed conditioning $pr(D|\Phi)$ —better known as the likelihood function—is obtainable. The likelihood function can be written as

$$pr(D|\Phi) = \prod_{j=1}^{n_{\text{dat}}} \frac{1}{\sqrt{2\pi\sigma^2}} \exp\left(-\frac{1}{2\sigma^2} \left[d_j - \sum_{\mu=1}^{n_{\text{mod}}} k_{j\mu}\phi_{\mu}\right]^2\right). \quad (\text{A5})$$

The model for estimating the unknown function can be found in Bayes theorem,

$$pr(\Phi|D) = \frac{pr(\Phi)pr(D|\Phi)}{pr(D)}, \quad (\text{A6})$$

with $pr(D)$ being a normalizing factor to ensure that the sum of the probabilities of all possible solutions is equal to one. This formula represents one of the most relevant mathematical fundamentals of data analysis. Considering the $pr(D|\Phi)$ as given and $pr(D)$ being a normalizing constant, the only remaining unknown term is the prior probability distribution of Φ , denoted as $pr(\Phi)$. The pointwise probability

$$pr(\Phi|m, \alpha) \propto \exp((\alpha S(\Phi, m))), \quad (\text{A7})$$

reflects the most important part of the quantified entropic prior.⁴⁴ The two parameters m and α represent a model for Φ and an inverse measure of the expected spread of values of Φ about m . The pointwise joint probability distribution is given by

$$pr(\Phi, D|m, \alpha) = \left(\frac{\alpha}{2\pi}\right)^{r/2} \prod \frac{1}{\sqrt{2\pi\sigma^2}} \times \exp\left(\alpha S(\Phi, m) - \frac{1}{2}C(\Phi, D)\right), \quad (\text{A8})$$

where the function $S(\Phi, m)$ denotes the Shannon–Jaynes entropy. The pointwise joint probability is proportional to the posterior probability by

$$pr(\Phi|m, \alpha, D) = \frac{pr(\Phi, D|m, \alpha)}{pr(D|m, \alpha)}. \quad (\text{A9})$$

Since the Shannon–Jaynes entropy is a convex function with negative definite curvature and $C(f)$ a positive curvature, the posterior probability $pr(\Phi|m, \alpha, D)$ has a unique maximum at

$$\alpha \frac{\partial S}{\partial \Phi} - \frac{1}{2} \frac{\partial C}{\partial \Phi} = 0 \quad \text{at} \quad \Phi = \hat{\Phi}. \quad (\text{A10})$$

The obtained distribution $\hat{\Phi}$ is the single most probable PAD. The choice of a well-guessed kick-off solution is essential as it has a stabilizing and regularizing effect. Furthermore it shortens the time needed for the solution to converge. For this particular reason the algorithm uses a general optimal linear filter to compute a good kick-off solution. Designing a filter in this case means constructing a filter matrix F to solve the inverse problem by satisfying a minimization criterion. This is chosen to be the mean squared error between the “real” Φ and the one extracted by the filter F ,

$$\sum_v p_v \langle |F(K\Phi_v - D)|^2 \rangle_N = \min. \quad (\text{A11})$$

To obtain the coefficients of the filter F , the left side of Eq. (A11) has to be differentiated with respect to F and then equated to zero to satisfy the minimization criterion. This leads to a filter F to obtain the regularized solution

$$\Phi_r = FD, \quad (\text{A12})$$

with

$$F = \frac{C_\Phi K^T}{KC_\Phi K^T + C_N}, \quad (\text{A13})$$

where

$$C_\Phi = \sum_v p_v \Phi_v \Phi_v^T; \quad C_N = \langle NN^T \rangle. \quad (\text{A14})$$

¹ISO 354:2003, "Acoustics—Measurement of sound absorption in a reverberation room" (International Organization for Standardization, Geneva, Switzerland, 2003).

²W. Sabine, *Collected Papers on Acoustics* (Harvard University Press, Cambridge, 1922), pp. 3–68.

³F. V. Hunt, L. L. Beranek, and D. Y. Maa, "Analysis of sound decay in rectangular rooms," *J. Acoust. Soc. Am.* **11**(1), 80–94 (1939).

⁴H. Kuttruff, "Eigenschaften und Auswertung von Nachhallkurven (Characteristics and analysis of decay curves)," *Acta Acust. Acust.* **8**(4), 273–280 (1958).

⁵E. Nilsson, "Decay processes in rooms with non-diffuse sound fields. Part I: Ceiling treatment with absorbing material," *Build. Acoust.* **11**(1), 39–60 (2004).

⁶W. Davern and P. Dubout, "First report on Australasian comparison measurements of sound absorption coefficients," DBR Special Report, CSIRO Division of Building Research, Highett (1980).

⁷ASTM, "Interlaboratory study to establish precision statements for ASTM C423," Research Report E33-1010 (2006).

⁸A.-C. Thysell, "Test codes for suspended ceilings—Sound absorption RRT," Tyrens AB project no. 224628, Tyrens, A. B. Sweden (2011).

⁹L. Savioja and U. P. Svensson, "Overview of geometrical room acoustic modeling techniques," *J. Acoust. Soc. Am.* **138**(2), 708–730 (2015).

¹⁰M. Vorländer, "Computer simulations in room acoustics: Concepts and uncertainties," *J. Acoust. Soc. Am.* **133**(3), 1203–1213 (2013).

¹¹J. Allard, *Propagation of Sound in Porous Media: Modelling Sound Absorbing Materials* (Elsevier Science Publishers, Essex, England, 1993), p. 38.

¹²Y. Miki, "Acoustical properties of porous materials. Modifications of Delany-Bazley models," *J. Acoust. Soc. Am.* **11**(1), 19–24 (1990).

¹³S.-I. Thomasson, "On the absorption coefficient," *Acta Acust. Acust.* **44**(4), 265–273 (1980).

¹⁴M. R. Schroeder, "New method of measuring reverberation time," *J. Acoust. Soc. Am.* **37**(3), 409–412 (1965).

¹⁵P. Bruel, "The enigma of sound power measurements at low frequencies," *Bruel & Kjaer Tech. Rev.* **34**, 3–40 (1978).

¹⁶F. Jacobsen, *Fundamentals of General Linear Acoustics* (John Wiley & Sons, United Kingdom, 2013), pp. 151–153.

¹⁷F. Jacobsen, "Decay rates and wall absorption at low frequencies," *J. Sound Vib.* **81**(3), 405–412 (1982).

¹⁸ISO 3382-2:2008, "Acoustics—Measurement of room acoustic parameters—Part 2: Reverberation time in ordinary rooms" (International Organization for Standardization, Geneva, Switzerland, 2008).

¹⁹E. Nilsson, "Decay processes in rooms with non-diffuse sound fields. Part II: Effect of irregularities," *Build. Acoust.* **11**(2), 133–143 (2004).

²⁰J. Balint, F. Muralter, M. Nolan, and C.-H. Jeong, "Energy decay curves in reverberation chambers and the influence of scattering objects on the absorption coefficient of a sample," in *Conference Proceedings Euronoise 2018*, Crete, Greece (2018), pp. 2025–2030.

²¹J. Balint and G. Graber, "Gekruemmte Abklingkurven in Hallräumen (Curved energy decays in reverberation rooms)," in *Proceedings of the 44th Annual Meeting for Acoustics DAGA*, Munich, Germany (2018).

²²N. Xiang and P. M. Goggans, "Evaluation of decay times in coupled spaces: Bayesian parameter estimation," *J. Acoust. Soc. Am.* **110**(3), 1415–1424 (2001).

²³N. Xiang and P. M. Goggans, "Evaluation of decay times in coupled spaces: Bayesian decay model selection," *J. Acoust. Soc. Am.* **113**(5), 2685–2697 (2003).

²⁴N. Xiang and T. Jasa, "Evaluation of decay times in coupled spaces: An efficient search algorithm within the Bayesian framework," *J. Acoust. Soc. Am.* **120**(6), 3744–3749 (2006).

²⁵N. Xiang, P. Goggans, T. Jasa, and P. Robinson, "Bayesian characterization of multiple-slope sound energy decays in coupled-volume systems," *J. Acoust. Soc. Am.* **129**(2), 741–752 (2011).

²⁶A. Shukla, M. Peter, and L. Hoffmann, "Analysis of positron lifetime spectra using quantified maximum entropy and a general linear filter," *Nuclear Instrum. Methods Phys. Res. A* **335**, 310–317 (1993).

²⁷A. Shukla, L. Hoffmann, A. Manuel, and M. Peter, "Bayesian methods for lifetime analysis," *Mater. Sci. Forum* **175–178**, 939–946 (1995).

²⁸A. Shukla, L. Hoffmann, A. Manuel, and M. Peter, "Melt 4.0a a Program for Positron Lifetime Analysis," *Mater. Sci. Forum* **255–257**, 233–237 (1997).

²⁹L. Hoffmann, A. Shukla, M. Peter, B. Barbiellini, and A. Manuel, "Linear and non-linear approaches to solve the inverse problem: Applications to positron annihilation experiments," *Nuclear Instrum. Methods Phys. Res. Sec. A* **335**(1–2), 276–287 (1993).

³⁰C.-H. Jeong, S.-H. Choi, and I. Lee, "Bayesian inference of the flow resistivity of a sound absorber and the room's influence on the Sabine absorption coefficients," *J. Acoust. Soc. Am.* **141**(3), 1711–1714 (2017).

³¹N. Xiang and C. Landschoot "Bayesian inference for acoustic direction of arrival analysis using spherical harmonics," *Entropy* **21**(579), 2–21 (2019).

³²S. F. Gull and J. Skilling, "Maximum entropy method in image processing," *IEE Proc. F* **131**(6), 646–659 (1984).

³³R. K. Bryan, *Maximum Entropy and Bayesian Methods*, edited by P. F. Fougere (Kluwer, Dordrecht, 1990), Vol. 127(6), pp. 221–232.

³⁴H. Kuttruff, *Room Acoustics* (CRC Press, Boca Raton, FL, 2016), p. 302.

³⁵C.-H. Jeong, "Non-uniform sound intensity distributions when measuring absorption coefficients in reverberation chambers using a phased beam tracing," *J. Acoust. Soc. Am.* **127**(6), 3560–3568 (2010).

³⁶C.-H. Jeong, "Converting Sabine absorption coefficients to random incidence absorption coefficients," *J. Acoust. Soc. Am.* **133**(6), 3951–3962 (2013).

³⁷J. Brunskog, "The forced sound transmission of finite single leaf walls using a variational technique," *J. Acoust. Soc. Am.* **132**(3), 1482–1493 (2012).

³⁸J. Brunskog, "Sound radiation from finite surfaces," *J. Acoust. Soc. Am.* **133**(5), 3385–3385 (2013).

³⁹M. E. Delany and E. N. Bazley, "Acoustical properties of fibrous absorbent materials," *Appl. Acoust.* **3**(2), 105–116 (1970).

⁴⁰M. Berzborn and M. Vorländer, "Investigations on the directional energy decay curves in reverberation rooms," in *Conference Proceedings Euronoise 2018*, Crete, Greece (2018), pp. 2005–2010.

⁴¹M. Nolan, E. Fernandez-Grande, J. Brunskog, and C.-H. Jeong, "A wavenumber approach to quantifying the isotropy of the sound field in reverberant spaces," *J. Acoust. Soc. Am.* **143**(4), 2514–2526 (2018).

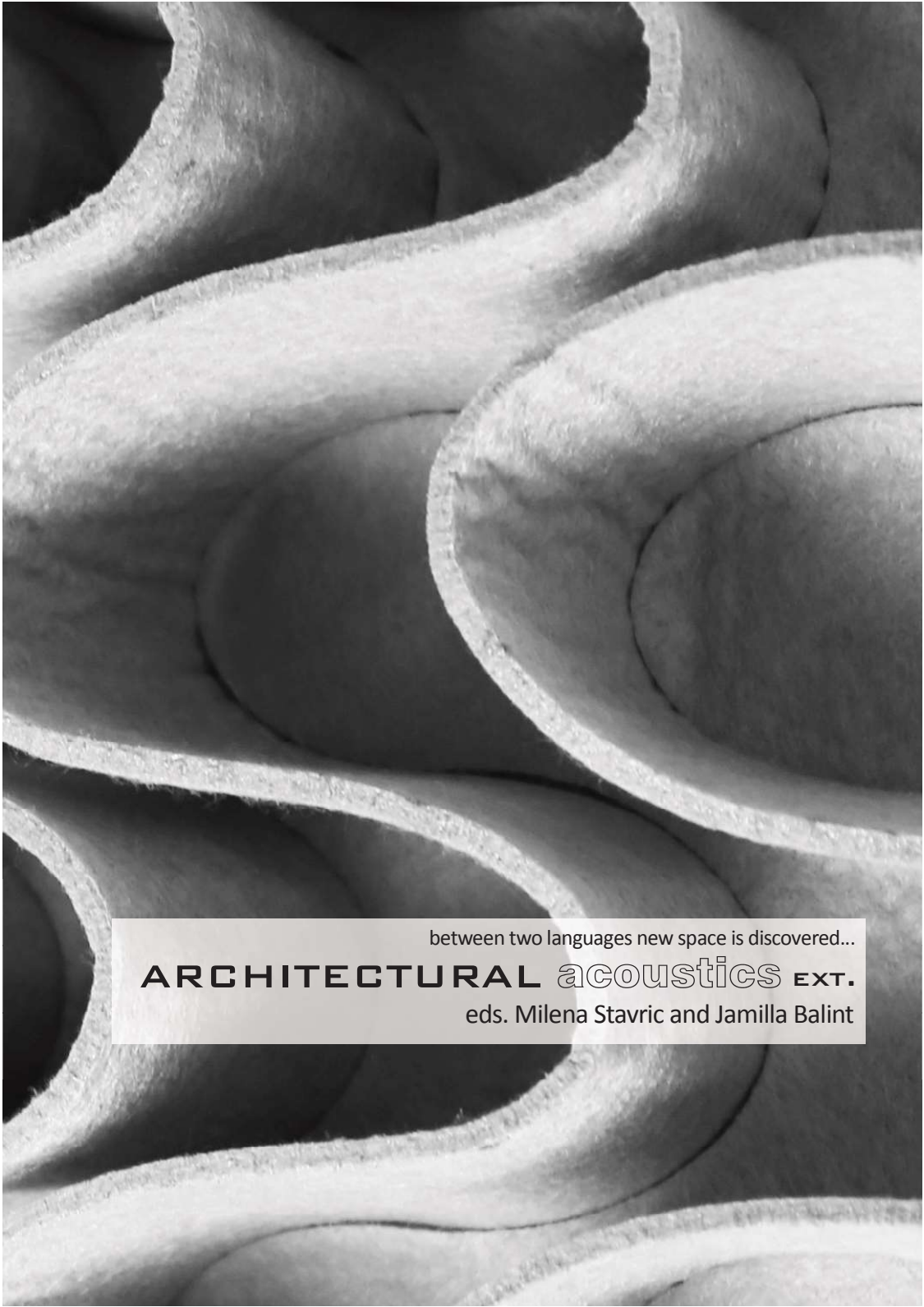
⁴²D. T. Bradley and L. M. Wang, "Quantifying the double slope effect in coupled volume room systems," *Build. Acoust.* **16**(2), 105–123 (2009).

⁴³F. Muralter and J. Balint, "Analysis tools for multi-exponential energy decay curves in room acoustics," in *Proceedings of the 45th Annual Meeting for Acoustics DAGA*, Rostock, Germany (2019).

⁴⁴J. Skilling, "Quantified maximum entropy," in *Maximum Entropy and Bayesian Methods* (Springer, New York, 1990), pp. 341–350.

Book (Ed.)

- Title: Architectural Acoustics extended, between two languages new space is discovered
- Editors: Milena Stavric, Jamilla Balint
- Published at Verlag der Technischen Universität Graz, 2019
- E-book: <https://www.tugraz-verlag.at/gesamtverzeichnis/architektur/architectural-acoustics-ext/>
- Pages: 1, 134, 135, 163

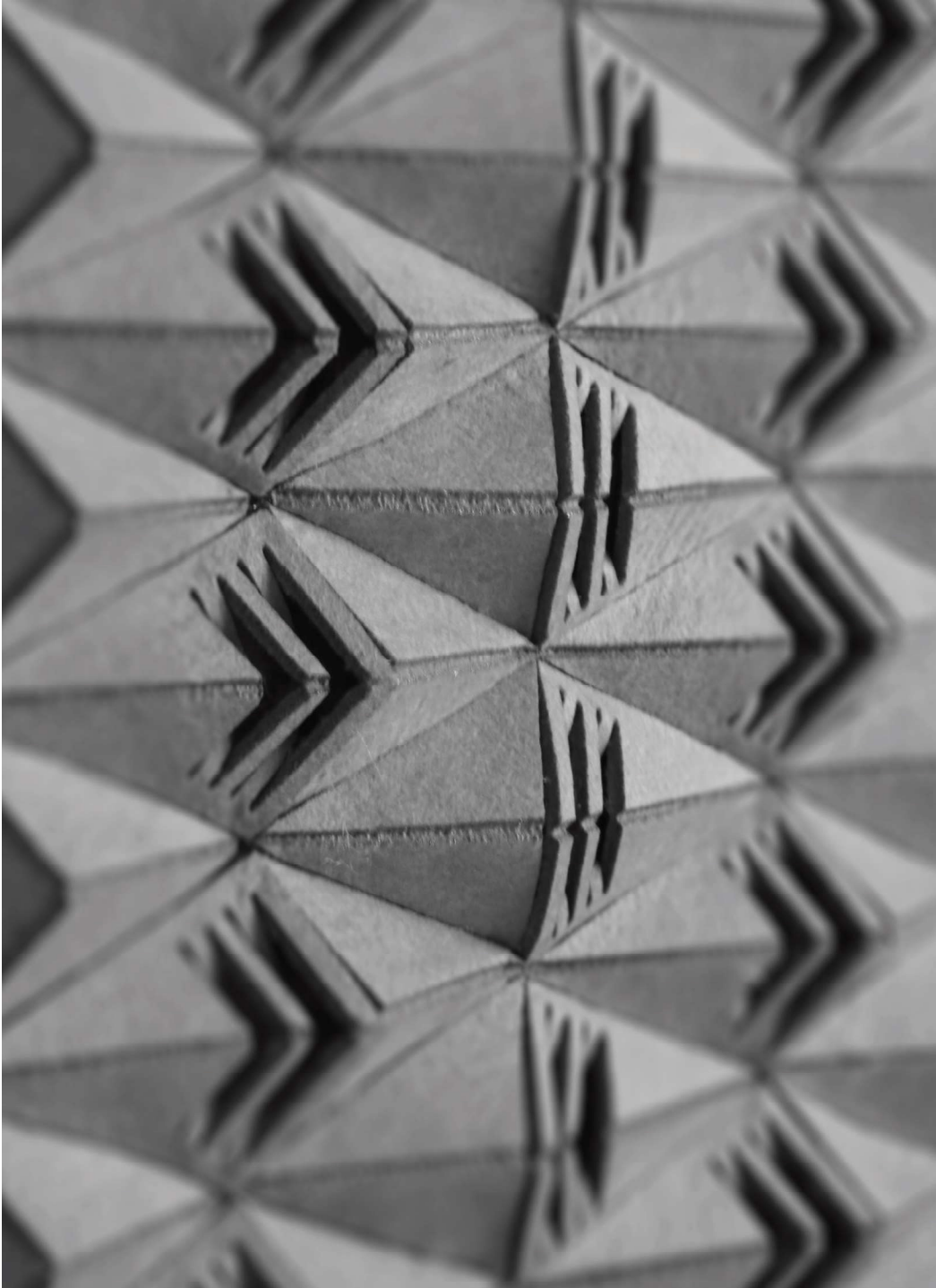


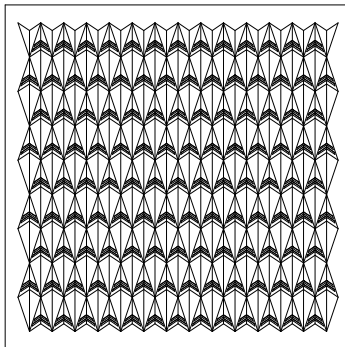
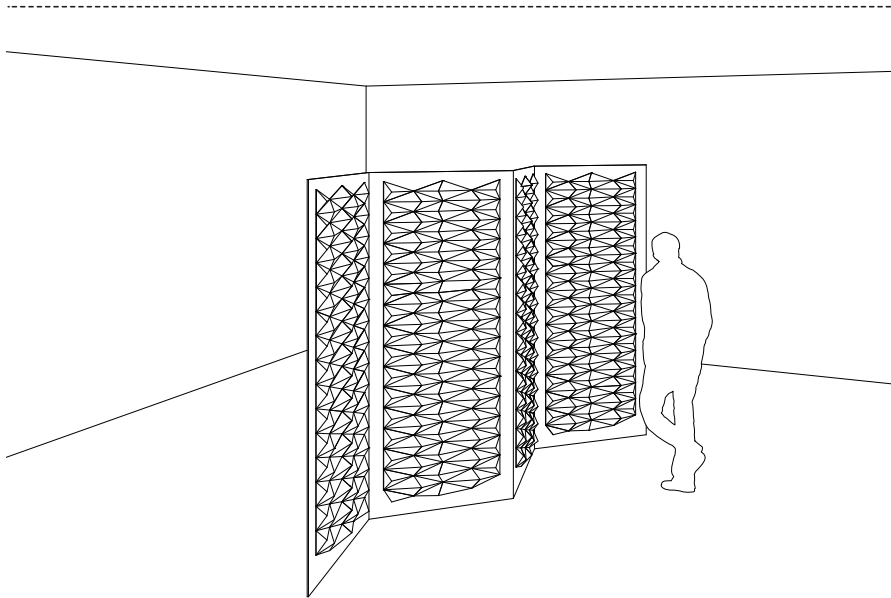
between two languages new space is discovered...

ARCHITECTURAL *acoustics* **EXT.**

eds. Milena Stavric and Jamilla Balint

132 FOLDED SURFACES / GEFALTETE OBERFLÄCHEN
diamond / Diamant





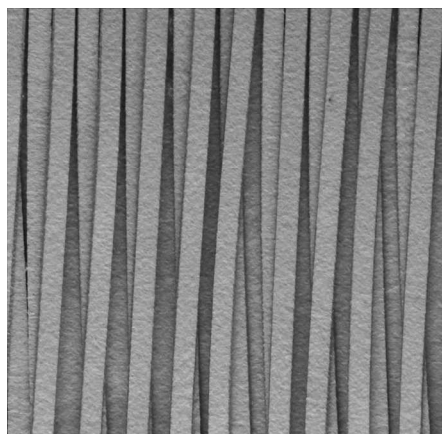
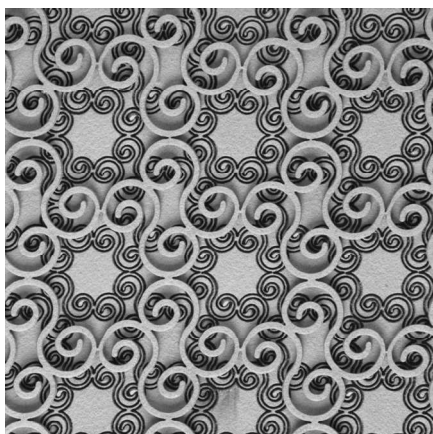
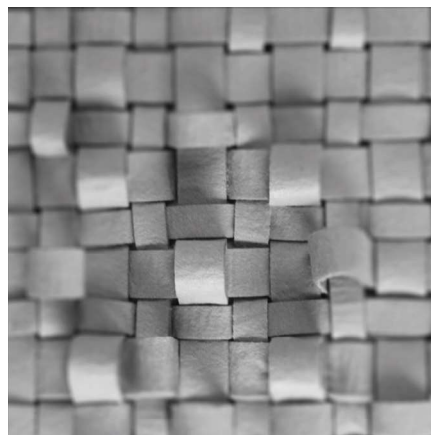
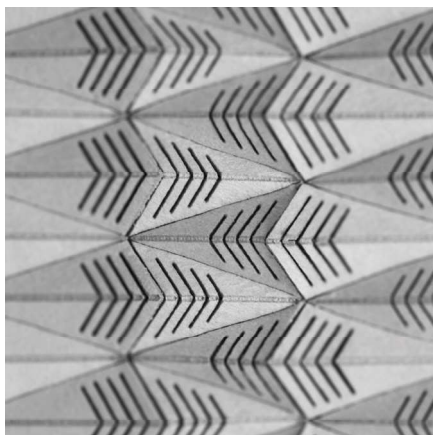
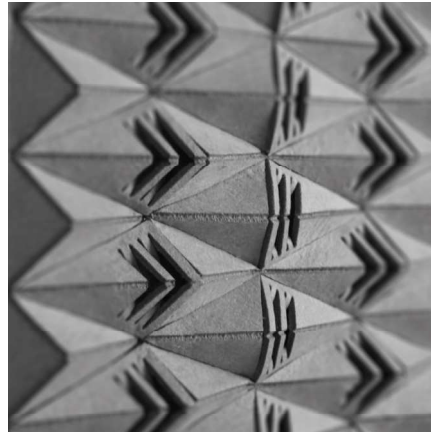
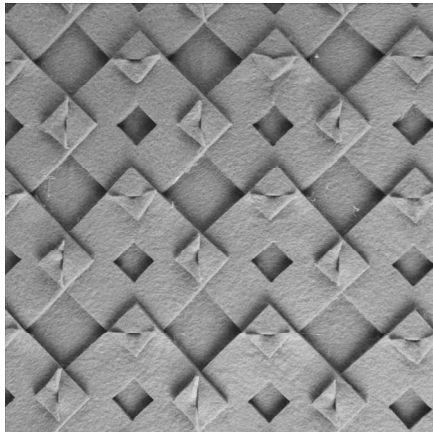
A simple design composed of individual rhombuses. The acoustic performance is enhanced by little slots in each element.

Ein einfaches Design bestehend aus Raute. Die akustische Wirkung wird durch kleine Schlitze in jedem Element optimiert.



| | | | | | | |
|----------------|------|------|------|------|------|------|
| f [Hz] | 63 | 125 | 250 | 500 | 1000 | 2000 |
| α_0 | 0.05 | 0.06 | 0.18 | 0.55 | 0.82 | 0.87 |
| α_{100} | 0.16 | 0.52 | 0.80 | 0.73 | 0.65 | 0.83 |

Absorption coefficient, felt on 25mm fiberboard, 0 mm and 100 mm air gap
 Absorptionsgrad, Filz auf 25mm Faserplatte, 0 mm und 100 mm Wandabstand

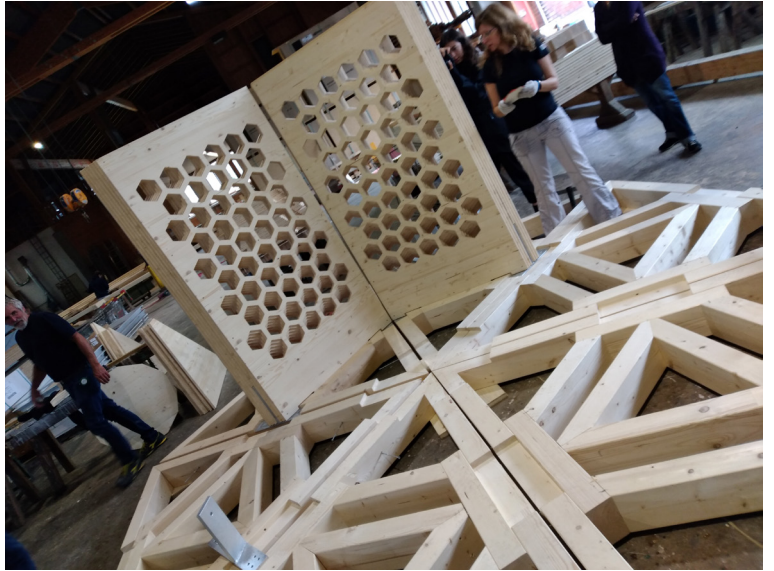


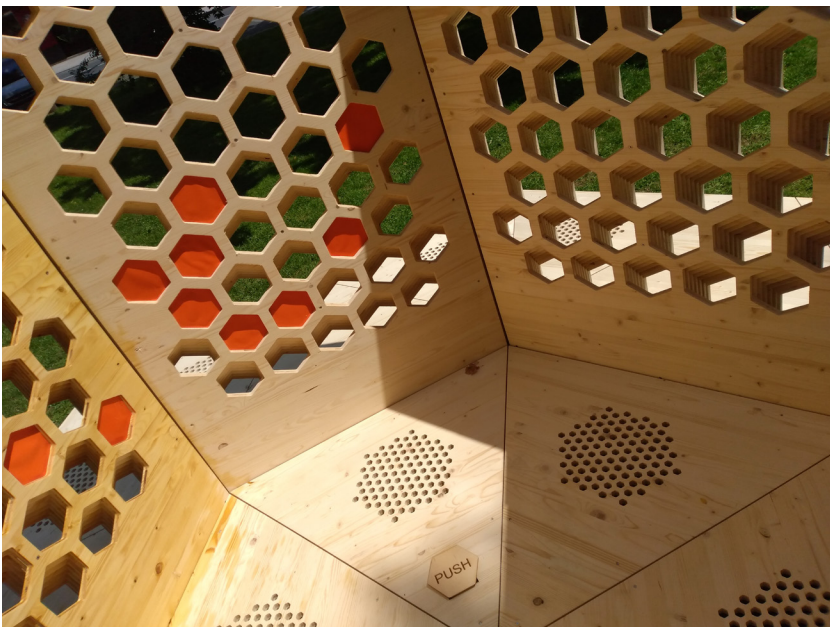
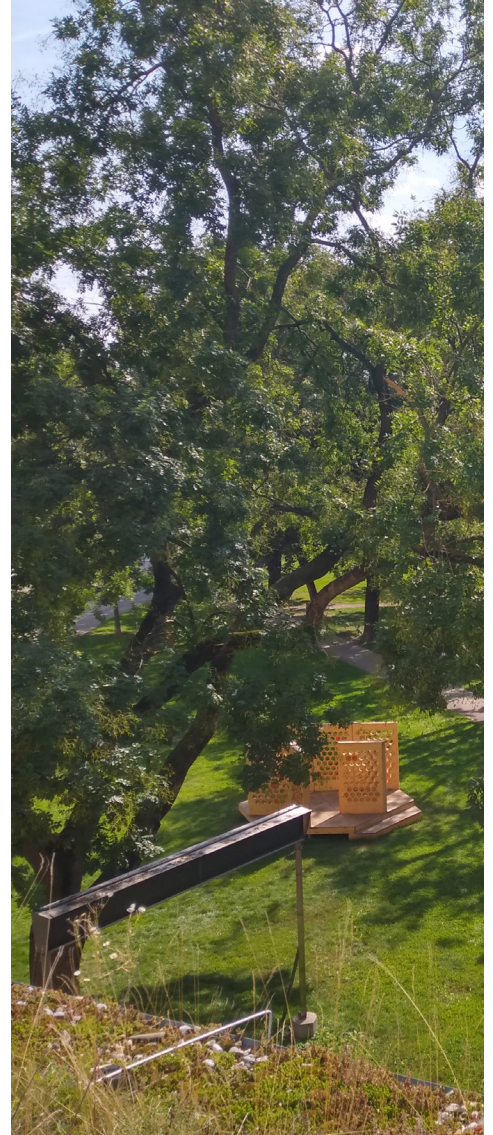
Art Project

- Title: Humming Room
- Artist: Elisabeth Harnik
- Acoustics: Jamilla Balint
- Architecture: Milena Stavric
- Sound Installation at Augarten, next to Musuem der Wahrnehmung
- Date: July 2020 - October 2020
- Picture Credits: Jamilla Balint

Humming room is a temporary sound installation in the public space (Graz, Augarten, next to Museum der Wahrnehmung). The form is based on the honeycomb structure and reflects the underlying theme of the project: merging urban sounds with nature (sound of bees) in a public space and sensitizing the perception of visitors on various levels. Six adjustable walls form a structure which reflect the sound depending on how they are aligned. From an acoustic point of view the challenge was to include an additional sound into the urban environment which is comforting rather than disturbing. The sound of humming bees was recorded and played back through six loudspeakers, which sound similar to white noise. Therefore it is not regarded as a source of annoyance. Basically one could say that white noise was added in a public space within an astonishing architectural structure to give visitors the possibility to pause for a moment and enjoy the natural/urban landscape.

Link to an interview with all project participants: <https://www.musicaustria.at/der-schluesel-ist-das-hin-hoeren-jamilla-balint-elisabeth-harnik-milena-stavric-humming-room-im-mica-interview/>





Appendix B - Data Sheets

Two data sheets from a lecture hall and a seminar room are shown. They were created within the Bachelor Projects, where the acoustic condition was assessed in 26 halls. [Frischmann et al., 2019, Mülleder et al., 2019]

TECHNISCHE UNIVERSITÄT GRAZ



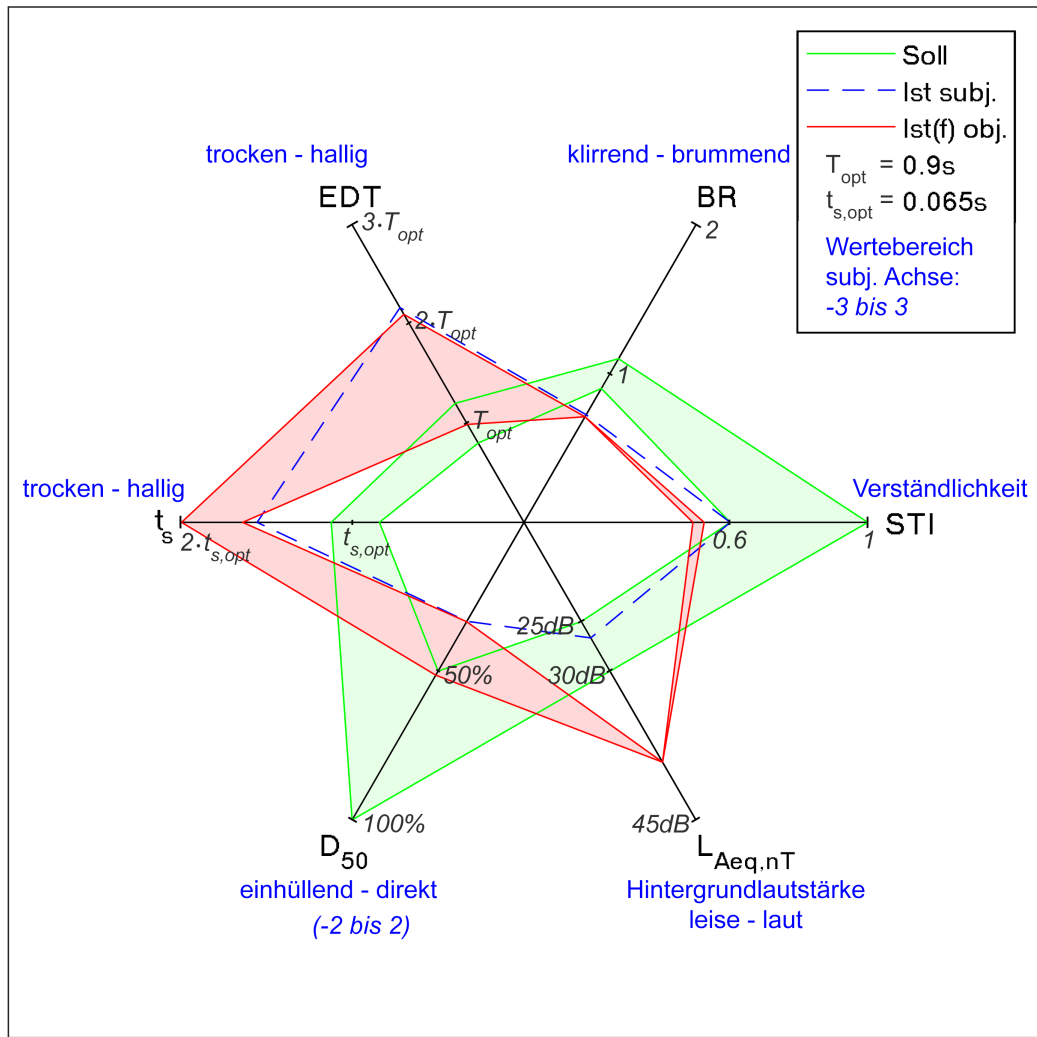
DATENBLATT HSi9



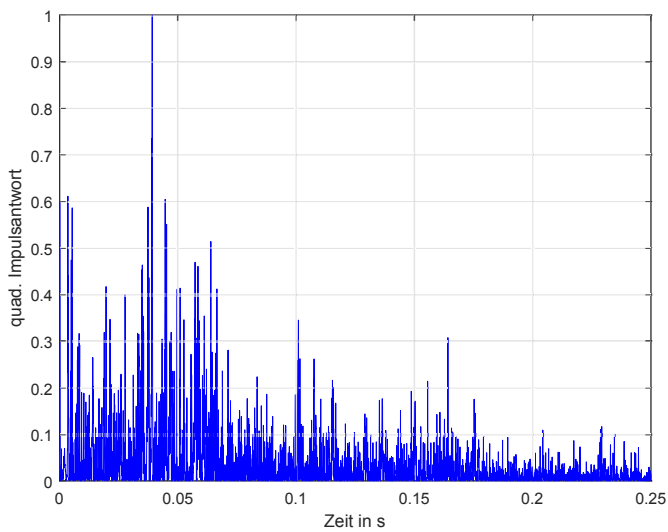
INFFELD GASSE 13

C. FRISCHMANN, K. SCHILLER, R. HOFER

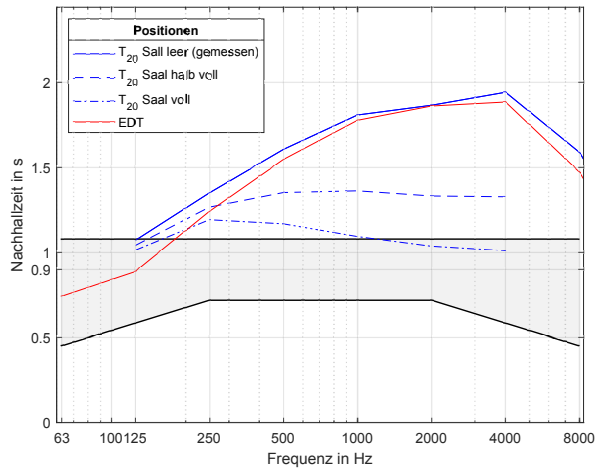
Sommersemester 2018



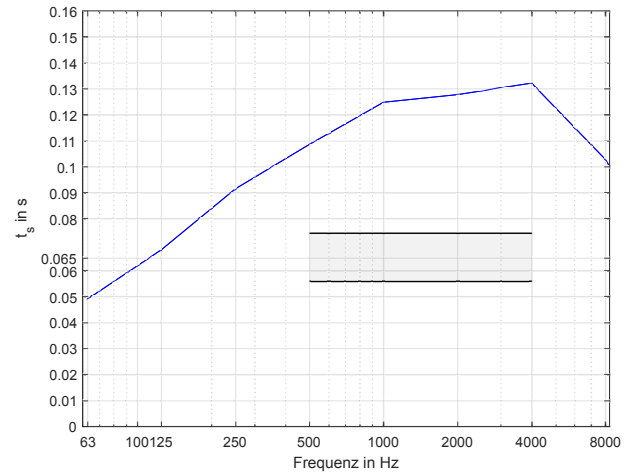
EDT... Anfangsnachhallzeit $L_{Aeq,nT}$... Anlagengeräuschpegel t_s ... Schwerpunktszeit
 D_{50} ... Deutlichkeitsgrad STI... Sprachübertragungsindex BR... Bassverhältnis



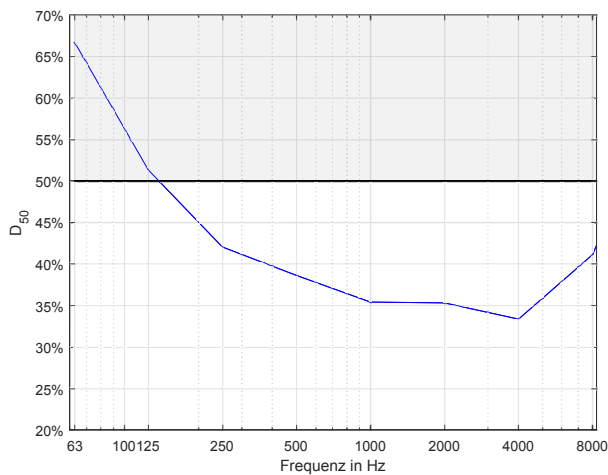
| Messbedingungen | |
|------------------|--------------------|
| Datum | 09.06.2018 |
| Messmethoden | MLS, Exp. Sweep |
| Personen im Raum | 1 |
| Raumvolumen | 643 m ³ |
| Temperatur | 23,4°C |
| Luftfeuchtigkeit | 63,3% |
| LAeq | 39,7 dB(A) |
| Bestuhlung | 70 Sessel Holz |
| Boden | Holzparkett |
| Wände | Fenster, Holz |
| Decke | Rigips |
| Absorber | Lochplatten |
| Reflektoren | Nein |



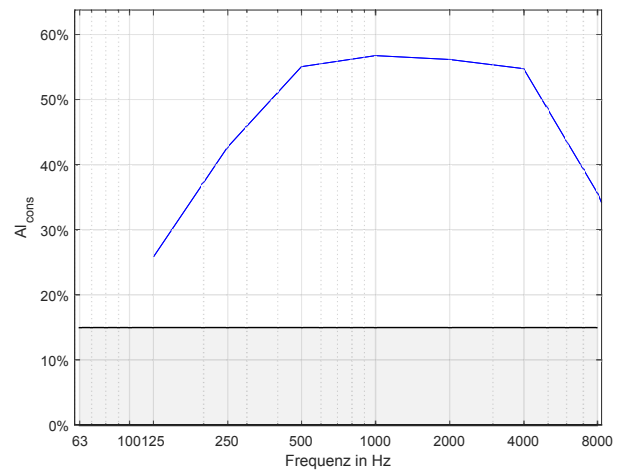
| Nachhallzeit | | | | | | | | |
|------------------------|------|------|------|------|------|------|------|------|
| f in Hz | 63 | 125 | 250 | 500 | 1000 | 2000 | 4000 | 8000 |
| T_{20} in s | 0.65 | 1.07 | 1.35 | 1.61 | 1.81 | 1.87 | 1.94 | 1.59 |
| T_{20} halbvoll in s | – | 1.04 | 1.27 | 1.35 | 1.36 | 1.33 | 1.33 | – |
| T_{20} voll in s | – | 1.01 | 1.19 | 1.17 | 1.09 | 1.04 | 1.01 | – |
| EDT in s | 0.74 | 0.89 | 1.24 | 1.55 | 1.78 | 1.86 | 1.89 | 1.47 |



| Schwerpunktzeit | | | | | | | | |
|-----------------|-------|-------|-------|-------|-------|-------|-------|-------|
| f in Hz | 63 | 125 | 250 | 500 | 1000 | 2000 | 4000 | 8000 |
| t_s in s | 0.049 | 0.068 | 0.092 | 0.109 | 0.125 | 0.128 | 0.132 | 0.103 |



| Deutlichkeitsgrad | | | | | | | | |
|-------------------|----|-----|-----|-----|------|------|------|------|
| f in Hz | 63 | 125 | 250 | 500 | 1000 | 2000 | 4000 | 8000 |
| D_{50} in % | 67 | 51 | 42 | 39 | 35 | 35 | 33 | 41 |



| Artikulationsverlust | | | | | | | | |
|----------------------|----|-----|-----|-----|------|------|------|------|
| f in Hz | 63 | 125 | 250 | 500 | 1000 | 2000 | 4000 | 8000 |
| Al_{cons} in % | 11 | 26 | 43 | 55 | 57 | 56 | 55 | 36 |

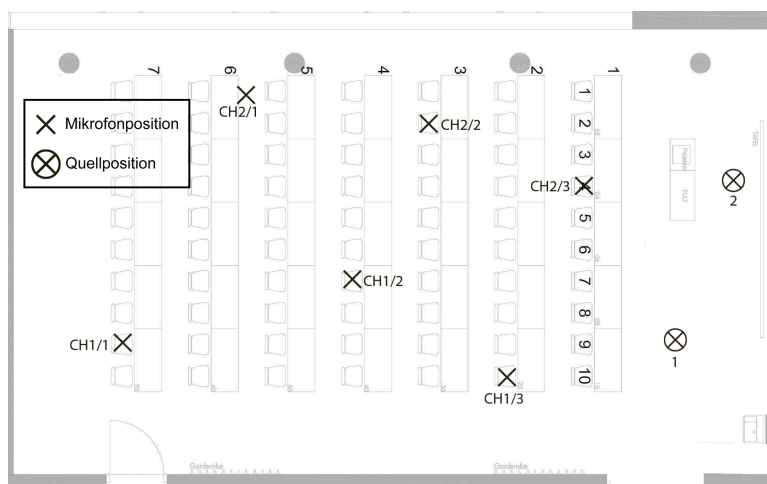
Diskussion:

Auffällig im HSi9 sind die enorm hohen Werte des Al_{cons} in den letzten beiden Reihen. Subjektiv wurde der Hörsaal in diesem Bereich als sehr hallig evaluiert. Der daraus resultierende Deutlichkeitsgrad ist im Großteil der Messpunkte zu niedrig.

Fazit:

Durch überwiegende Abweichungen im gesamten Frequenzbereich der Gütemaße und dem ergänzenden subjektiven Eindruck empfiehlt sich im HSi9 eine akustische Sanierung.

| | | f in Hz | | | | | | | |
|-----------------|-------|-----------|-------|-------|--------|--------|--------|--------|-------|
| Positionen | | 63 | 125 | 250 | 500 | 1000 | 2000 | 4000 | 8000 |
| T_{20} in s | Ch1/1 | 0.97 | 0.95 | 1.33 | 1.67 | 1.83 | 1.90 | 1.92 | 1.59 |
| | Ch2/1 | 0.56 | 1.10 | 1.37 | 1.58 | 1.84 | 1.87 | 1.97 | 1.61 |
| | Ch1/2 | 0.79 | 1.18 | 1.28 | 1.60 | 1.81 | 1.85 | 1.96 | 1.59 |
| | Ch2/2 | 0.64 | 1.00 | 1.41 | 1.61 | 1.81 | 1.86 | 1.91 | 1.59 |
| | Ch1/3 | 0.60 | 1.03 | 1.30 | 1.63 | 1.80 | 1.85 | 1.92 | 1.58 |
| | Ch2/3 | 0.52 | 1.18 | 1.41 | 1.55 | 1.77 | 1.87 | 1.98 | 1.57 |
| EDT in s | Ch1/1 | 0.77 | 1.16 | 1.48 | 1.52 | 1.82 | 1.84 | 1.91 | 1.49 |
| | Ch2/1 | 0.80 | 0.82 | 0.96 | 1.47 | 1.85 | 1.95 | 1.86 | 1.56 |
| | Ch1/2 | 1.18 | 1.09 | 1.29 | 1.69 | 1.73 | 1.86 | 1.87 | 1.48 |
| | Ch2/2 | 0.65 | 0.79 | 1.10 | 1.52 | 1.71 | 1.88 | 1.97 | 1.43 |
| | Ch1/3 | 0.63 | 0.79 | 1.38 | 1.54 | 1.78 | 1.84 | 1.91 | 1.46 |
| | Ch2/3 | 0.41 | 0.68 | 1.24 | 1.55 | 1.78 | 1.80 | 1.79 | 1.40 |
| t_s in s | Ch1/1 | 0.041 | 0.073 | 0.095 | 0.115 | 0.137 | 0.142 | 0.140 | 0.110 |
| | Ch2/1 | 0.055 | 0.069 | 0.075 | 0.115 | 0.131 | 0.141 | 0.141 | 0.115 |
| | Ch1/2 | 0.074 | 0.088 | 0.097 | 0.122 | 0.133 | 0.137 | 0.140 | 0.112 |
| | Ch2/2 | 0.047 | 0.061 | 0.092 | 0.116 | 0.134 | 0.128 | 0.136 | 0.099 |
| | Ch1/3 | 0.048 | 0.062 | 0.096 | 0.092 | 0.111 | 0.109 | 0.120 | 0.092 |
| | Ch2/3 | 0.029 | 0.055 | 0.095 | 0.093 | 0.104 | 0.111 | 0.117 | 0.089 |
| A_{cons} in % | Ch1/1 | 48.41 | 46.47 | 90.52 | 100.00 | 100.00 | 100.00 | 100.00 | 77.63 |
| | Ch2/1 | 12.04 | 46.88 | 73.69 | 96.85 | 100.00 | 100.00 | 98.90 | 59.31 |
| | Ch1/2 | 16.67 | 27.59 | 33.15 | 53.60 | 56.74 | 55.31 | 53.40 | 31.18 |
| | Ch2/2 | 6.84 | 16.42 | 31.87 | 41.88 | 44.09 | 42.74 | 39.12 | 24.07 |
| | Ch1/3 | 4.77 | 9.76 | 16.10 | 25.15 | 25.61 | 24.51 | 22.94 | 13.54 |
| | Ch2/3 | 1.42 | 7.78 | 10.71 | 12.89 | 14.09 | 14.42 | 14.16 | 7.88 |
| D_{50} in % | Ch1/1 | 81.99 | 51.04 | 44.47 | 38.42 | 33.83 | 27.60 | 30.05 | 37.57 |
| | Ch2/1 | 65.67 | 55.39 | 56.51 | 29.26 | 32.12 | 29.69 | 28.61 | 35.74 |
| | Ch1/2 | 48.25 | 32.61 | 35.31 | 36.39 | 27.50 | 27.78 | 29.05 | 35.05 |
| | Ch2/2 | 66.92 | 54.92 | 37.44 | 29.83 | 27.02 | 36.15 | 33.26 | 43.30 |
| | Ch1/3 | 54.34 | 56.46 | 38.80 | 49.60 | 43.84 | 45.40 | 39.13 | 46.80 |
| | Ch2/3 | 83.62 | 57.67 | 39.89 | 48.37 | 48.30 | 45.38 | 40.19 | 48.44 |



| Positionen | STI | BR |
|------------|------|------|
| Ch1/1 | 0.50 | 0.65 |
| Ch2/1 | 0.51 | 0.72 |
| Ch1/2 | 0.48 | 0.72 |
| Ch2/2 | 0.51 | 0.70 |
| Ch1/3 | 0.53 | 0.68 |
| Ch2/3 | 0.54 | 0.78 |

Das Datenblatt wurde im Rahmen der Bachelorarbeit „Akustische Bestandsaufnahme der TU-Hörsäle Inffeldgasse“ erstellt. Details zur Messung, Berechnung und Auswertung werden in der genannten Arbeit erläutert.

TECHNISCHE UNIVERSITÄT GRAZ



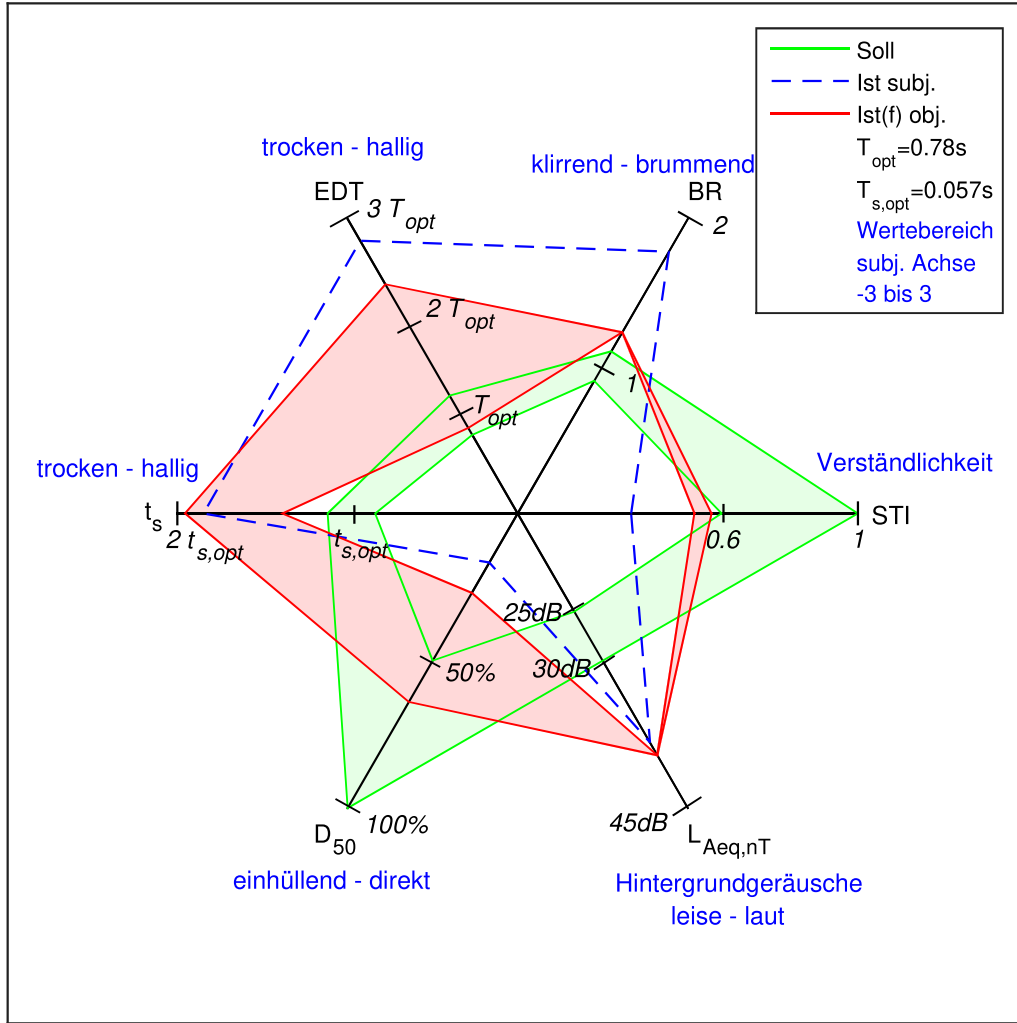
DATENBLATT LS XIV (ARCH II)



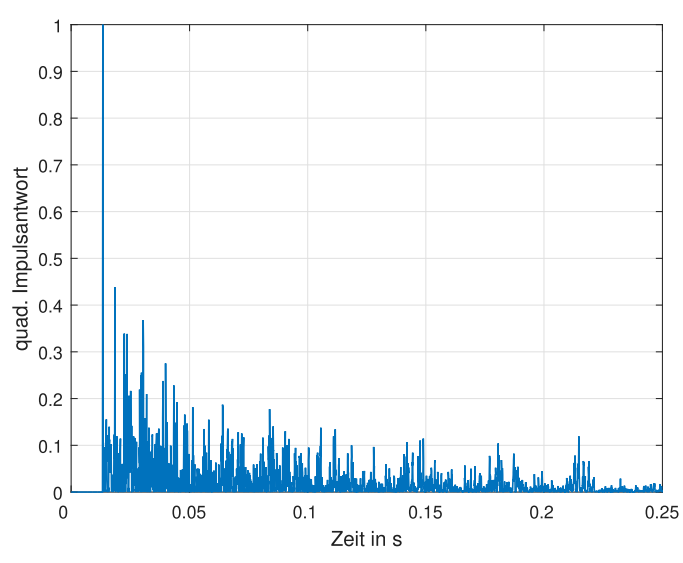
KRONESGASSE 5

DJ. PERINOVIC, L. RADOVANOVIC, A. MÜLLEDER

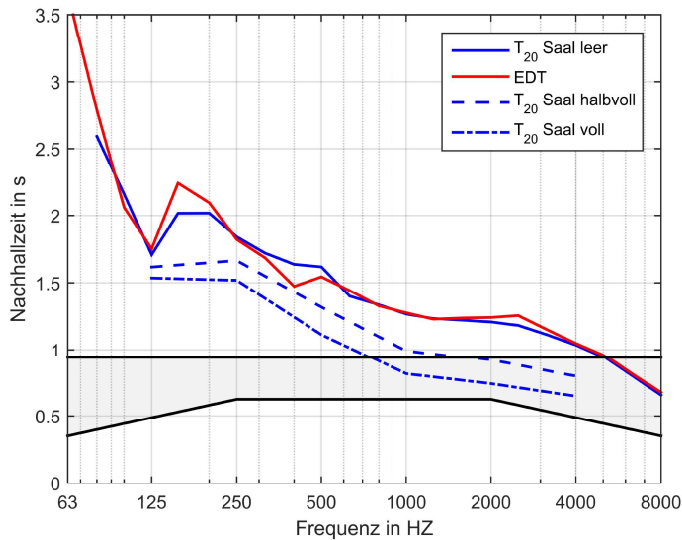
Wintersemester 2018/2019



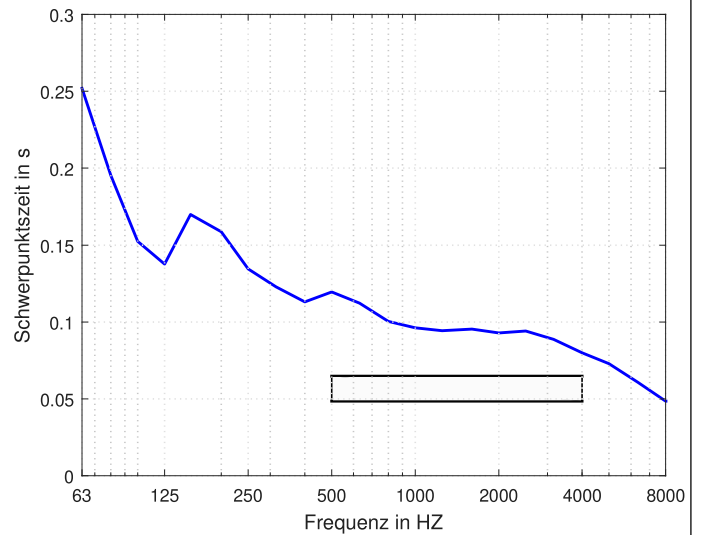
EDT... Anfangsnachhallzeit $L_{Aeq,nT}$... Hintergrundgeräuschpegel t_s ... Schwerpunktszeit
 D_{50} ... Deutlichkeitsgrad STI... Sprachübertragungsindex BR... Bassverhältnis



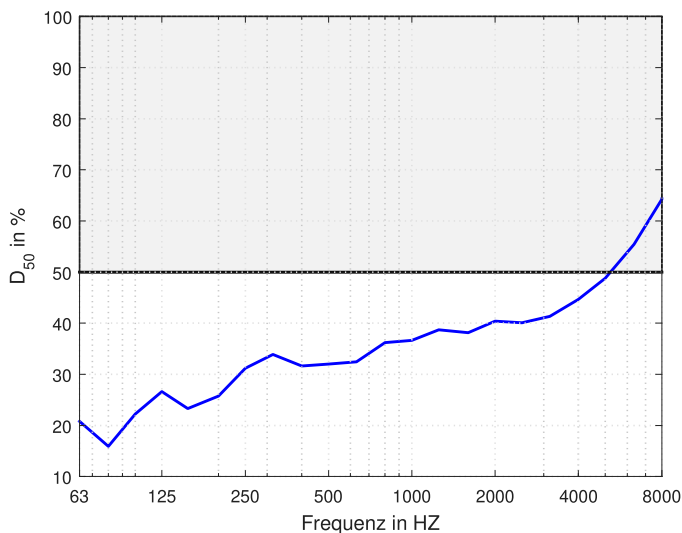
| Messbedingungen | |
|------------------|----------------------|
| Datum | 02.02.2019 |
| Messmethoden | Exp. Sweep |
| Personen im Raum | 3 |
| Raumvolumen | 308,5 m ³ |
| Temperatur | 22,9°C |
| Luftfeuchtigkeit | 34% |
| L_{Aeq} | 39,6 dB(A) |
| Bestuhlung | 41 Sitze Holz |
| Boden | Linoleum |
| Wände | Verputz, Beton |
| Decke | Verputz |
| Absorber | Nein |
| Reflektoren | keine |



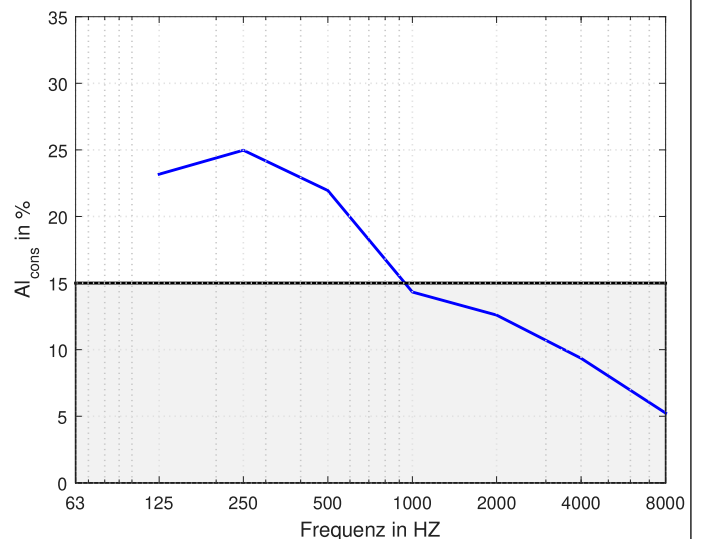
| Nachhallzeit | | | | | | | | |
|------------------------|------|------|------|------|------|------|------|------|
| <i>f</i> in Hz | 63 | 125 | 250 | 500 | 1000 | 2000 | 4000 | 8000 |
| T_{20} in s | — | 1.71 | 1.84 | 1.62 | 1.27 | 1.21 | 1.04 | 0.66 |
| T_{20} halbvoll in s | — | 1.62 | 1.67 | 1.32 | 0.99 | 0.92 | 0.80 | — |
| T_{20} voll in s | — | 1.54 | 1.52 | 1.11 | 0.82 | 0.74 | 0.65 | — |
| EDT in s | 3.69 | 1.75 | 1.82 | 1.54 | 1.28 | 1.24 | 1.05 | 0.68 |



| Schwerpunktszeit | | | | | | | | |
|------------------|-------|-------|-------|-------|-------|-------|-------|-------|
| <i>f</i> in Hz | 63 | 125 | 250 | 500 | 1000 | 2000 | 4000 | 8000 |
| t_s in s | 0.254 | 0.137 | 0.134 | 0.119 | 0.096 | 0.093 | 0.080 | 0.048 |



| Deutlichkeitsgrad | | | | | | | | |
|-------------------|----|-----|-----|-----|------|------|------|------|
| <i>f</i> in Hz | 63 | 125 | 250 | 500 | 1000 | 2000 | 4000 | 8000 |
| D_{50} in % | 21 | 27 | 31 | 32 | 37 | 40 | 45 | 64 |



| Artikulationsverlust | | | | | | | | |
|----------------------|----|-----|-----|-----|------|------|------|------|
| <i>f</i> in Hz | 63 | 125 | 250 | 500 | 1000 | 2000 | 4000 | 8000 |
| Al_{cons} in % | — | 23 | 25 | 22 | 14 | 13 | 9 | 5 |

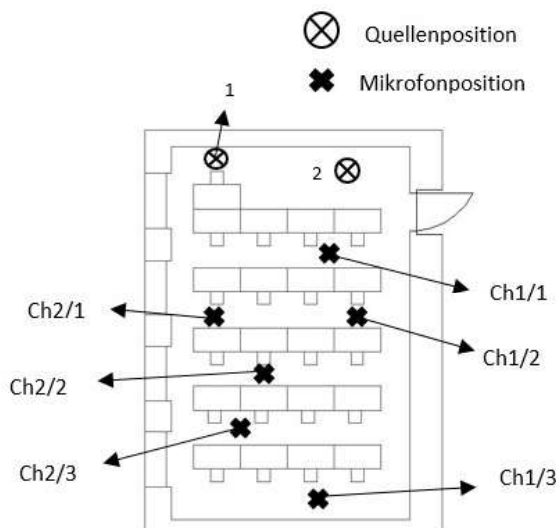
Diskussion:

In diesem Raum gibt es bisher keine Absorber oder sonstigen Maßnahmen, die einer guten Akustik dienen. Die gekrümmten Pberflächen an der Decke wirken wie Diffusoren, die in diesem Fall negative Auswirkungen haben. Bemerkenswert ist auch, dass es fast nicht möglich ist, Sprache zu verstehen, sobald zwei oder mehr Personen gleichzeitig reden. Alle objektiven Parameter sind fast ausschließlich außerhalb der zu erfüllenden Grenzen, was ebenfalls dem subjektiven Eindruck entspricht.

Fazit:

Durch die lange Nachhallzeit ist die Sprachverständlichkeit nicht gegeben. Eine akustische Sanierung ist unbedingt notwendig.

| | | f in Hz | | | | | | | |
|---------------------|-------|-----------|-------|-------|-------|-------|-------|-------|-------|
| Positionen | | 63 | 125 | 250 | 500 | 1000 | 2000 | 4000 | 8000 |
| T_{20} in s | Ch1/1 | 3.71 | 1.64 | 1.78 | 1.73 | 1.25 | 1.26 | 1.04 | 0.65 |
| | Ch2/1 | 3.37 | 1.78 | 1.80 | 1.56 | 1.27 | 1.19 | 0.98 | 0.66 |
| | Ch1/2 | 3.45 | 1.67 | 1.89 | 1.58 | 1.25 | 1.25 | 1.01 | 0.64 |
| | Ch2/2 | 4.07 | 1.39 | 1.72 | 1.67 | 1.29 | 1.17 | 1.05 | 0.66 |
| | Ch1/3 | – | 1.79 | 1.84 | 1.59 | 1.21 | 1.24 | 1.07 | 0.65 |
| | Ch2/3 | 4.66 | 2.08 | 2.25 | 1.76 | 1.26 | 1.16 | 1.08 | 0.65 |
| EDT in s | Ch1/1 | 3.66 | 2.45 | 1.47 | 1.50 | 1.17 | 1.42 | 0.98 | 0.60 |
| | Ch2/1 | 3.41 | 1.70 | 2.20 | 1.60 | 1.48 | 1.29 | 1.04 | 0.65 |
| | Ch1/2 | 3.51 | 1.68 | 1.98 | 1.73 | 1.18 | 1.18 | 1.07 | 0.63 |
| | Ch2/2 | 3.53 | 1.94 | 1.55 | 1.46 | 1.31 | 1.28 | 1.05 | 0.70 |
| | Ch1/3 | 3.42 | 1.80 | 2.46 | 1.39 | 1.21 | 1.30 | 1.06 | 0.73 |
| | Ch2/3 | 4.23 | 1.89 | 1.37 | 1.29 | 1.45 | 1.31 | 1.06 | 0.75 |
| t_s in s | Ch1/1 | 0.238 | 0.183 | 0.118 | 0.097 | 0.086 | 0.081 | 0.068 | 0.041 |
| | Ch2/1 | 0.230 | 0.112 | 0.133 | 0.127 | 0.101 | 0.102 | 0.074 | 0.044 |
| | Ch1/2 | 0.243 | 0.116 | 0.156 | 0.142 | 0.090 | 0.088 | 0.083 | 0.049 |
| | Ch2/2 | 0.208 | 0.174 | 0.130 | 0.125 | 0.109 | 0.112 | 0.086 | 0.055 |
| | Ch1/3 | 0.231 | 0.165 | 0.190 | 0.110 | 0.101 | 0.089 | 0.087 | 0.053 |
| | Ch2/3 | 0.249 | 0.164 | 0.121 | 0.114 | 0.105 | 0.103 | 0.089 | 0.055 |
| $A_{I_{cons}}$ in % | Ch1/1 | – | 12.06 | 13.00 | 11.43 | 7.45 | 6.56 | 4.87 | 2.72 |
| | Ch2/1 | – | 16.85 | 18.16 | 15.96 | 10.41 | 9.16 | 6.81 | 3.80 |
| | Ch1/2 | – | 27.70 | 29.86 | 26.23 | 17.12 | 15.06 | 11.19 | 6.25 |
| | Ch2/2 | – | 36.00 | 38.81 | 34.10 | 22.25 | 19.57 | 14.55 | 8.12 |
| | Ch1/3 | – | 80.05 | 86.30 | 75.83 | 49.48 | 43.52 | 32.35 | 18.07 |
| | Ch2/3 | – | 59.04 | 63.65 | 55.93 | 36.49 | 32.10 | 23.86 | 13.32 |
| D_{50} in % | Ch1/1 | 12.09 | 21.18 | 29.82 | 48.16 | 40.21 | 54.81 | 54.47 | 73.03 |
| | Ch2/1 | 24.45 | 48.73 | 32.42 | 24.79 | 37.21 | 30.11 | 48.63 | 68.05 |
| | Ch1/2 | 20.85 | 41.70 | 29.06 | 22.60 | 39.95 | 41.50 | 42.79 | 62.92 |
| | Ch2/2 | 32.86 | 4.55 | 27.36 | 30.03 | 27.64 | 24.60 | 39.23 | 55.18 |
| | Ch1/3 | 27.48 | 9.22 | 13.08 | 34.93 | 30.55 | 50.50 | 38.85 | 61.68 |
| | Ch2/3 | 31.87 | 14.44 | 26.72 | 26.50 | 32.60 | 33.04 | 40.09 | 58.64 |

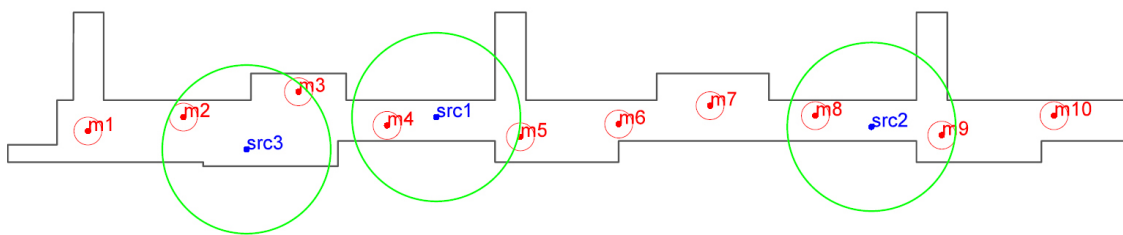


| Positionen | STI | BR |
|------------|------|------|
| Ch1/1 | 0.57 | 1.15 |
| Ch2/1 | 0.53 | 1.27 |
| Ch1/2 | 0.54 | 1.26 |
| Ch2/2 | 0.52 | 1.05 |
| Ch1/3 | 0.54 | 1.30 |
| Ch2/3 | 0.54 | 1.43 |

Das Datenblatt wurde im Rahmen der Bachelorarbeit „Architectural Acoustics - Acoustic Design of Lecture Halls“ erstellt. Details zur Messung, Berechnung und Auswertung werden in der genannten Arbeit erläutert.

Appendix C - Student Projects

Bachelor Thesis 1

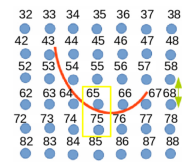


- Title: Prevention of flutter echoes in architecturally demanding spaces
- Author: Maximilian Giller, July 2015
- Link: <https://www.spsc.tugraz.at/student-projects/prevention-of-flutter-echos-in-architectural-demanding-spaces.html>

Abstract:

This bachelor thesis deals with the problem of utter echoes inside enclosed spaces and possible measures to prevent them. Flutter echoes result from repeated sound reflections between parallel walls with insufficient absorption; they are mostly perceived as disturbing and can noticeably impair speech intelligibility. After a summary of some theoretical fundamentals of acoustics and measurement techniques, measurements are performed in the interior space of the university building Inffeldgasse 16 c, Graz, regarding the general acoustic situation and the flutter echoes in the building. Trying to find valid measures for the whole space and to detect the echoes in the measured impulse responses, different problems resulting from the size and the shape of the building were encountered. A simulation of the whole building in CATT-Acoustic was created. The comparison with the measurement data shows significant differences, which again can likely be traced back to the room geometry. Finally, various possible strategies for prevention of flutter echoes, both in general and with regard to the situation in the examined enclosure, are presented and reviewed by means of simulations.

Bachelor Thesis 2

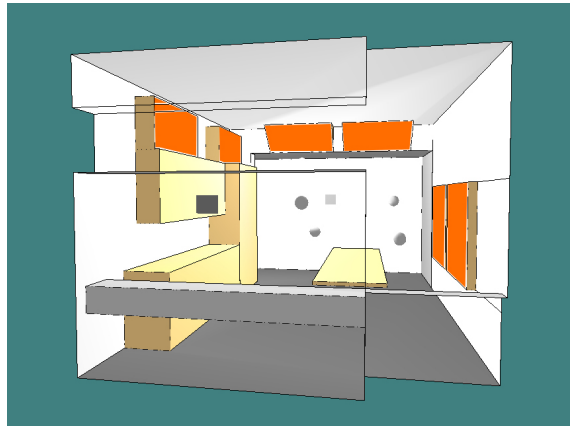


- Title: Schallausbreitung im Hallraum
- Author: Martina Kreuzbichler, October 2015
- Link: <https://www.spsc.tugraz.at/student-projects/sound-propagation-in-a-reverberation-chamber.html>
- Published [Kreuzbichler et al., 2016] at the 42. Jahrestagung fuer Akustik, Aachen, 2016. *Sound Propagation in a Reverberation Chamber*. Martina Kreuzbichler, Jamilla Balint, Gerhard Graber

Conclusion: [Kreuzbichler et al., 2016]

In this research we investigated the energy distribution around a panel diffuser in a reverberation chamber after excitation. We placed a diffuser in the middle of the chamber and looked at the energy level in the area behind the diffuser and compared it to the area in front of it which was facing the sound source. We animated the measurement results of the energy distribution over time to illustrate the different energy levels in the reverberation chamber from the point of excitation through the entire decay process. Our measurements showed that the energy level of the broadband signal in front of the diffuser is higher up to a time frame of 35 ms after excitation. At around 35 ms the reflections from the reverberation chamber's surface start to weight in. After this time, the energy is distributed almost equally in the entire measurement area and the difference between the measurement positions reach a minimum value. For low frequency bands the density of room modes is very low and the energy distribution in the room is unequal, therefore large fluctuations appear. This can be seen in the animations for 63 Hz and 125 Hz. For frequency bands above 125 Hz the energy is distributed almost equally after 35 ms after excitation. Reverberation chambers are usually equipped with more than one diffusers. Although the energy in the reverberation chamber in our research is almost equally distributed after 35 ms above the Schroeder frequency, it is questionable how the energy distribution looks like when the sound field around more than one diffuser is analysed. Usually the diffusers are cascaded in the upper half of the reverberation chamber. Therefore it could take longer until equal energy levels are reached. Moreover the panel diffusers could reduce the volume and be one of the reasons why the measured absorption coefficients differ so much in each reverberation chamber. This has to be evaluated in future research.

Bachelor Thesis 3



- Title: Entwurf und Bau einer variablen Akustik
- Author: Stefan Ziesemer, Oktober 2016
- Link: <https://www.spsc.tugraz.at/student-projects/entwurf-und-bau-einer-variablen-akustik.html>

Abstract:

This thesis deals with the room acoustical improvement of a conference and break room of the SPSC laboratory, located at Inffeldgasse 16, University of Technology Graz. At first, the actual state is determined by measuring the room impulse response and creating a simulation model. The concept of the new acoustic is acquired by placing sound absorbers in the room, using the Austrian standard OENORM B 8115-3 as a guideline. An important criterion for the absorbers is, that they can be mounted variable, to provide different room acoustic scenarios for the developers of the DIRHA-system (a speech interaction system for smart home applications), which is also installed in that very room. The absorption coefficient of the absorber is measured in the impedance tube. With those results the absorbers are designed, build and installed. Finally room acoustical measurements and simulations of the new situation are repeated, to evaluate the achieved improvements.

Comment: The response from the lab members were very good. Coffee breaks were no longer a loud event, even when many people joined the informal meetings. Furthermore, the construction plans served as templates for acoustic improvements at the new Congress Centre Alpbach. Due to too much reverberation, the seminar rooms were not suited for their purpose. After installing some of Stefan's wall absorbers, the rooms are fit for congresses and seminars. Before completing his studies, Stefan worked as a study assistant and help me to design the new exercise 'Raumakustik, Uebung'.



Recording studio at KUG, photo credits: Jan Godde

Bachelor Thesis 4

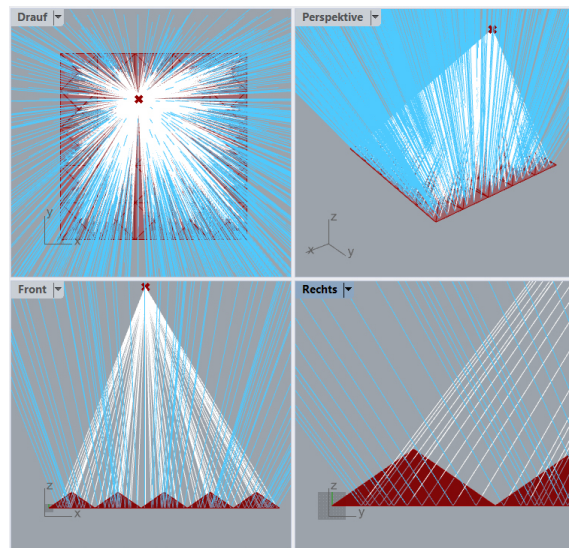
- Title: Raumakustische Optimierung eines Aufnahmerraumes im Tonstudio der Kunstuniversität Graz
- Author: Jan Godde, Valentin Huber, Februar 2017
- Link: <https://www.spsc.tugraz.at/student-projects/raumakustische-optimierung-eines-aufnahmerraumes-im-tonstudio-der-kunstuniversitaet-graz.html>
- Published [Huber et al., 2018] at the 44. Jahrestagung fuer Akustik, Muenchen. *Hoher Anspruch auf kleinem Raum: Tieffrequente Herausforderungen bei der akustischen Sanierung eines Aufnahmerraumes*. Valentin Huber, Jan Godde, Jamilla Balint

Abstract:

The present work is dealing with the acoustic design of a recording studio. It is intended to achieve similar acoustic conditions as in an already existing live room. The challenges occurring especially in small spaces are introduced and a number of acoustical absorbers are presented. The types of absorbers capable of damping the low frequency room modes are discussed. The acoustic measurements are evaluated, the reverberation time is selected as a significant criterion and a low, frequency-independent target value is chosen. A 3D-model for the acoustic simulation software is built and on the basis of the simulations, various optimisation measures are developed. Concerning an adequate dampening of the room modes, edge or corner absorbers are selected as the basic concept for the enhancement and compound panel absorbers are planned to be installed on the walls. For prevention of flutter echoes and a sufficient gain of absorption and diffusion, a panel system on the ceiling is designed. Finally, the acoustical measures taken are presented and evaluated, specifically regarding the reverberation time, room modes and reflections.

Comment: The ideas and the design impressed the head of the recording studio so much that the students were commissioned to conduct the refurbishment. After the successful redesign, recordings were made in both rooms to compare the sound and impression with the calculations. After completing his Bachelor studies, Valentin now runs his own company for acoustic consulting.

Bachelor Thesis 5

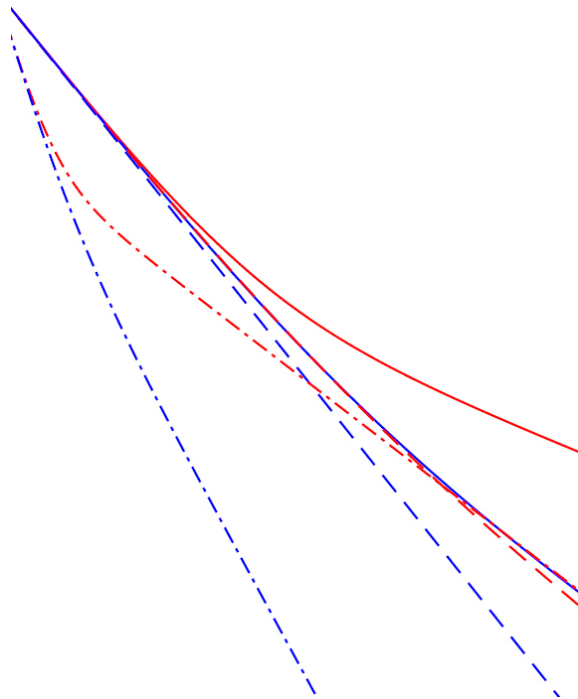


- Title: Adaptive Acoustics
- Author: Christian Bloecher, Michael Sattler, Oktober 2019
- Link: <https://www.spsc.tugraz.at/student-projects/adaptive-acoustics.html>

Abstract:

The aim of this thesis was to design new kinds of acoustic panels which are able to change their form and therefore their acoustic characteristics through mechatronical control. This was conceived to be part of the seminar Design of Specialised Topics with the topic Adaptive Acoustics. During the seminar architecture students and audio-engineering students worked in collaboration with the staff of the Institute of Architecture and Media and the Signal Processing and Speech Communication Laboratory of the University of Technology Graz. In order to assist the architecture students in acquiring a basic understanding of acoustics and sound propagation and thereby facilitate the cooperation between the two disciplines a sound reflection simulation was created using the CAD-program Rhinoceros 3D and its plug-in Grasshopper. This learning tool demonstrates basic acoustic phenomena during sound reflection - such as diffraction, scattering, and frequency-dependent absorption - through ray-tracing techniques. Another part of the thesis consists of the measurement and comparison of the acoustic properties of panel models and different kinds of perforated plates designed by the students. After the construction of the panels is finished they are planned to be installed inside two lecture halls at the University of Technology Graz. The adaptive acoustics will then allow to adjust acoustic characteristics of the room including reverberation time, speech intelligibility and other acoustic quality criteria to fit different kinds of applications.

Master Thesis 1

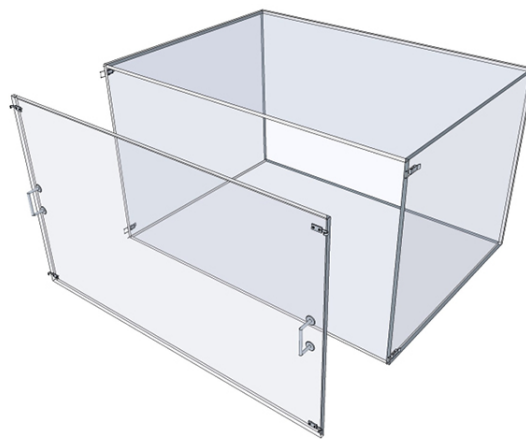


- Title: Statistical energy analysis for room acoustics
- Author: Nikolaus Fankhauser, August 2016
- Link: <https://www.spsc.tugraz.at/student-projects/statistical-energy-analysis-for-room-acoustics.html>

Abstract:

The following master thesis deals with Statistical Energy Analysis for room acoustics. In the first chapters of the work SEA is introduced and the theory of SEA is described. Based on the energy equations of simple resonators for different excitation scenarios, the calculations are extended to coupled systems and it is presented how to determine the energy equations for complex systems. The goal of this thesis is to calculate the energy decay curves (that means temporally dependent and not stationary results) of different rooms with SEA: at first the easiest case of a rectangular room is described, then the energy decay curves of coupled rooms are dealt with and in the last experiment a rectangular room containing plates is discussed. Moreover it is shown how the reverberation time of the analysed rooms can be determined based on the decay curves. The three experiments are evaluated by comparing the results with methods used in literature and measurements respectively. Therefore a method is developed that can be used to simulate the reverberation time of rooms.

Master Project 1

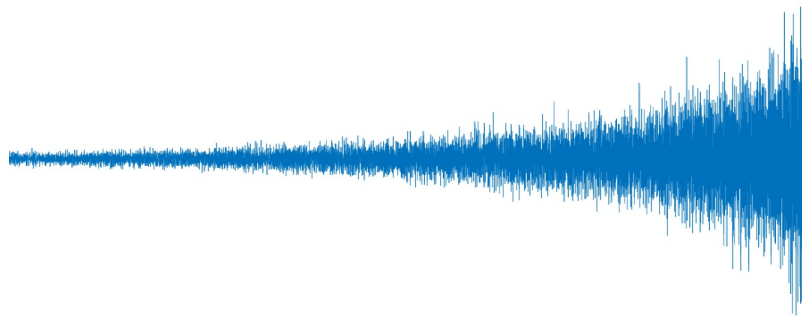


- Title: Entwurf und Bau eines Modellhallraums im Masstab 1:10
- Author: Martin Mueller, November 2016
- Link: <https://www.spsc.tugraz.at/student-projects/design-and-construction-of-a-110-scale-model-reverberation-chamber.html>

Abstract:

The project work at hand documents the design and construction of a 1:10 scale model reverberation chamber and a suitable sound source, as well as the implementation of a software necessary for operating the resulting measurement system. Said system aims to satisfy the requirements of OENORM EN ISO 354 sound absorption measurements in reverberation chambers in a 1:10 scale model context. In conclusion a soundfield diffusivity examination suggested by the norm was performed to test the functionality of the model reverberation chamber using both boundary and hanging diffusors (i.e. volume diffusors and conventional panel diffusors respectively). The resulting product built during this project is intended to serve as a test-bench in future scientific studies concerning the research of diffuse sound fields in reverberation chambers.

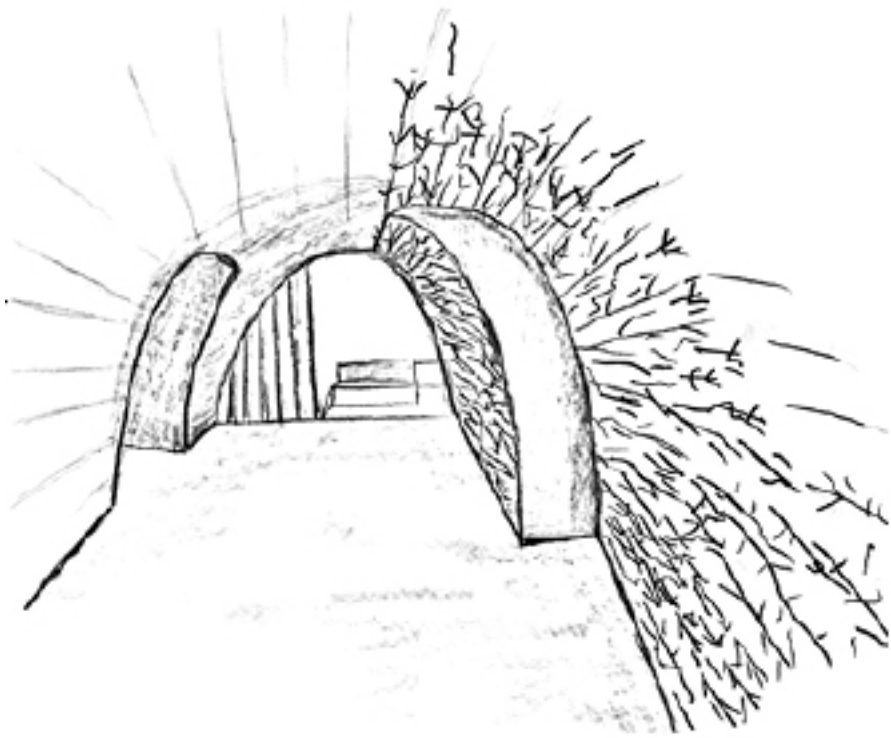
Master Project 2



- Title: Raumakustik: Grundlagen, Konzepte und Anwendungsbeispiele
- Author: Daniel Reisinger, Juni 2018
- Link: <https://www.spsc.tugraz.at/student-projects/raumakustik-grundlagen-konzepte-und-anwendungsbeispiele.html>

Abstract:

The acoustic properties of a room determine its suitability for specific uses. The requirements and specifications for music performance, teaching or industry are significantly different. As part of this project, the relevant standards and guidelines of various sectors were considered. In room acoustic evaluations the room impulse response is an easy-to-determine size to calculate acoustically interesting parameters such as reverberation time or quality measures. For this purpose, a tool for ISO-compliant impulse response processing was programmed in Matlab. In addition to calculation options for quality measures and stage measured quantities, this includes an algorithm to minimize the influence of noise when calculating reverberation time. A further section is dedicated to the room acoustics of venues. Concert halls and operas fascinate not only with their visual appearance and ambience, but also with their outstanding acoustic qualities. Based on research by the acousticians Beranek and Adelman-Larsen, a selection of venues in room acoustics was considered. In addition, it explains how the subjective perception of hearing can be linked to acoustically measurable factors and why room acoustics parameters of venues have to be regarded with respect to the performed musical genre.



Design Michael Schöllauf | wine acoustics

Collaborative Teaching

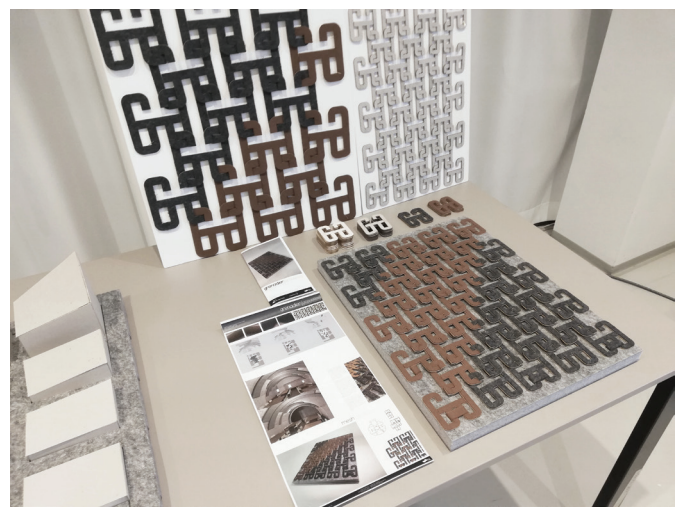
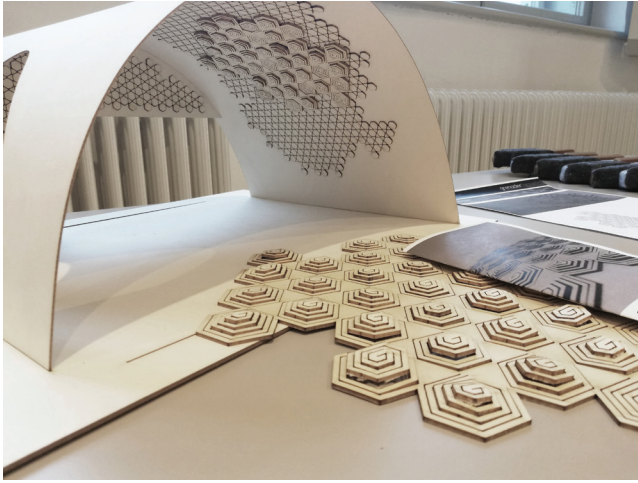


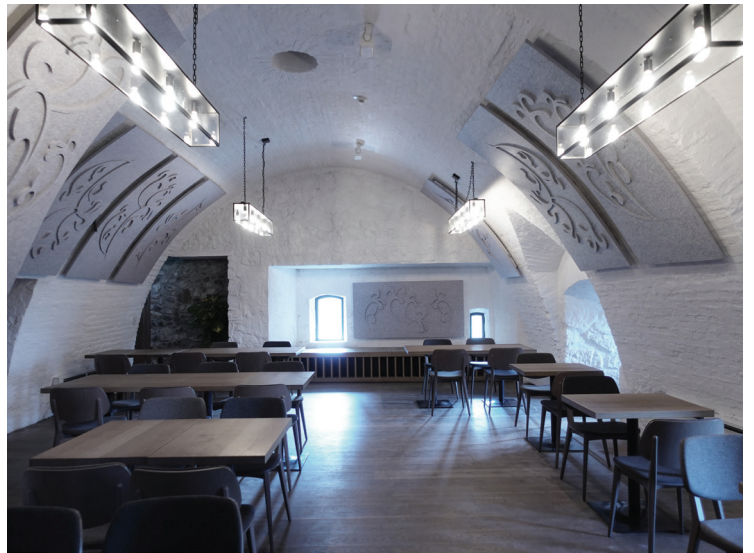
- Title: Grenadier Acoustics
- Course: Entwerfen spezialisierter Themen
- Instructors: Milena Stavric, Jamilla Balint, Albert Wiltsche
- Organisation: Institute of Architecture and Media, TUG
- Date: Summer Term 2020
- Picture credits: Albert Wiltsche

- Students: Brunner Viktoria Sabrina, Hosseini Badr Hoda, Guger Matthias, Williams J-Carl Grant, Jäger Fabian, Kubin Thomas, Stjepanovic Savo, Penz Lara Mercedes, Presnik Lisa, Rigler Fabian Yves, Schöllauf Michael, Ott Cornelia, Gal Filip

Abstract:

In a joint teaching project the acoustics of a space within a restaurant should be improved. Students from architecture were introduced to the fundamentals of acoustics and had to design innovative acoustic measures to decrease the reverberation time. Measurements were carried out before and after the refurbishment and the reverberation time could be decreased from 1.7 s to 0.7 s at 500 Hz.





Appendix D - Derivation of decay times

The theory is based on [Jacobsen, 2013] and is shown for the sake of completeness. The sound pressure can be expressed as a sum of modal terms:

$$\psi_m(x, y, z) = \sqrt{\varepsilon_x \varepsilon_y \varepsilon_z} \cos\left(\frac{n_x \pi x}{l_x}\right) \cos\left(\frac{n_y \pi y}{l_y}\right) \cos\left(\frac{n_z \pi z}{l_z}\right), \quad (6.1)$$

with normalisation constants

$$\varepsilon_x, \varepsilon_y, \varepsilon_z = 1 \text{ for } n = 0 \quad (6.2)$$

$$\varepsilon_x, \varepsilon_y, \varepsilon_z = 2 \text{ for } n > 0 \quad (6.3)$$

Decay time of modes expressed as the total energy of a mode divided by the sound power absorbed:

$$\tau_m = \frac{E_{a,m}}{P_{a,abs,m}} = \frac{1}{\rho c} \frac{\int_V \psi_m^2 dV}{\int_S \psi_m^2 \operatorname{Re}\{Y_s\} dS} \quad (6.4)$$

The volume integral in the numerator equals the total volume V and the surface integral in the denominator follows as (with the assumption that $l_x = l_y = l_z$ so that each wall has an area of $S/6$ and uniform wall admittance):

6 Conclusion

(1) Oblique modes ($n_x > 0, n_y > 0, n_z > 0$):

$$\begin{aligned}
 \int_S \psi_m^2 dS &= \sqrt{\varepsilon_x \varepsilon_y \varepsilon_z}^2 \int_S \cos^2\left(\frac{n_x \pi x}{l_x}\right) \cos^2\left(\frac{n_y \pi y}{l_y}\right) \cos^2\left(\frac{n_z \pi z}{l_z}\right) dS \\
 &= 8 \int \cos^2\left(\frac{n_x \pi x}{l_x}\right) \cos^2\left(\frac{n_y \pi y}{l_y}\right) \cos^2\left(\frac{n_z \pi z}{l_z}\right) \Big|_{z=0, l_z} dx dy \\
 &= 8 \left(\underbrace{\cos^2\left(\frac{n_z \pi 0}{l_z}\right)}_{=1} + \underbrace{\cos^2\left(\frac{n_z \pi l_z}{l_z}\right)}_{=1} \right) \int_0^{l_x} \cos^2\left(\frac{n_x \pi x}{l_x}\right) dx \int_0^{l_y} \cos^2\left(\frac{n_y \pi y}{l_y}\right) dy \\
 &= 8 \cdot 2 \cdot \left(\frac{x}{2} + \frac{\sin(2\frac{n_x \pi}{l_x} x)}{4\frac{n_x \pi}{l_x}} \right) \Big|_0^{l_x} \left(\frac{y}{2} + \frac{\sin(2\frac{n_y \pi}{l_y} y)}{4\frac{n_y \pi}{l_y}} \right) \Big|_0^{l_y} \\
 &= 8 \cdot 2 \cdot \frac{l_x}{2} \frac{l_y}{2} \Big|_{l_x l_y = \frac{S}{6}} \\
 &= 4 \cdot \frac{S}{6} \dots \Big|_{x=0, l_x} \Big|_{y=0, l_y} \\
 &= 2 \cdot S
 \end{aligned}$$

$$\boxed{\tau_m = \frac{1}{2} \frac{V}{S \rho c^2 \operatorname{Re}\{Y_s\}}} \quad (6.5)$$

(2) Tangential modes:

$$\int_S \psi_m^2 dS = \sqrt{\varepsilon_x \varepsilon_y \varepsilon_z}^2 \underbrace{\int_S \cos^2\left(\frac{n_x \pi x}{l_x}\right) \cos^2\left(\frac{n_y \pi y}{l_y}\right) \cos^2\left(\frac{n_z \pi z}{l_z}\right) dS}$$

$$\begin{aligned} & \text{for } n_x = 0, n_y > 0, n_z > 0 \\ & = 2 \int dx \int \cos^2(a_y y) dy \\ & = 2 \cdot l_x \cdot \frac{l_y}{2} \\ & = \frac{S}{6} \end{aligned}$$

$$\begin{aligned} & \text{for } n_x > 0, n_y = 0, n_z > 0 \\ & = 2 \int \cos^2(a_x x) dx \int dy \\ & = 2 \cdot \frac{l_x}{2} \cdot l_y \\ & = \frac{S}{6} \end{aligned}$$

$$\begin{aligned} & \text{for } n_x > 0, n_y > 0, n_z = 0 \\ & = 2 \int \cos^2(a_x x) dx \int \cos^2(a_y y) dy \\ & = 2 \cdot \frac{l_x}{2} \cdot \frac{l_y}{2} \\ & = \frac{S}{12} \end{aligned}$$

$$\int_S \psi_m^2 dS = 4 \cdot \frac{5}{12} \cdot S = \frac{5}{3} \cdot S$$

$$\boxed{\tau_m = \frac{3}{5} \frac{V}{S \rho c^2 \operatorname{Re}\{Y_s\}}} \quad (6.6)$$

6 Conclusion

(3) Axial modes:

$$\int_S \psi_m^2 dS = \sqrt{\varepsilon_x \varepsilon_y \varepsilon_z}^2 \underbrace{\int_S \cos^2\left(\frac{n_x \pi x}{l_x}\right) \cos^2\left(\frac{n_y \pi y}{l_y}\right) \cos^2\left(\frac{n_z \pi z}{l_z}\right) dS}$$

$$\begin{aligned} & \text{for } n_x = 0, n_y = 0, n_z > 0 \\ & = 2 \int dx \int dy \\ & = 2 \cdot l_x \cdot l_y \\ & = \frac{S}{3} \end{aligned}$$

$$\begin{aligned} & \text{for } n_x = 0, n_y > 0, n_z = 0 \\ & = 2 \int dx \int \cos^2(a_y y) dy \\ & = 2 \cdot l_x \cdot \frac{l_y}{2} \\ & = \frac{S}{6} \end{aligned}$$

$$\begin{aligned} & \text{for } n_x > 0, n_y = 0, n_z = 0 \\ & = 2 \int \cos^2(a_x x) dx \int dy \\ & = 2 \cdot \frac{l_x}{2} \cdot l_y \\ & = \frac{S}{6} \end{aligned}$$

$$\int_S \psi_m^2 dS = 2 \cdot \frac{2}{3} \cdot S = \frac{4}{3} \cdot S$$

$$\tau_m = \frac{3}{4} \frac{V}{S \rho c^2 \operatorname{Re}\{Y_s\}}$$

(6.7)

In case of non-uniform wall admittance, where all the losses are concentrated on $z = 0$:

(1) Oblique modes:

$$\begin{aligned}
 \int_S \psi_m^2 dS &= \sqrt{\varepsilon_x \varepsilon_y \varepsilon_z}^2 \int_S \cos^2\left(\frac{n_x \pi x}{l_x}\right) \cos^2\left(\frac{n_y \pi y}{l_y}\right) \cos^2\left(\frac{n_z \pi z}{l_z}\right) dS \\
 &= 8 \int \cos^2\left(\frac{n_x \pi x}{l_x}\right) \cos^2\left(\frac{n_y \pi y}{l_y}\right) \cos^2\left(\frac{n_z \pi z}{l_z}\right) \Big|_{z=0} dx dy \\
 &= 8 \underbrace{\cos^2\left(\frac{n_z \pi 0}{l_z}\right)}_{=1} \int_0^{l_x} \cos^2\left(\frac{n_x \pi x}{l_x}\right) dx \int_0^{l_y} \cos^2\left(\frac{n_y \pi y}{l_y}\right) dy \\
 &= 8 \cdot \left(\frac{x}{2} + \frac{\sin(2\frac{n_x \pi}{l_x} x)}{4\frac{n_x \pi}{l_x}}\right) \Big|_0^{l_x} \left(\frac{y}{2} + \frac{\sin(2\frac{n_y \pi}{l_y} y)}{4\frac{n_y \pi}{l_y}}\right) \Big|_0^{l_y} \\
 &= 8 \cdot \frac{l_x l_y}{2 \cdot 2} \\
 &= 2 \cdot l_x l_y
 \end{aligned}$$

(2) Tangential modes:

$$\begin{aligned}
 &\text{for } n_x = 0, n_y > 0, n_z > 0 \\
 &= \int dx \int \cos^2(a_y y) dy \\
 &= l_x \cdot \frac{l_y}{2}
 \end{aligned}$$

$$\begin{aligned}
 &\text{for } n_x > 0, n_y = 0, n_z > 0 \\
 &= \int \cos^2(a_x x) dx \int dy \\
 &= \frac{l_x}{2} \cdot l_y
 \end{aligned}$$

6 Conclusion

$$\begin{aligned}
 & \text{for } n_x > 0, n_y > 0, n_z = 0 \\
 & = \int \cos^2(a_x x) dx \int \cos^2(a_y y) dy \\
 & = \frac{l_x}{2} \cdot \frac{l_y}{2}
 \end{aligned}$$

(3) Axial modes:

$$\begin{aligned}
 & \text{for } n_x = 0, n_y = 0, n_z > 0 \\
 & = \int dx \int dy \\
 & = l_x l_y
 \end{aligned}$$

$$\begin{aligned}
 & \text{for } n_x = 0, n_y > 0, n_z = 0 \\
 & = \int dx \int \cos^2(a_y y) dy \\
 & = l_x \cdot \frac{l_y}{2}
 \end{aligned}$$

$$\begin{aligned}
 & \text{for } n_x > 0, n_y = 0, n_z = 0 \\
 & = \int \cos^2(a_x x) dx \int dy \\
 & = \frac{l_x}{2} \cdot l_y
 \end{aligned}$$

Resulting 2 groups of decay times:

$$\tau_m \Big|_{n_z=0} = \frac{l_z}{\rho c^2 \operatorname{Re}\{Y_s\}} \quad (6.8)$$

$$\tau_m \Big|_{n_z \neq 0} = \frac{1}{2} \frac{l_z}{\rho c^2 \operatorname{Re}\{Y_s\}} \quad (6.9)$$

Bibliography

- [Allard, 1993] Allard, J. (1993). *Propagation of sound in porous media: modelling sound absorbing materials*. Elsevier Science Publishers.
- [ArchitonicAG, 2020] ArchitonicAG (2020). <https://www.architonic.com/de/project/herzog-de-meuron-the-elbphilharmonie-hamburg/5103708>, last visited on september 17th, 2020.
- [ASTM, 2006] ASTM (2006). Interlaboratory Study to establish precision statements for ASTM C423. *Research Report E33-1010*.
- [Balint and Graber, 2018] Balint, J. and Graber, G. (2018). Gekruemmte Abklingkurven in Hallraeuumen, (Curved energy decays in reverberation rooms). In *Proceedings of the 44th annual meeting for acoustics DAGA, Munich, Germany*.
- [Balint and Kaiser, 2018] Balint, J. and Kaiser, F. (2018). Non-exponential decay curves in auditoriums. In *Auditorium Acoustics 2018*, volume Proceedings of the Institute of Acoustics Volume 40 Pt.3.
- [Balint and Muralter, 2019] Balint, J. and Muralter, F. (2019). The effect of absorber placement on absorption coefficients obtained from reverberation chamber measurements. In *Proceedings of the 23rd Int. Congress on Acoustics, Aachen*.
- [Balint et al., 2018] Balint, J., Muralter, F., Nolan, M., and Jeong, C.-H. (2018). Energy decay curves in reverberation chambers and the influence of scattering objects on the absorption coefficient of a sample . In *Conference Proceedings Euronoise 2018, Crete, Greece*, pages 2025–2030.
- [Balint et al., 2019] Balint, J., Muralter, F., Nolan, M., and Jeong, C.-H. (2019). Bayesian decay time estimation in a reverberation chamber for absorption measurements. *J. Acoust. Soc. Am.*, 146(3).
- [Balint et al., 2016] Balint, J. and Nolan, M., Fernandez-Grande, E., Brunskog, J., Jeong, C., Xiang, N., and Graber, G. (2016). Decay curves in coupled, reverberant spaces. In *Proceedings of the 22nd Int. Conference on Acoustics, Buenos Aires*.
- [Barron, 1995] Barron, M. (1995). Interpretation of early decay times in concert halls. *Acustica*, 81:320–331.
- [Barron, 2000] Barron, M. (2000). The current state of acoustic design of concert halls and opera houses. In *National Congress of Acoustics, TechniAcoustica, Spain*.
- [Beranek, 2004] Beranek, L. L. (2004). *Concert Halls and Opera Houses*. Springer-Verlag New York.
- [Berzborn and Vorländer, 2018] Berzborn, M. and Vorländer, M. (2018). Investigations on the directional energy decay curves in reverberation rooms. In *Conference Proceedings Euronoise 2018, Crete, Greece*, pages 2005–2010.

Bibliography

- [Blöcher and Sattler, 2019] Blöcher, C. and Sattler, M. (2019). Adaptive Acoustics - Entwurf und Herstellung von adaptiven Akustikpaneelen. Technical report, Graz University of Technology.
- [Bodlund, 1980] Bodlund, K. (1980). Monotonic curvature of low frequency decay records in reverberation chambers. *Journal of Sound and Vibration*, 73(1):19–29.
- [Bradley et al., 2014] Bradley, D. T., Müller-Trapet, M., Adelgren, J., and Vorländer, M. (2014). Effect of boundary diffusers in a reverberation chamber: Standardized diffuse field quantifiers. *The Journal of the Acoustical Society of America*, 135(4):1898–1906.
- [Bradley and Wang, 2005] Bradley, D. T. and Wang, L. M. (2005). The effects of simple coupled volume geometry on the objective and subjective results from nonexponential decay. *J. Acoust. Soc. Am.*, 118(3):1480–1490.
- [Bradley and Wang, 2009] Bradley, D. T. and Wang, L. M. (2009). Quantifying the Double Slope Effect in Coupled Volume Room Systems. *Building Acoustics*, 16(2):105–123.
- [Bradley and Wang, 2010] Bradley, D. T. and Wang, L. M. (2010). Optimum absorption and aperture parameters for realistic coupled volume spaces determined from computational analysis and subjective testing results. *The Journal of the Acoustical Society of America*, 127(1):223–232.
- [Bruel, 1978] Bruel, P. (1978). The enigma of sound power measurements at low frequencies. *Bruel & Kjaer Technical Review*, 34:3–40.
- [Brunskog, 2012] Brunskog, J. (2012). The forced sound transmission of finite single leaf walls using a variational technique. *J. Acoust. Soc. Am.*, 132(3):1482–1493.
- [Brunskog, 2013] Brunskog, J. (2013). Sound radiation from finite surfaces. *J. Acoust. Soc. Am.*, 133(5):3385–3385.
- [Castillo-Rutz et al., 2019] Castillo-Rutz, N., Hederer, F., Pirró, D., and Rutz, H. (2019). <https://www.researchcatalogue.net/view/595459/595460>, last visited on september 17th, 2019.
- [Cremer, 1961] Cremer, L. (1961). *Die wissenschaftlichen Grundlagen der Raumakustik*, volume II. S. Hirzel Stuttgart.
- [C.W.Kosten, 1960] C.W.Kosten (1960). International comparison measurements in the reverberation room. *Acustica*, 106:400–411.
- [Davern and Dubout, 1980] Davern, W. and Dubout, P. (1980). First Report on Australasian comparison measurements of sound absorption coefficients. *DBR Special Report, CSIRO Division of Building Research, Highett*.
- [Delany and Bazley, 1970] Delany, M. E. and Bazley, E. N. (1970). Acoustical properties of fibrous absorbent materials. *Appl. Acoust.*, 335:105–116.

- [Ermann and Johnson, 2002] Ermann, M. and Johnson, M. (2002). Pilot study: Exposure and materiality of the secondary room and its impact on the impulse response coupled-volume concert halls. *J. Acoust. Soc. Am.*, 111.
- [Eyring, 1931] Eyring, C. F. (1931). Reverberation time measurements in coupled rooms. *The Journal of the Acoustical Society of America*, 3(2A):181–206.
- [Frischmann et al., 2019] Frischmann, C., Hofer, R., and Schiller, K. (2019). Akustische Bestandsaufnahme der TU Hörsäle Inffeldgasse. Technical report, Graz University of Technology.
- [Gropius, 1923] Gropius, W. (1923). Idee und Aufbau des staatlichen Bauhauses Weimar. *Bauhausverlag GmbH. München*.
- [Gull and Skilling, 1984] Gull, S. F. and Skilling, J. (1984). Maximum entropy method in image processing. *IEE Proceedings F - Communications, Radar and Signal Processing*, 131(6):646–659.
- [Harrison and Madaras, 2001] Harrison, B. and Madaras, G. (2001). Computer modeling and prediction in the design of coupled volumes for a 1000-seat concert hall at Goshen College. *J. Acoust. Soc. Am.*, 109(5).
- [Hoffmann et al., 1993] Hoffmann, L., Shukla, A., Peter, M., Barbiellini, B., and Manuel, A. (1993). Linear and non-linear approaches to solve the inverse problem: applications to positron annihilation experiments. *Nuclear Instruments and Methods in Physics Research Section A: Accelerators, Spectrometers, Detectors and Associated Equipment*, 335(1-2):276–287.
- [Huber et al., 2018] Huber, V., Godde, J., and Balint, J. (2018). Hoher Anspruch auf kleinem Raum: Tieffrequente Herausforderungen bei der akustischen Sanierung eines Aufnahme- raumes. In *Proceedings of the 44. Jahrestagung fuer Akustik, Muenchen*.
- [Hunt et al., 1939] Hunt, F. V., Beranek, L. L., and Maa, D. Y. (1939). Analysis of sound decay in rectangular rooms. *J. Acoust. Soc. Am.*, 11(1):80–94.
- [ISO 3382-2, 2008] ISO 3382-2 (2008). Acoustics – Measurement of room acoustic parameters – Part 2: Reverberation time in ordinary rooms.
- [ISO 354, 2003] ISO 354 (2003). Acoustics – Measurement of sound absorption in a reverberation room.
- [Jacobsen, 1982] Jacobsen, F. (1982). Decay rates and wall absorption at low frequencies. *J. Sound and Vib.*, 81(3):405–412.
- [Jacobsen, 2013] Jacobsen, F. (2013). *Fundamentals of general linear acoustics*. John Wiley & Sons, United Kingdom.
- [Jeong et al., 2018] Jeong, C., Nolan, M., and Balint, J. (2018). Difficulties in comparing diffuse sound field measures and data/code sharing for future collaboration. In *Conference Proceedings Euronoise 2018, Crete, Greece*.

Bibliography

- [Jeong, 2010] Jeong, C.-H. (2010). Non-uniform sound intensity distributions when measuring absorption coefficients in reverberation chambers using a phased beam tracing. *J. Acoust. Soc. Am.*, 127(6):3560–3568.
- [Jeong, 2013] Jeong, C.-H. (2013). Converting Sabine absorption coefficients to random incidence absorption coefficients. *J. Acoust. Soc. Am.*, 133(6).
- [Jeong et al., 2017] Jeong, C.-H., Choi, S.-H., and Lee, I. (2017). Bayesian inference of the flow resistivity of a sound absorber and the room's influence on the Sabine absorption coefficients. *J. Acoust. Soc. Am.*, 141(3):1711–1714.
- [Jordan, 1970] Jordan, V. L. (1970). Acoustical criteria for auditoriums and their relation to model techniques. *The Journal of the Acoustical Society of America*, 47(2A):408–412.
- [Kahle, 2001] Kahle, E. (2001). Das Geheimnis der Salle Blanche. *tec21*, 48:12–14.
- [Kahle, 2013] Kahle, E. (2013). Room acoustical quality of concert halls: perceptual factors and acoustic criteria - return from experience. *Building acoustics*, 20(4):265–282.
- [Kahle, 2018] Kahle, E. (2018). Halls without qualities - or the effect of acoustics diffusion. In *Proceedings of the Institute of Acoustics*, volume 40(3), pages 169–173.
- [Kaiser, 2009] Kaiser, F. (2009). Acoustic enhancement systems, graz university of technology. Bachelor Thesis.
- [KKLManagementAG, 2020] KKLManagementAG (2020). <https://www.kkl-luzern.ch/en/dienstleistungen/das-kl-luzern/akustik/>, last visited on september 7th, 2020.
- [Kreuzbichler et al., 2016] Kreuzbichler, M., Balint, J., and Graber, G. (2016). Sound propagation in a reverberation chamber. In *Proceedings of the 42. Jahrestagung fuer Akustik, Aachen*.
- [Kuttruff, 1958] Kuttruff, H. (1958). Eigenschaften und Auswertung von Nachhallkurven, (Characteristics and analysis of decay curves). *Acta Acustica united with Acustica*, 8(4):273–280.
- [Kuttruff, 1981] Kuttruff, H. (1981). Sound decay in reverberation chambers with diffusing elements. *The Journal of the Acoustical Society of America*, 49(6):1716–1723.
- [Kuttruff, 2016] Kuttruff, H. (2016). *Room Acoustics*. CRC Press, Boca Raton.
- [Kuttruff and Jusofie, 1969] Kuttruff, H. and Jusofie, M. J. (1969). Messungen des nachhallverlaufes in mehreren Räumen, ausgeführt nach dem Verfahren der integrierten Impulsantwort. *Acustica*, 21(1):1–9.
- [Kuttruff and Straßen, 1980] Kuttruff, H. and Straßen, T. (1980). Zur Abhängigkeit des Raumnachhalls von der Wanddiffusität und von der Raumform. *Acustica*, 45:246–255.

- [Lokki and Pätynen, 2011] Lokki, T. and Pätynen, J. (2011). Concert hall acoustics assessment with individually elicited attributes. *The Journal of the Acoustical Society of America*, 130(2):835–849.
- [Lokki and Pätynen, 2018] Lokki, T. and Pätynen, J. (2018). Concert halls should primary please the ear, not the eye. In *Proceedings of the Institute of Acoustics*, volume 40 (3), pages 378–385.
- [Lokki et al., 2016] Lokki, T., Pätynen, J., Kuusinen, A., and Tervo, S. (2016). Concert hall acoustics: Repertoire, listening position and individual taste of listeners influence the quality attributes and preferences. *The Journal of the Acoustical Society of America*, 160(1):551–562.
- [Loos, 1912] Loos, A. (1912). Das Mysterium der Akustik. *Der Merker, Österreichische Zeitschrift für Musik und Theater, III. Jahrgang, I. Quartal, Heft 1, S. 9 f.*
- [Luizard et al., 2013] Luizard, P., Polack, J.-D., and Katz, B. (2013). Auralization of coupled spaces based on a diffusion equation model. *Open Access Article*.
- [McGurk and MacDonald, 1976] McGurk, H. and MacDonald, J. (1976). Hearing lips and seeing voices. *Nature*, 264:746–748.
- [Miki, 1990] Miki, Y. (1990). Acoustical properties of porous materials. Modifications of Delany-Bazley models. *J. Acoust. Soc. Am.*, 11(1):19–24.
- [Mülleder et al., 2019] Mülleder, A., Radovanovic, L., and Perinovic, D. (2019). Raumakustische Vermessung und Sanierung von Hörsälen. Technical report, Graz University of Technology.
- [Muralter, 2018] Muralter, F. (2018). Analysis tool for multiexponential energy decay curves in room acoustics. Master’s thesis, Graz University of Technology.
- [Muralter and Balint, 2019] Muralter, F. and Balint, J. (2019). Analysis tools for multiexponential energy decay curves in room acoustics. In *Proceedings of the 45th annual meeting for acoustics DAGA, Rostock, Germany*.
- [Nilsson, 2004a] Nilsson, E. (2004a). Decay processes in rooms with non-diffuse sound fields. Part II: Effect of irregularities. *Building Acoustics*, 11(2):133–143.
- [Nilsson, 2004b] Nilsson, E. (2004b). Decay processes in rooms with non-diffuse sound fields. Part I: Ceiling treatment with absorbing material. *Building Acoustics*, 11(1):39–60.
- [Nolan et al., 2020] Nolan, M., Berzborn, M., and Fernandez-Grande, E. (2020). Isotropy in decaying reverberant sound fields. *The Journal of the Acoustical Society of America*, 148(2):1077–1088.
- [Nolan et al., 2018] Nolan, M., Fernandez-Grande, E., Brunskog, J., and Jeong, C.-H. (2018). A wavenumber approach to quantifying the isotropy of the sound field in reverberant spaces. *J. Acoust. Soc. Am.*, 143(4):2514–2526.

Bibliography

- [Nolan et al., 2019] Nolan, M., Verburg, S., Brunskog, J., and Fernandez-Grande, E. (2019). Experimental characterization of the soundfield in a reverberation room. *J. Acoust. Soc. Am.*, 145(4).
- [Nolan et al., 2014] Nolan, M., Vercammen, M., Jeong, C.-H., and Brunskog, J. (2014). The use of a reference absorber for absorption measurements in a reverberation chamber. In *Proceedings of Forum Acusticum*.
- [OENORM B 8115-3, 2005] OENORM B 8115-3 (2005). (schallschutz und raumakustik im hochbau - teil 3: Raumakustik).
- [Oliveros, 2010] Oliveros, P. (2010). *Sounding the Margins: Collected Writings 1992-2009*. Deep Listening.
- [Popper and Lorenz, 1985] Popper, K. and Lorenz, K. (1985). Die Zukunft ist offen. *Piper*, S. 52, ISBN 3-492-00640-X.
- [Pätynen and Lokki, 2016a] Pätynen, J. and Lokki, T. (2016a). Concert halls with strong and lateral sound increase the emotional impact of orchestra music. *The Journal of the Acoustical Society of America*, 139(3):1214–1224.
- [Pätynen and Lokki, 2016b] Pätynen, J. and Lokki, T. (2016b). Perception of music dynamics in concert hall acoustics. *The Journal of the Acoustical Society of America*, 140(5).
- [R.E.Halliwell, 1983] R.E.Halliwell (1983). Interlaboratory variability of sound absorption measurement. *J. Acoust. Soc. Am.*, 73(3):880–886.
- [Sabine, 1931] Sabine, P. E. (1931). A Critical Study of the Precision of Measurement of Absorption Coefficients by Reverberation Methods. *The Journal of the Acoustical Society of America*, 3(1A):139–154.
- [Sabine, 1935] Sabine, P. E. (1935). What is Measured in Sound Absorption Measurements. *The Journal of the Acoustical Society of America*, 6(4):239–245.
- [Sabine, 1936] Sabine, P. E. (1936). The Beginnings of Architectural Acoustics. *The Journal of the Acoustical Society of America*, 7(4):242–248.
- [Sabine, 1922] Sabine, W. (1922). *Collected Papers on Acoustics*. Harvard University Press, Cambridge.
- [Savioja and Svensson, 2015] Savioja, L. and Svensson, U. P. (2015). Overview of geometrical room acoustic modeling techniques. *J. Acoust. Soc. Am.*, 138(2):708–730.
- [Schroeder, 1965] Schroeder, M. R. (1965). New Method of Measuring Reverberation Time. *J. Acoust. Soc. Am.*, 37(3):409–412.
- [Schroeder, 1966] Schroeder, M. R. (1966). Complementarity of sound buildup and decay. *J. Acoust. Soc. Am.*, 40:549–551.

- [Schultz, 1971] Schultz, T. (1971). Diffusion in reverberation chambers. *Journal of Sound and Vibration*, 16(1):17–28.
- [Shukla et al., 1995] Shukla, A., Hoffmann, L., Manuel, A., and Peter, M. (1995). Bayesian methods for lifetime analysis. *Materials Science Forum*, 175-178:939–946.
- [Shukla et al., 1997] Shukla, A., Hoffmann, L., Manuel, A., and Peter, M. (1997). Melt 4.0a a Program for Positron Lifetime Analysis. *Materials Science Forum*, 255-257:233–237.
- [Shukla et al., 1993] Shukla, A., Peter, M., and Hoffmann, L. (1993). Analysis of positron lifetime spectra using quantified maximum entropy and a general linear filter. *Nuclear Instruments and Methods in Physics Research*, A(335):310–317.
- [Skilling, 1990] Skilling, J. (1990). Quantified maximum entropy. In *Maximum Entropy and Bayesian Methods*, pages 341–350. Springer.
- [Stavric and Balint, 2019a] Stavric, M. and Balint, J. (2019a). Architectural Acoustics Ext. In *Exhibition Catalogue*.
- [Stavric and Balint, 2019b] Stavric, M. and Balint, J., editors (2019b). *Architectural Acoustics Extenden, Between two languages new space is discovered*. Verlag der Technischen Universität Graz.
- [Stavric and Balint, 2020] Stavric, M. and Balint, J., editors (2020). *Grenadier Acoustics*. Institut für Architektur und Medien.
- [Svensson, 1994] Svensson, P. (1994). *On reverberation enhancement in auditoria*. PhD thesis, Department of Applied Acoustics, Göteborg.
- [Thomasson, 1980] Thomasson, S.-I. (1980). On the Absorption Coefficient. *Acta Acustica united with Acustica*, 44(4):265–273.
- [Thompson, 2004] Thompson, E. (2004). *The Soundscape of Modernity, Architectural Acoustics and the Culture of Listening in America, 1900–1933*. MIT Press.
- [Thysell, 2011] Thysell, A.-C. (2011). Test Codes for suspended ceilings – Sound absorption RRT. *Tyrens AB project no. 224628, Tyrens AB, Sweden*.
- [Vercammen, 2010] Vercammen, M. (2010). Improving the accuracy of sound absorption measurements according to ISO 354. In *Proc. of the Int. Symp. on Room Acoustics*.
- [von Fischer, 2013] von Fischer, S. (2013). *Hellhörige Häuser, Akustik als Funktion der Architektur, 1920-1970*. PhD thesis, ETH Zürich.
- [Vorländer, 2013] Vorländer, M. (2013). Computer simulations in room acoustics: Concepts and uncertainties. *J. Acoust. Soc. Am.*, 133(3):1203–1213.
- [Waterhouse, 1955] Waterhouse, R. (1955). Inference patterns in reverberant sound fields. *J. Acoust. Soc. Am.*, 27(2).

Bibliography

- [Werner, 2008] Werner, V. (2008). Der virtuelle Konzertsaal, Elektroakustische Raumk-
langerzeugung im Überblick. Master's thesis, Universität für Musik und darstellende Kunst,
Wien.
- [Xiang, 2020] Xiang, N. (2020). Model-based Bayesian analysis in acoustics—A tutorial. *The
Journal of the Acoustical Society of America*, 148(2):1101–1120.
- [Xiang et al., 2011] Xiang, N., Goggans, P., Jasa, T., and Robinson, P. (2011). Bayesian char-
acterization of multiple-slope sound energy decays in coupled-volume systems. *J. Acoust.
Soc. Am.*, 129(2):741–752.
- [Xiang and Goggans, 2001] Xiang, N. and Goggans, P. M. (2001). Evaluation of decay times
in coupled spaces: Bayesian parameter estimation. *J. Acoust. Soc. Am.*, 110(3):1415–1424.
- [Xiang and Goggans, 2003] Xiang, N. and Goggans, P. M. (2003). Evaluation of decay times
in coupled spaces: Bayesian decay model selection. *J. Acoust. Soc. Am.*, 113(5):2685–2697.
- [Xiang and Jasa, 2006] Xiang, N. and Jasa, T. (2006). Evaluation of decay times in coupled
spaces: An efficient search algorithm within the Bayesian framework. *J. Acoust. Soc. Am.*,
120(6):3744–3749.